Die to Survive

- Functional Analysis of Grapevine Metacaspases Responsive to Effector - Triggered Immunity (ETI)-Related Cell Death

Zur Erlangung des akademischen Grades eines

DOKTORS DER/ NATURWISSENSCHAFTEN

(Dr. rer. nat.)

der KIT-Fakultät für Chemie und Biowissenschaften

Karlsruher Institut für Technologie (KIT) - Universitätsbereich

genehmigte

DISSERTATION

von

Peijie Gong

aus

Gansu, China

KIT-Dekan: Prof. Dr. Willem Klopper

Referent: Prof. Dr. Peter Nick

Korreferent: Prof. Dr. Eva Zyprian

Tag der mündlichen Prüfung: 26.07. 2017

Die vorliegende Dissertation wurde am Botanischen Institut des Karlsruher Instituts für Technologie (KIT), Botanisches Institut, Lehrstuhl 1 für Molekulare Zellbiologe, von Oktober 2013 bis Juni 2017 angefertigt.

Hiermit erkläre ich, dass ich die vorliegende Dissertation, abgesehen von der Benutzung der angegebenen Hilfsmittel, selbständig verfasst habe.

Alle Stellen, die gemäß Wortlaut oder Inhalt aus anderen Arbeiten entnommen sind, wurden durch Angabe der Quelle als Entlehnungen kenntlich gemacht.

Diese Dissertation liegt in gleicher oder ähnlicher Form keiner anderen Prüfungsbehörde vor.

Zudem erkläre ich, dass ich mich beim Anfertigen dieser Arbeit an die Regeln zur Sicherung guter wissenschaftlicher Praxis des KIT gehalten habe, einschließlich der Abgabe und Archivierung der Primärdaten, und dass die elektronische Version mit der schriftlichen übereinstimmt.

Karlsruhe, im Juni 2017

Peijie Gong

Acknowledgements

Firstly, the dissertation was accomplished under a grateful instruction by my supervisor Prof. Dr. Peter Nick. His innovative thoughts and motivation are continuously supporting me through every step of my research. I really appreciate for all his help, patience, trust, kindness and encouragement. I am deeply thankful to him for giving me this valuable chance to be one of his team in Botanical Institute and let me enjoyed a good scientific research time over the past four years.

I am grateful that Prof. Dr. Eva Zyprian agreed to be my co-examiner immediately and I really appreciate her time, devotion and expertise.

I sincerely give my special thanks to Dr. Michael Riemann for his countless suggestions and help during each group meeting and discussion time, and for critical reading of this thesis.

I would like to thank all the members working in Botanical Institute. I appreciate the outstanding work of our lab technician Sybille Wörner, Ernst Heene, and Sabine Purper, for resolving any technical troubles while I needed help. Thanks our Azubi Ronja Kammerrich and Jonas Müller, for cooperating with my leaf disc experiment and cell culture work to accelerate the progress of my research. My sincere thanks extend to Joachim Daumann and Kerstin Huber from Botanical garden, for well taking care of our plant materials. I am really thankful to Dr. Qiong, Dr. Fan, Dr. Manish, Dr. Vaidurya Dr. Dong, Dr. Viktoria, Dr. Rita, Dr. Sarhar, Dr. Ningning, Lixin, Xiaolu, Xiang, Ye, Fan, Yingnan, Hao, Ruipu, and Preshobha from whom I always learned many things and get unselfish help. My special thanks also to master/bachelor students Bernadette Gross, Armin Markel, Daniel Kuhn and Nadja Stöffler whom I got nice cooperation.

I appreciate that this research was also obtained generous support from other university or institute. Thanks a lot for Prof. Dr. Otmar Spring and Dr. Javier Gómez-Zeledón, from Botanical Institute of Hohenheim University, for providing us

single-sporangia strains of *Plasmopara viticola* and corresponding techniques; Prof. Dr. Jochen Bogs and Dr. Patrick R. Merz, from Dienstleistungszentrum Laendlicher Raum Rheinpfalz, Neustadt for providing us luciferase vector pLuc of gateway version, for our promoter activity assay.

Finally, I would like to thank my parents. For various reasons I did not return home for four years, but my parents totally understand my situation and support me with their unconditional love. Besides, I especially thank my wife Wen Zheng for living abroad with me and care my daily life during the last three years.

This work was supported by the China Scholarship Council (CSC).

Gong, Peijie

2017 June

Table of contents

Abbreviations

BY-2: Tobacco *Nicotiana tabacum* L. cv. bright yellow 2

CTAB: cetyltrimethylammonium bromide

DM: downy mildew

DPI: diphenyleneiodonium

dpi: day(s) post infection

DTT: dithiothreitol

ER: Endoplasmic reticulum

ETH: Ethylene

ETI: effector-triggered immunity

GFP: green fluorescent protein

hpi: hours post infection

HR: hypersensitive response

JA: jasmonic acid

MC: metacaspase

MeJA: methyljasmonate

MS: Murashige and Skoog

NB-LRR: nucleotide binding-leucine rich repeat

OxVrMC2-GFP: Overexpressed VrMC2 fused with GFP

OxVrMC5-GFP: Overexpressed VrMC5 fused with GFP

PAMPs: pathogen associated molecular patterns

PCD: programmed cell death

PR gene: pathogenesis related gene

PRRs: pattern recognition receptors

PTI: PAMP-triggered immunity

qPCR: quantitative PCR

R genes/proteins: resistance genes/proteins

ROS: reactive oxygen species

Rpv3: resistance to *P. viticola* 3

RT-PCR: reverse transcription-PCR

SA: salicylic acid

SAR: systemic acquired resistance

WT: wild type

2, 4-D: 2, 4-dichlorophenoxyacetic acid

Zusammenfassung

Der programmierte Zelltod (programmed cell death, PCD) ist ein unverzichtbarer Vorgang, welcher sowohl bei Pflanzen als auch bei Tieren durch ein intrazelluläres Programm vermittelt wird. Vor allem im pflanzlichen Immunitätssystem ist er als letztes Mittel eine unentbehrliche Strategie, um im Rahmen einer sogenannten hypersensitiven Antwort (hypersensitive response, HR) die Ausbreitung von biotrophen Pathogenen zu unterbinden. Als fortgeschrittener Zelltodmechanismus erscheint die hypersensitive Antwort häufig als Gipfelpunkt des zweiten Immunitätsniveaus einer Pflanze, die als Effektor-vermittelte Immunität (effector-triggered immunity, ETI) bezeichnet wird und ein Zeichen höherer Resistenz darstellt. Unsere bisherige Arbeit hat bereits eine Cystein-abhängige Protease-Genfamilie in der Weinrebe identifiziert, eine so genannte Metacaspase (MC), die eine wesentliche Rolle bei Prozessen des programmierten Zelltods in der Entwicklung von Pflanzen spielt. Ziel dieser Doktorarbeit ist es, zentrale MC-Genkandidaten zu screenen, die auf den ETI-induzierten HR-Prozess reagieren und die zelluläre Funktion und den entsprechenden Regulationsmechanismus der Kandidaten zu verstehen. Die Doktorarbeit besteht wie folgt aus drei progressiven Teilen.

Wir verwendeten ein typisches biotrophes Pathogenisolat, Plasmopara viticola, als HR-Elicitor auf Blattscheibenbioassays, um die Unterschiede der nekrotischen Zone während der Infektion von neun Genotypen auf Weinrebenblätter zu beobachten. Zwei gegensätzliche Genotypen wurden untersucht: Das Kultivar "Müller Thurgau" steht für einen anfälligen Genotyp, wohingegen *Vitis rupestris* für einen HR-resistenten Genotyp steht. Eine weitere Genexpressionsanalyse zeigte, dass nach der Infektion nur VrMC2 und VrMC5 von *V. rupestris* zunehmend exprimiert wurden, was 24 h vor dem Auftreten der hypersensitive Antwort erfolgte. Daher wurden diese beiden Gene als Kandidaten ausgewählt.

In einer Suspensionszelllinie wurde Harpin als ein wirksamer, die hypersensitive Antwort auslösender Elicitor eingesetzt, der den Zelltod spezifisch für *V. rupestris* und

“Pinot Noir” induzieren konnte. Die Genexpressionsanalyse zeigte, dass nach 24 h mit 18 µg / ml Harpinbehandlung VrMC2 und VrMC5 entsprechend hochreguliert wurden. Dieses Ergebnis entsprach unseren früheren Ergebnissen auf Blattscheiben. Bezüglich ihrer zellulären Funktionen wurden VrMC2 und VrMC5 durch heterologe Expression in BY-2 Tabakzellen charakterisiert. Die subzellulären Lokalisierungsstudien zeigten, dass sich VrMC2 am endoplasmatischen Retikulum (ER) um die Kern herum und VrMC5 im Zytoplasma und dem Kernbereich befand. Dies legt nahe, dass in der Weinrebe zwei verschiedene Typen von Metacaspasen wahrscheinlich die Rolle des programmierten Zelltods in verschiedenen subzellulären Orten in der Zelle übernehmen. Darüber hinaus zeigte ein Zellmortalitätsassay, dass beide VrMC2- und VrMC5-BY-2-Überexpressionslinien stark auf den durch Harpin-induzierten Zelltod reagierten. Darüber hinaus ist diese Mortalität signalabhängig, was durch die Zugabe von exogenem Methyljasmonat (MeJA), ein wichtiger Überträger der basalen Immunität, oder Diphenyleniodonium (DPI), einem Inhibitor von Nicotinamid-Adenin- Dinukleotid-Phosphat-Wasserstoff (NADPH) Oxidasen, welche apoplastisches Superoxid erzeugen, vermindert werden konnte.

Die 5'-Upstream-Sequenz-Promotoren von MC2 (pMC2) und MC5 (pMC5) wurden aus beiden Kultivaren, "Müller Thurgau" und *V. rupestris*, kloniert, um den durch Genexpression regulierten Mechanismus weiter zu untersuchen. Die Verteilung der auf die Abwehrreaktion bezogenen cis-Elemente von pMC2 und pMC5 wurde in den zwei Genotypen weiter analysiert. Die Ergebnisse zeigten, dass es fünf verschiedene Arten cis-Elementen gibt, die sowohl auf pMC2 als auch auf pMC5 verteilt sind, wie z. B. die W-Box, die TC-reiche Region und das GT-1-Motiv. Die Gesamtelementanzahl von pVrMC2 und pVrMC5 ist höher als die Anzahl von pVvMC2 und pVvMC5. Nicht zuletzt wurde mit Hilfe eines Dual-Luciferase-Systems zum Nachweis der Promotoraktivität von pVrMC2 und pVrMC5 gezeigt, dass nach der Harpinbehandlung sowohl die Aktivität von pVrMC2 als auch die von pVrMC5 zumeist verdoppelt wurden. Jedoch zeigte pVrMC2 keine Antwort auf MeJA. Außerdem verringerte sich sogar die pVrMC5-Aktivität durch Zugabe von MeJA. Diese Ergebnisse bestätigten, dass die VrMC2- und VrMC5-Genexpressionsmuster teilweise durch ihre entsprechenden Promotoraktivitäten reguliert wurden.

Abstract

In both plants and animals, programmed cell death (PCD) is an indispensable process that is mediated by an intracellular program. Especially in plant defence response, PCD works as a last resort to block the spread of biotrophic pathogens and this phenomenon is called hypersensitive response (HR) or hypersensitive cell death. As an advanced suicide defence mechanism, HR often appears as a culmination of a plant's second immunity level, termed an effector-triggered immunity (ETI), and a mark of higher resistance. Our previous work has already identified one cysteine-dependent protease gene family in grapevine, a so-called *Metacaspase (MC)*, which is reported to play an essential role in plant developmental PCD processes. In this study, the scope is to screen central *MC* gene candidates which respond to the ETI-induced HR process and understand the cellular function and related regulation mechanism of the candidates. The whole study consists of three progressive parts as follows.

As a first step, two extreme genotypes differed in their HR response elicited by a typical biotrophic pathogen isolate *plasmopara viticola* were selected by screening 9 genotypes of the host grapevine using leaf discs bio-assay. As a result, *V. vinifera* cv. 'Mueller Thurgau' stands for susceptible genotype and *V. rupestris* stands for HR-resistant genotype were chosen. By comparing the expression profile of *MC* genes, it is shown that the expression level of *VrMC2* and *VrMC5* in *V. rupestris* increased steadily within 24 hours after infection in *V. rupestris* not in the susceptible cultivar Mueller Thurgau.

In order to have a detailed understanding of *VrMC2* and *VrMC5*, suspension cell line of *V. rupestris* and cv 'Pinot Noir' was employed in the following studies in which HR can be induced by harpin elicotor. Gene expression analysis showed that *VrMC2* and *VrMC5* were up-regulated after 24h in response to harpin treatment at 18 µg / ml. This result was in accordance with our former results on leaf discs. Subcellular localization of *VrMC2* and *VrMC5* has been characterized upon heterologous expression in tobacco BY-2 cells which is much easier to transform. Fluorescent microscopy

showed that *VrMC2* located on Endoplasmic reticulum (ER) around the nuclear zone, and *VrMC5* located in the cytoplasm and nucleus. These results suggest that there are two different types of grape MCs probably involved PCD and function in different subcellular location. Moreover, a cell mortality assay showed both overexpressed *VrMC2* and *VrMC5* BY-2 cell lines responded highly to harpin induction (activating defence-related cell death). In addition, this mortality is signal-dependent, which could be mitigated by either the addition of exogenous methyljasmonate (MeJA; an important transducer of basal immunity) or diphenyleneiodonium (DPI), an inhibitor of Nicotinamide adenine dinucleotide phosphate hydrogen (NADPH) oxidases that generate apoplastic superoxide.

The 5' upstream sequences promoters of *MC2* (*pMC2*) and *MC5* (*pMC5*) were cloned from both cv. 'Mueller Thurgau' and *V. rupestris* to further investigate the gene expression-regulation mechanism. The distribution of defence-related cis-elements was further analysed from *pMC2* and *pMC5* between two genotypes. Results showed there are five different kinds of key defence-related cis-elements distributed on both *pMC2* and *pMC5*, such as the W box, TC-rich region and GT-1 motif. The total element numbers from *pVrMC2* and *pVrMC5* are higher than the numbers from *pVvMC2* and *pVvMC5*. Last but not least, by using a dual-luciferase system to detect the promoter activity of *pVrMC2*, *pVrMC5*, the results revealed that both *pVrMC2* and *pVrMC5* activities were mostly doubled after harpin treatment. However, *pVrMC2* showed no response to MeJA, and even *pVrMC5* activity decreased by adding MeJA. These findings verified that the *VrMC2* and *VrMC5* gene expression trends were partially regulated by their corresponding promoter activities.

1. INTRODUCTION

1.1 Plant immune system

Plants encounter a variety of unfavourable factors surrounding their environment at each stage of their life cycle, such as pathogenic microorganisms (e.g. fungi, bacteria, viruses, oomycetes and mycoplasma), pests and other stress factors. Among them, one of the hot topics is the interaction between pathogens and host plants, which is dynamic and sophisticated. During a long history of co-evolution, plants have evolved multiple layers of defence strategies, termed plant immune systems, to identify and defend against various invaders. On the other hand, pathogens could only survive and reproduce on the host if they can overcome each of those layers (Jones and Dangl, 2006). It is essential for the development of novel plant protections strategies to clarify the details of how plants communicate with pathogen infections.

1.1.1 The 1st defence layer: mechanical barriers

Firstly, pathogens need to pass through the host plant's mechanical barriers. Plant epidermis possesses for example wax layers, rigid cell walls and cuticular lipids, that can protect itself from the entry of pathogens (Reina-Pinto and Yephremov, 2009). Most of the invasions of potential pathogens are primarily prevented by these barriers. Only a few pathogens can break through the host plant's mechanical barriers by the direct penetration of the plant surface or invasion through physical wounds or natural openings, such as stomata (Getz *et al.*, 1983; Huang, 1986). Pathogens commonly use mechanical pressure, pathogen-secreted enzymes, toxic proteins and hormones to enter through the host plant's surface (Spoel and Dong, 2012).

Once the first layer is overcome, the pathogen faces the host plant's second layer of defence, which is its own immune system. The plant's immune system is similar to that of animals, and is divided into an innate and acquired immune system, respectively (Coll *et al.*, 2011; Zipfel, 2009).

1.1.2 Innate immune system

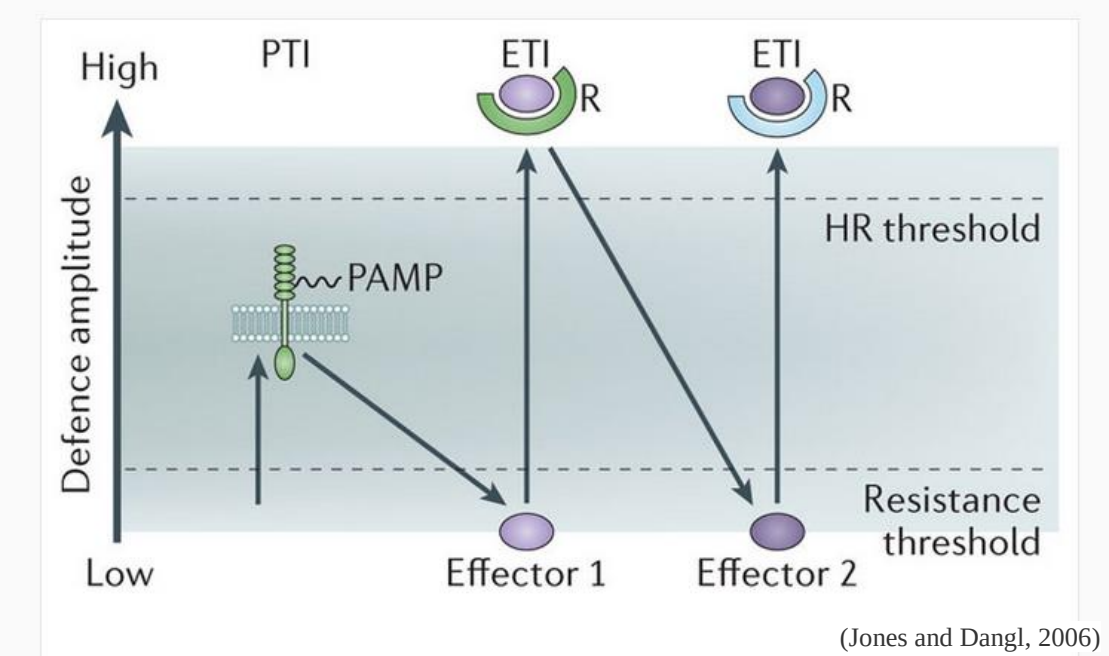

(Jones and Dangl, 2006)

Figure 1.1 The zigzag model illustrates the quantitative output in plant immunity system. ETI: effector-triggered immunity; HR: hypersensitive response; PAMPs: pathogen associated molecular patterns; PTI: PAMP-triggered immunity; R: R protein

Pathogen-host interactions are defined by a constant arms race in innate immune systems: pathogens find varying ways to compromise plant defence and proliferate inside the organism. Plants have developed corresponding ways to confront these threats for their own self-protection. There is a system based upon two main distinct levels of immunity to resist pathogen invasion (Coll *et al.*, 2011): the first level is provided by transmembrane proteins, called pattern recognition receptors (PRRs), which can recognise pathogen-associated molecular patterns (PAMPs) from invaders, and initiate a broad defence response against a whole group of pathogens. We termed this step as PAMP-triggered immunity (PTI). However, this basal defence could be recognised and conquered by some successful microbial pathogens which secrete molecules, so-called effectors, to suppress the PTI process (Tsuda and Katagiri, 2010). Therefore, plants respond to the further attack with a second level of immunity which has been evolved by recognition of such specialized effectors, resulting in so-called ETI, which is a more advanced and strain-specific immunity level (Boller and He, 2009; Coll *et al.*, 2011).

Jones and Dangl (2006) proposed the famous “zigzag model” of plant-pathogen interaction, which provides new insights into the study of innate immunity systems in

plants. Subsequently, Bent and Mackey (2007) further developed this model and provided more detailed annotations (Fig. 1.1). This model is regarded as the "central law" of plant pathology. It elaborates the evolution and competition between plants and pathogens in more detail during the process of interaction.

According to the model, plant-pathogen interaction can be divided into four phases. In phase I, PRRs recognise pathogenic PAMPs in microorganisms, activating PTI. The PAMPs are characteristic, highly conserved molecules of pathogenic microorganisms, which do not exist in host plant cells. Typical examples are flg22 (a peptide with 22 amino acids derived from the N-terminal region of flagellin), elf18 (the first 18 amino acids of the N-terminus of elongation factor Tu) and LPS (lipopolysaccharide), which are essential for the pathogenicity or survival of pathogenic microorganisms (Zipfel, 2008, 2009). The PTI can activate various initial defence responses rapidly, including the accumulation of callose for reinforcement of the cell wall (Brown *et al.*, 1998), regulation of ion channels, such as the Ca^{2+}-conducting channel (Jeworutzki *et al.*, 2010), activation of a mitogen-activated protein kinase (MAPK) cascade, which plays a pivotal role in mediating the production of reactive oxygen species (ROS), transcription of defence genes, phytoalexin accumulation and stomatal closure (Gomez-Gomez and Boller, 2000; He *et al.*, 2006; Nomura *et al.*, 2008; Nurnberger, 1999; Zipfel *et al.*, 2006).

In phase II, some successful pathogens start to deliver toxic effectors that could inhibit the PTI of the host, resulting in effector-triggered susceptibility (ETS). The *Pseudomonas syringae* strain DC3000, for instance, secreted the effector proteins AvrPto and AvrPtoB through a type III secretion system. These two molecules could interact directly with one type of PRR – FLS2 – in the host plant, thereby inhibiting either kinase activity or preventing the interaction of FLS2 complexes with other proteins (Qi *et al.*, 2011), which terminates the PTI defence process. In addition, some effectors not only quell plant defence responses, but also regulate the physiological process to accommodate fungal invaders and provide them with nutrients (Presti *et al.*, 2015).

In phase III, plants evolved R-specific genes which could directly or indirectly recognise pathogen-specific effectors and further mediate ETI. The latter could

accelerate and amplify the effect of PTI to improve the strength of plant disease resistance (Muthamilarasan and Prasad, 2013). This second line is to achieve a higher defence through new molecular receptors, such as the N-terminal coiled-coil domain, nucleotide-binding site, leucine-rich repeats (CC-NBS-LRRs), encoded by the R gene, that could recognise the effector released by the pathogen and induce defence response. There are generally several different classes of R-specific genes in plants and the major ones are the NBS-LRR genes, which contain a variable N-terminal structure, a nucleotide binding site (NBS) and an LRR (Qi *et al.*, 2011). The structure of NB-LRRs not only holds true for the proteins in plants, but is also very similar to the structure of the mammalian Nod-like receptors (NLRs). They can bind and recognise different types of effectors by using unique and specific R proteins directly or indirectly. Therefore, ETI is also well-known as the "gene-for-gene relationship" resistance (Jones and Dangl, 2006). In many cases, ETI accompanies hypersensitive response (HR). It is a plant-specific type of PCD, often followed by systemic acquired resistance (SAR) of the host (Heath, 2000).

In the final phase IV, pathogens produce new or more toxic effectors under natural selection to suppress ETI, causing plants to develop susceptibility. Many pathogens have even evolved new strategies to inhibit HR from playing its fundamental role in fighting infections (Greenberg and Yao, 2004). For further defence, plants, under natural selection pressure, will produce new R-specific genes to activate ETI to inhibit new or more toxic effects, in order to maintain their own survival and propagation (Bent and Mackey, 2007; Jones and Dangl, 2006). Thus, the arms race never stops and is a dynamic development.

1.1.3 Acquired immunity system

Not only at the local injury site, but also in distal tissues cells get prepared for confronting infection. The site of pathogen invasion into the plant will release the signal, which could spread to other uninfected parts of the host plant, and even other plant individuals. Subsequently the immune response in those distal parts or neighbouring plants is activated (Durrant and Dong, 2004). If a secondary infection occurs, the plant is already primed. This process is the so called systemic acquired resistance (SAR), which strengthens the resistance of the host against infecting pathogens and other subsequent pathogens for the next weeks or even months after the

1st infestation (Fu and Dong, 2013). Therefore SAR can also be called the plant immune "memory". In contrast to ETI leading to HR, SAR will lead to a better survival of cells (Fu and Dong, 2013).

Moreover, there is an extremely complex and interrelated signal transduction network system in plants to regulate SAR. Among them, Salicylic Acid (SA), Jasmonic Acid (JA) and Ethylene (Eth) are the most important signalling molecules (Luna *et al.*, 2012). Lastly as a key point during regulation of SAR, expression of pathogenesis related gene（PR gene) occurs and is regarded as a hallmark for activation of the system (Durrant and Dong, 2004).

As described in this section, plant immunity is complex. This complexity has to be understood in the context of different nutritional strategies of plant pathogens

1.2 Life styles of plant pathogens

According to the different nutrient strategies on host plant by various pathogens and also according to their lifestyles, phytopathogens are broadly divided into three categories (Fig. 1.2): necrotrophic, hemibiotrophic and biotrophic pathogens (Freeman and Beattie, 2008). Necrotrophs derive nutrition from killed cells. So they need to invade and kill plant tissue rapidly and then live saprophytically on the dead remains, such as grey mold fungus, *Botrytis cinerea* (Dodds and Rathjen, 2010). Hemibiotrophs obtain nutrition available from either living cells, or from the necrotic host. They often require a living host initially, but kill at later stage of infection, for instance, the bacterium *Pseudomonas syringae* and the fungus *Magnaporthe grisea* (Dodds and Rathjen, 2010).

The third type, biotrophs are able to establish a long-term feeding relationship with living cells of their hosts for deriving energy and nutrition, rather than killing the host cells as part of the infection process. By their feeding activities, they create a nutrient sink to the infection site, so that the host is affected negatively but is not killed. This type of pathogen, such as *Golovinomyces cichoracearum* or *Plasmopara viticola*, can

result in serious economic losses of crop plants, and it can reduce the competitive abilities of the host in natural environments (Hammond-Kossack and Jones, 2000).

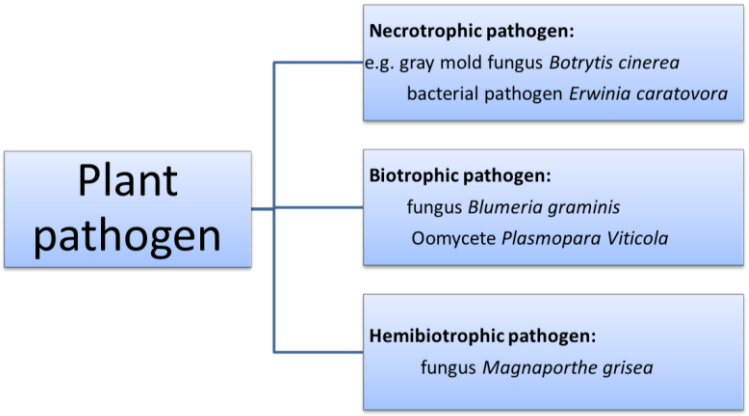

Figure 1.2 Three categories of Phytopathogens devided by different nutrient absorbing ways absorbing ways (Freeman and Beattie, 2008)

The cellular defence strategy against a pathogen depends on its nutritional strategy (Freeman and Beattie, 2008). While warding off a necrotrophic pathogen will require cellular adaptation, this strategy does not work in case of a biotrophic pathogen. Here, a seemingly paradox strategy is more efficient: kill yourself to kill your enemy. The death of the individual cell will bring life to the entire organism. This type of adaptive cell death, so called programmed cell death (PCD), is known in many organisms, but it is important to consider the commonalities and specific differences to get a deeper understanding of plant immunity.

1.3 Programmed cell death (plants versus animals)

1.3.1 Definition and functions of PCD

PCD, as an academic term, firstly used and reported in 1964, functions related to enhance inter-segmental muscles in insect tissue development (Lockshin and Williams, 1964). Since then, PCD became a more general concept and has been reported to play crucial roles in the development of multicellular organisms, organogenesis, and carcinogenesis (Jacobson *et al.*, 1997; Ouyang *et al.*, 2012).

Compared with several other terms, like apoptosis, necrosis and autophagy which are mainly related to morphological descriptions of events, PCD possesses a more general and broader sense in animals. The definition of PCD nowadays can be described as follows: a genetically programmed and highly ordered cell suicide process that removes unwanted or damaged cells in a certain physiological or pathological condition, in order to maintain the stability of the internal environment and better adapt to the living environment.

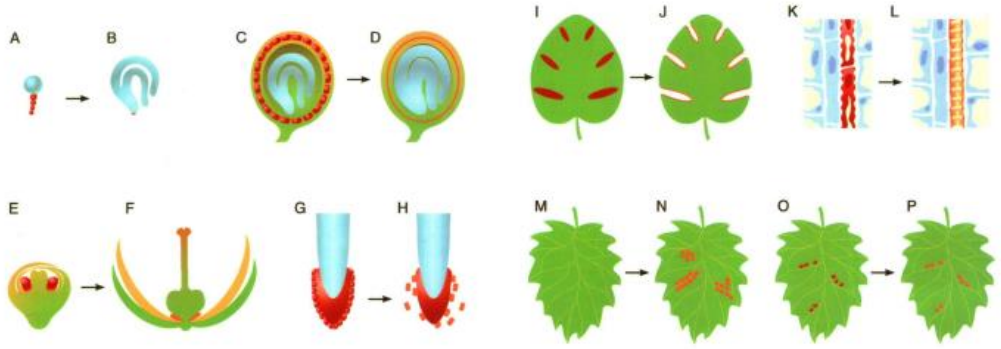

(Pennell et al, 1997)

Figure 1.3 Functions of PCD in Plants.

(A) to (D) Deletion of cells with temporary functions. These include deletion of suspensor cells in embryos ([A] and [B]) and of aleurone cells in seeds ([C] and [D]). (E) to (H) Deletion of unwanted cells. These include stamen primordia cells in unisexual flowers ([E] and [F]) and root cap cells ([G] and [H]). (I) and (J), deletion of cells during sculpting of the plant body. (K) and (L), deletion of cells during cell specialization in TEs. (M) to (P), deletion of cells during plant interactions with pathogens. These include cells in an HR ([M] and [N]) and cells in uninfected leaves in response to HR-derived signals ([O] and [P]). The red regions represent cells that have been targeted for PCD, and the orange regions represent cells that have died by PCD.

Compare with animals, the study of plant PCD started much later and less advanced (Pennell and Lamb, 1997). However, with the deepening of knowledge, it can be stated that PCD occurs universally in processes of plant growth and development, such as the formation of embryos and vascular bundles catheters, as well as plant regeneration, seed development and leaf aging (Fig. 1.3) (Gadjev *et al.*, 2008; Gunawardena, 2008). This type of PCD could be also called developmental cell death (DCD), where cell death plays specific functions itself during a terminal stage or by contrast, cells die after having accomplished their role. Moreover, PCD is also

essential in the response of plants to external environmental stimuli, e.g., non-biological stress or resistance to pathogen infection (Fig. 1.3) (Lam, 2004; Pennell and Lamb, 1997).

1.3.2 Similarities and differences of PCD between animals and plants

On cell morphology level, morphological changes of plant PCD have been investigated and they share some similarities with animal apoptosis in the early stage. They all begin with cytoplasm shrinkage and chromatin condensation. Then the fragmentation of the nucleus occurs in dying cells (Danon *et al.*, 2000). It is regarded as a very specific hallmark of PCD. The genomic DNA degrades randomly and in some cases results in a DNA ladder which could be detected when the DNA is separated on agarose gel. Alternatively, DNA fragmentation can be also detected using an in situ method called terminal deoxynucleotidyltransferase-mediated dUTP nick end labelling reaction (TUNEL), which detects free 3'-OH DNA breaks in both animals and plants (Gorczyca *et al.*, 1994).

At the very end of animal apoptosis, the fragmentation of the entire cell occurs, apoptotic bodies are formed subsequently (nucleus fragments and plasma membrane fragments surrounded by cell material), which are then phagocytized by adjacent cells. Plant cells are surrounded by cell walls and no phagocytosis exists. Therefore during end of PCD, no apoptotic body is formed and cells must degrade the substance by themselves (van Doorn and Woltering, 2005). Instead a plant pathway might involve autophagy in the process of PCD under developmental or abiotic stress (Iakimova *et al.*, 2005), whereas non-lysosomal systems might be involved in the process of HR under biotrophic pathogen infection (Greenberg and Yao, 2004). So, since some of the terminal hallmarks of animal apoptosis are absent, the term "apoptotic-like phenomenon" or a more general concept of PCD in plants should be used instead of apoptosis.

On the molecular level, the apoptotic pathway of animal cells is mediated by a class of highly conserved aspartic acid-specific cysteine protease, called caspases (Cohen, 1997). Caspases are also known as death proteases. Caspase-like activity can also be detected in plants in certain context, such as after pathogen infection, chemical

treatment, NO treatment and heat shock treatment(Clarke *et al.*, 2000; De Jong *et al.*, 2000; del Pozo and Lam, 1998; Tian *et al.*, 2000). Meanwhile, the commonly used inhibitors of caspase can also such plant caspase-like activities. However, no orthologous caspases have been identified in plants.

1.3.3 An essential type of PCD in plant defence: Hypersensitive response (HR)

As described above, necrotrophic pathogens infect and kill host tissue and extract nutrients from the dead host cells, while most (hemi)biotrophic and entire biotrophic pathogens colonize living plant tissue and obtain nutrients sustainably (Coll *et al.*, 2011b). Therefore, in many cases, the ETI in the host plant culminates in the hypersensitive response (HR), which is a plant-specific form of programmed cell death (PCD) providing an efficient strategy to block pathogens (Heath, 2000). Based on a long coevolution history of host plant and pathogens, HR always associates with a high degree of plant resistance (Pontier *et al.*, 1998). Since HR is a rapid and localized plant cell death induced by rust fungi, it becomes visible as necrotic spots at the site of infection or it develops to visible brown lesions, in case a sufficient number of cells died (Heath, 2000). The infected plant benefits from sacrificing infested cells as most other cells will remain unaffected and can form a healthy tissue.

1.4 HR regulating gene families in plants

As described above, caspases in animal cells, as one kind of aspartic acid-specific cysteine protease, ultimately induce PCD and control the process (Cohen, 1997; Kitanaka and Kuchino, 1999). Caspases are usually synthesized *de novo* in inactive forms, termed procaspases, in the cytoplasm and are activated via self-proteolysis. The activated caspases further activate other downstream caspases or related protein substrates by hydrolysing their C terminal aspartic acid residue (P1 position). Caspase activation leads to cell structure and metabolic changes and mediates the occurrence of PCD (Earnshaw *et al.*, 1999).

However, how is HR or even broader process of PCD regulated in plants? Compared to animals during PCD, higher plants do not own any proteins orthologous to caspases.

Interestingly, caspase-like enzymatic activity has been found and it is essential in many forms of plant PCD (del Pozo and Lam, 1998; Woltering *et al.*, 2002). Moreover, HR-like phenotypes as one kind of PCD, has also been described in many plant species, including corn, tomato, barley, *Arabidopsis* and grapevine (Bellin *et al.*, 2009; Greenberg and Ausubel, 1993; Hoisington. *et al.*, 1982; Langford, 1948; Wolter *et al.*, 1993). Finally, with identification work expanding, a type of cysteine-dependent proteases with "caspase-like" activity has finally emerged as the best candidates to replace caspases in plants (Piszczek and Gutman, 2007). As of now, the identified cysteine-dependent proteases participating in PCD in plants can be further classified into 2 protein families: proteases from the legumain family—VPEs (vacuolar processing enzymes) and the metacaspase family (Piszczek and Gutman, 2007).

1.4.1 Vacuolar processing enzymes (VPEs)

In 1987, an enzyme responsible for maturation of various storage proteins in the protein-storage vacuoles was characterized from maturing pumpkin seeds (Hara-Nishimura and Nishimura, 1987), then the enzyme was purified from maturing seeds of castor bean (*Ricinus communis*) and was designated vacuolar processing enzyme (VPE) (Hara Nishimura, et al.,1991). VPEs are the legumain family proteases that belong to clan CD of the C13 family (Hara-Nishimura *et al.*, 1993). VPEs were originally identified as a protease responsible for maturation of various seed proteins in protein-storage vacuoles and play an important role in seed maturating process (Hara-Nishimura, et al. 1991). But since 2004, numerous researches indicate another key role for VPEs that these enzymes participate in plant cell death induced by various stress conditions, playing a similar function as caspases in animals (Piszczek and Gutman, 2007).

Four members have been identified in *Arabidopsis* VPE family at present, including αVPE, βVPE, γVPE and δVPE (Gruis *et al.*, 2002; Kinoshita *et al.*, 1995). They are divided into two subfamilies by their homology and expression pattern analysis, including vegetative type: αVPE and γVPE, and seed type: βVPE and δVPE, respectively (Yamada *et al.*, 2005). Both αVPE and γVPE participate in the

maturation of proteins in typical lytic vacuoles for vegetative organs and in the PCD process induced by environmental stress and organ senescence (Hatsugai *et al.*, 2004; Kinoshita *et al.*, 1999). On the other hand, βVPE has been reported as one of the most essential enzymes to process seed storage proteins. But δVPE was detected to express in the inner integument layer, where PCD occurs during the formation of seed coat. Furthermore, Recently three novel grapevine *VPE* gene members were also identified, named as *VvβVPE*, *VvγVPE*, and *VvδVPE*, respectively (Tang *et al.*, 2016). Interestingly, *VvβVPE* as a homologus gene with βVPE in *Arabidopsis* was reported to have functions related to PCD process during ovule abortion in seedless grapes (Tang *et al.*, 2016).

1.4.2 Metacaspase

A family of cysteine-dependent proteases with "caspase-like" activity, termed *metacaspases*, was found in plants, fungi and protozoa (Uren *et al.*, 2000). Metacaspase structures are similar to caspases but the two enzyme types are distantly phylogenetically related and differ in their substrate specificity. The predicted secondary structure of metacaspases contains conserved domains and motifs in all members of the caspase/metacaspase/paracaspase superfamily (Vercammen *et al.*, 2007). For example, the catalytic dyad of cysteine and histidine is in the α/β fold, which is characteristic of the caspase-hemoglobinase fold (CHF)-containing proteins (Aravind and Koonin, 2002). Phylogenetic analysis of eukaryotic caspases, metacaspases, and paracaspases suggested that these groups are about equally distant from each other (Vercammen *et al.*, 2004). In recent years, research on the biochemical characteristics and biological functions of metacaspase enzymes has become a hot topic, especially the question of whether metacaspases have caspase-like enzymatic activities (Carmona-Gutierrez *et al.*, 2010; Enoksson and Salvesen, 2010). The reason is that metacaspases lack the substrate specificity to recognize and cleave the amino acid after aspartic acid and have a different cleavage specificity than caspases; metacaspases hydrolyze proteins after arginine or lysine(Carmona-Gutierrez *et al.*, 2010; Enoksson and Salvesen, 2010; Vercammen *et al.*, 2007). The substrates of most metacaspases also have not yet been identified. The recent identification of Tudor staphylococcal nuclease (TSN) as a common substrate for both the Norway spruce metacaspase mcII-Pa and the human caspase-3 suggests

that metacaspases can execute PCD like caspases, but this phenomenon has not been identified in other plants (Sundström *et al.*, 2009).

Plant metacaspases can be divided into two subclasses on the basis of similarities in amino acid sequence and general domain structure: Type I and Type II (Lam, 2004). Both kinds of metacaspases have putative small (p10) and large (p20) subunits, which contain the catalytic amino acid dyad histidine/cysteine. The catalytic histidine lies in the H(Y/F) SGHG sequence and the catalytic cysteine in the active-site pentapeptide DXCHS (where X is A or S) sequence (Piszczek and Gutman, 2007; Suarez *et al.*, 2004). Type I plant pro-metacaspases contain a proline-rich or glutamine-rich N-terminal prodomain of about 80–120 amino acids. This prodomain contains zinc finger motifs, similar to the *Arabidopsis* regulatory protein LSD1 (LESIONS SIMULATING DISEASE 1) expressed during the hypersensitive response in plants (Coll *et al.*, 2010; Watanabe and Lam, 2004). Type II metacaspases only exist in plants and lack the prodomain but harbor a linker region of about 90-150 aa between the putative large (p20) and small (p10) subunits (Rahman and Mahmudur, 2010), whereas the linker region of Type I metacaspases has only about 30aa. These metacaspases also have a relatively high degree of amino acid sequence identity, from 56 to 71% (Watanabe and Lam, 2005). The number of metacaspase genes varies in the genomes of different organisms and many metacaspase genes have been cloned and analyzed in different organisms, such as *Arabidopsis thaliana*, tobacco, tomato and Norway spruce.

Metacaspases initiate PCD during embryo patterning and provide a functional connection between PCD and embryogenesis in plants. RNA interference suppression of *McII-Pa*, a Type II metacaspase in Norway spruce (*Picea abies*), led to failure of establishment of the embryo, embryonic mass and terminal differentiation of the embryo suspensor, which suggested that metacaspase-dependent programmed cell death is essential for plant embryogenesis (Suarez *et al.*, 2004). UVC, H_2O_2 or methyl viologen (herbicide) can induce PCD under oxidative stress via up-regulating the gene expression level of metacaspase8 (*AtMC8*) (He *et al.*, 2008). In addition, the involvement of metacaspases in cell death has been also reported in response to ROS and age-mediated senescence (Ahmad *et al.*, 2012; Watanabe and Lam, 2011a).

There is more evidence indicating that metacaspases also play a very essential role to regulate HR in plant biotic stress process. In tobacco, *NbMCA1* may have a direct role in host defence by affecting a virulence factor of *Colletotrichum destructivum* during infection (Hao *et al.*, 2007). In *Arabidopsis thaliana*, there is a pair of Type I metacaspases, *AtMC1* and *AtMC2*, antagonistically controlling hypersensitive cell death response induced by either the obligate biotrophic oomycete *Hyaloperonospora arabidopsidis* (Hpa; isolate Emwa1), or the hemibiotrophic bacterium *Pseudomonas syringae* pv. tomato [Pto; strain DC3000 (avrRpm1)] (Coll *et al.*, 2010). Besides, *AtMC4* (*AtMCP2d*) plays as a positive regulatory role in mycotoxin fumonisin B1-induced PCD (Watanabe and Lam, 2011a) and exhibits a strict Ca^{2+} dependency for its catalytic activation that is apparently mediated by intramolecular self-cleavage mechanism (Watanabe and Lam, 2011b).

1.5 (Rpv3-dependent resistance to *Plasmopara viticola*): Case study between HR and resistance in grapevine

Grapevine (*Vitis vinifera* L.) as one of the most important economical fruit species, used in the global industry to produce wine, juice, table grapes, and dried fruit, etc. Among various biotic stresses, downy mildew (DM) has become one of the most important diseases in viticulture, seriously affecting the yield and fruit quality. It is caused by a classical biotrophic pathogen, one kind of oomycete called *Plasmopara viticola* (This *et al.*, 2006). Almost all European *V. vinifera* L. grapevine cultivars are susceptible to DM, due to the lack of co-evolutionary history. In contrast, North American grapes such as *V. rupestris*, *V. riparia*, *V. cinerea*, sharing the same origin with *P. viticola*, possess a higher resistance which is associated with ETI and also accompanied by an HR process (Munson, 1909). In fact, due to genetic diversity and geographical linkage of host and pathogen, the resistance ability against DM infection has evolved according to the zigzag model (Schroder *et al.*, 2011). Therefore downy mildew (DM) resistance is regarded as a quantitative trait exhibiting variable levels of resistance in North American grapes (Welter *et al.*, 2007). For searching this genetic factor, molecular markers for establishing genetic maps could be used to localize specific QTL (quantitative trait loci) which is responsible for HR at the infection sites.

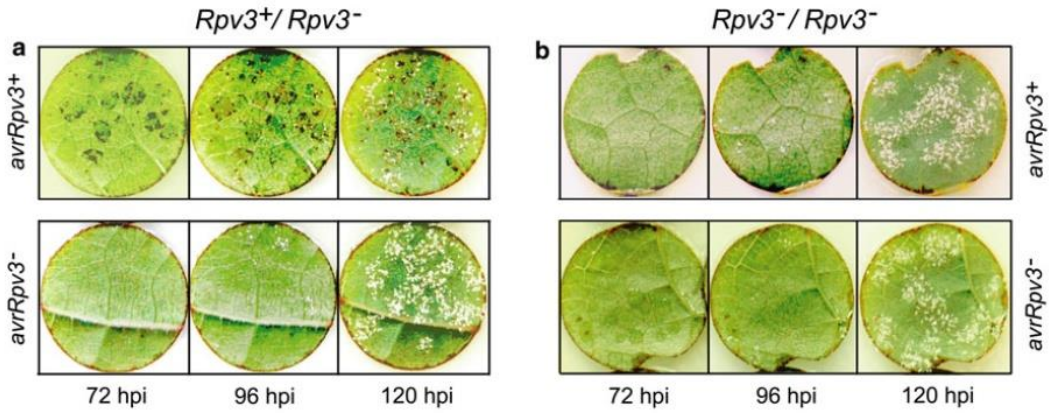

(Casagrande et al., 2011)

Figure 1.4 Outcome of the host–pathogen interaction, depending on host and pathogen genotypes. a, Leaf discs of the Rpv3^{+}/Rpv3^{-}hostinoculated with avrRpv3^{+}or avrRpv3^{-}isolates of P. viticola: HR triggered by the avrRpv3^{+}isolate (above); absence of plant response and abundant sporulation upon infection with the avrRpv3^{-}isolate (below). b, Leaf discs of the Rpv3^{-}/Rpv3^{-}host inoculated with isolates of *P. viticola.*

As expected, a major QTL locus, named Rpv3, was first identified by interval mapping in 'Regent', a resistant variety, where it explained up to 56% of the phenotypic variance effects on downy mildew resistance (Fischer *et al.*, 2004; Welter *et al.*, 2007). Further research on 'Bianca', retaining resistance originally present in its North American ancestors, has located Rpv3 locus on the lower arm of chromosome 18. Rpv3 contains a cluster of disease resistance genes, such as R genes encoding TIR-NB-LRR and LRR-kinase receptor-like proteins (Casagrande *et al.*, 2011). Using artificial inoculation, researchers further confirmed that haplotype type of grapes Rpv3^{+}/Rpv3^{-} could cause a reduction of avrRpv3^{+} pathogen development and be associated with HR in the proximity of infected sites within 3-5 days post inoculation (Fig 1.4) (Bellin *et al.*, 2009; Casagrande *et al.*, 2011). To sum up, the Rpv3 locus is a major determinant of DM resistance derived from North America and associated with the ability of mounting a localized hypersensitive response (HR).

1.6 Scope of the study

Overall, in both plants and animals, programmed cell death (PCD) is an indispensable process that removes redundant cells in the course of development, damage or

infection. Especially during plant-pathogen interaction, programmed cell death (PCD) is an indispensable and ultimate mean to block the spread of pathogens in the plant defence (so called hypersensitive response, HR). Metacaspases, one type of cysteine-dependent protease, was reported to play an essential role in plant PCD processes. However, its interplay with other HR factors and specificity is far from being understood. In our previous work, we have identified the whole metacaspase gene family in grapevine (containing 6 members), and reported *VvMC1*, *VvMC3*, and *VvMC4* play an essential role in PCD process during ovule abortion of seedless grapes (Zhang *et al.*, 2013). This leads to the central question of our current study: whether there are metacaspases members which specifically participate in the HR process during plant defence? To approach these open points in this study, we use *P.viticola* induced HR as experimental model and put forward three questions to work on the *Vitis* metacaspase families:

1.6.1 What is the expression pattern of each metacaspase member during HR process in grapevine?

The first step of our study was the establishment of an effective and stable HR induced system. We have investigated a panel of 9 grape genotypes (genotype $Rpv3^{+}$ or $Rpv3^{-}$) to show possible differences with the incidence of HR necrotic lesions after infection with *P. viticola* strain 1191-B15 containg $avrRpv3^{+}$. Afterwards one $Rpv3^{-}$ susceptible and another $Rpv3^{+}$ resistant cultivar were selected. Expression patterns of metacaspase genes were measured including 8 time points after inoculation on both cultivars, to investigate temporal and spatial patterns of *Vitis* metacaspase members. Based on this transcript analysis, *VrMC2* and *VrMC5* were chosen as candidates that showed up-regulation only in *V. rupestris* after 1191-B15 infection but before appearance of necrosis, for further analysis.

In parallel, gene expression pattern has also been examined in grape suspension cell cultures, using harpin (activating cell-death related defence) as elicitor to treat two cell lines: *V. rupestris* as resistant line, and 'Pinot Noir' as susceptible line. Similar results showed that only *VrMC2* and *VrMC5* in *V. rupestris* were up-regulated after 24h with 18 μg/ml harpin treatment.

1.6.2 What is the cellular location and cellular function of *VrMC2* and *VrMC5* in ETI-induced cell death process?

To further get insight into the biological function of *VrMC2* and *VrMC5*, we have cloned and overexpressed separate full-length ORFs fused with GFP into tobacco BY-2 suspension cells. Since metacaspases shows uncommon subcellular localization patterns in different types or plant species, the subcellular localization of *VrMC2* and *VrMC5* was firstly well-addressed via different co-visualization strategies using spinning-disc confocal microscopy. In the next step, we further asked whether *VrMC2* or *VrMC5* possess cell death executing function during plant ETI stage. In the same stable overexpression lines, cell mortality has been tested to reveal the function of *VrMC2* or *VrMC5* and HR related signalling, after induction of different defence related cell death elicitors using Evans Blue staining.

1.6.3 Could promoters of metacaspase affect their own gene expression?

Based on the results that both *VrMC2* and *VrMC5* are HR inducible genes, it led us to further excavate the regulation mechanism behind gene expression. Since HR is always associated with the ETI immunity level, we asked whether promoters of *VrMC2* or *VrMC5* mediate their own gene expression as HR-inducible promoter. To get insight this question, promoters of *MC2* and *MC5* were first isolated from both cultivars *V. rupestris* and cv. 'Müller-Thurgau'. Then cis-element analysis has been done and the different distribution of pathogen- or defence-response motives was compared between *pVrMC2*, *pVrMC5*, *pVvMC2*, and *pVvMC5*. Furthermore, using transient dual promoter–reporter assays in grape suspension cells, we revealed both *pVrMC2* and *pVrMC5* were activated in response to harpin treatment, whereas no induction occurred in 'Müller-Thurgau' promoters.

2. MATERIALS AND METHODS

2.1 Plant material

2.1.1 Leaf discs material

Nine grapevine genotypes differing regarding the presence of the locus *Resistance to Plasmopara viticola 3* (*Rpv3*) were used in this study. The *Rpv3* positive genotypes include wild North American grapevines *V. rupestris* (voucher KIT 5888) and *V. riparia* (voucher KIT 6548), which are the presumed natural sources of *Rpv3*; the rootstock genotype 'Börner' (voucher KIT 5890), derived from a cross between *V. riparia* and *V. cinerea*; and the resistant *vinifera* variety 'Regent' (voucher KIT 5895), derived from a complex pedigree comprising different crosses and back-crosses of various North American grapes with *vinifera* varieties (Fischer *et al.*, 2004). By contrast, the European *vinifera* varieties 'Müller-Thurgau' (voucher KIT 5585), 'Pinot Blanc' (voucher KIT 7473) and 'Augster Weiss' (voucher KIT 7443), and the European Wild Grape genotypes *V. sylvestris* 'Hö29' (voucher KIT 6188) and *V. sylvestris* 'K83' (voucher KIT 6235) were *Rpv3*-negative. All genotypes are cultivated as living vouchers in the collection of the Botanical Garden of the Karlsruhe Institute of Technology, Germany, and have been verified by microsatellite markers (Nick, 2014) and ampelographic descriptors of the *Organisation Internationale de la Vigne et du Vin* (Olmo, 1976). Leaf discs of 1.5 cm in diameter were collected from the fourth to the seventh leaves from the top of each shoot by means of a cork borer and used further for infection with *P. viticola*. The leaf discs were then cultivated under conditions of 22/18 ℃ (day/night) temperature and a 14/10 h (light/dark) photoperiod in a phytochamber (CLF plantclimatics, Model: E-36L). Prior to shock freezing in liquid nitrogen for RNA extraction, a smaller (1.3 cm diameter) central disc was excised from the infected leaf disc. This 'disc-in-the-disc' harvest was employed to avoid the pathogen response of gene expression being overlaid by wounding responses in the peripheral 2 mm of the disc. The frozen samples were stored at -80 ℃ till RNA extraction, which was conducted a few days later. Leaf discs were taken directly from the phytochamber at specific time points for microscope observation.

2.1.2 Cell culture

Cell suspension cultures of *Vitis rupestris* (as resistant line) and *Vitis vinifera* cv. 'Pinot Noir' (as a susceptible line, also as receptor cells for transient expression) were investigated for subsequent experiments. They were established from the callus tissue of young, non-woody internodes (pith parenchymatic cells), as described previously (Seibicke, 2002). The cells were subcultivated every seven days by inoculation of 6 or 8 ml of stationary cells into 30 ml of fresh, autoclaved liquid medium with 4.3 $g \cdot L^{-1}$ MS (Murashige and Skoog) salts (Duchefa, http://www.duchefa.com), 30 $g \cdot L^{-1}$ sucrose, 200 $mg \cdot L^{-1}$ KH_2PO_4, 100 $mg \cdot L^{-1}$ inositol, 1 $mg \cdot L^{-1}$ thiamine, and 0.2 $mg \cdot L^{-1}$ (0.9 μM) 2, 4-dichlorophenoxyacetic acid (2, 4-D), at pH 5.8. All the cells were cultivated at 26 ℃ in 100-ml Erlenmeyer flasks on an orbital shaker (KS260 basic, IKA Labortechnik, http://www.ika.de) at 150 rpm. The tobacco BY2 cell strain *Nicotiana tabacum* L. cv Bright Yellow 2 was used to obtain transgenic suspension cells and the latter were subcultivated in the same medium as mentioned above (Nagata *et al.*, 1992), but supplemented with 45 $mg \cdot L^{-1}$ Hygromycin or 25 $mg \cdot L^{-1}$ kanamycin (details in Appendix 5.1).

2.2 Pathogen material

Single sporangia strains of *Plasmopara viticola* were used rather than field isolates to ensure the high reproducibility of results. The strains 1191-B15, 1135-F2 and 1137-C20 were kindly provided by the group of Prof. Dr. Otmar Spring, Botanical Institute of Hohenheim University, and have been described in Gomez-Zeledon *et al.* (2013). If not stated otherwise, the experiments were run with 1191-B15, a strain that cannot overcome *Rpv3*-mediated resistance and induces HR on *Rpv3*-positive hosts. Additionally, this strain can infect European genotypes intensively. The fourth to the seventh leaf of cv. 'Müller-Thurgau' shoots were detached for propagation and thoroughly rinsed at both sides with distilled water (Fig 2.1). Mature sporangia of strain 1191-B15 were collected from well-infected leaves as inoculum. In some cases, dried sporangia stored at -80 ℃ were used. Freshly excised leaves were placed with their abaxial side down on the surface of the sporangial suspension and kept in a phytochamber (CLF plantclimatics, Model: E-36L) with a high humidity at 21 ℃ in darkness for 24 h. Afterwards, the leaves were turned, placing on wet filter paper with

their abaxial side up and further incubated under a photoperiod of 14 h light (25 μmol·m-2 s^{-1}) with full spectrum lamps and 10 h darkness (0 μmol·m-2 s^{-1}) at 21 ℃ till sporulation.

Figure 2.1 *Vitis vinifera* cv. 'Müller-Thurgau' leaf well-infected with *P.viticola* (Photographed by Peijie Gong, May 2014).

2.3 Leaf discs HR-related bioassay

Infected 'Müller-Thurgau' leaves were cut into small pieces and immersed in 5 ml distilled water in a Schott flask to release zoospores from sporangia. After shaking gently, the leaf pieces were removed. The suspension of sporangia was then prepared and the concentration was adjusted to approximately 40,000 sporangia· ml^{-1}. A hemacytometer (Fuchs-Rosenthal, Thoma, Freiburg) was used to ensure the concentration amount and optimal inoculation effect (Kiefer *et al.*, 2002). The solution was then incubated at 16 ℃ in a climate chamber in the dark for 1.5 – 2 h to let the zoospores emerge and release. An amount of 30 ul droplets of sporangial suspension was added onto the centre of abaxial surface on each disc for infection treatment. All infected discs were placed in Petri dishes on wet filter paper and incubated under a 16 h light and 8 h darkness photoperiod.

2.3.1 Leaf discs phenotype observation after *Plasmopara viticola* 1191-B15 infection

Five leaf discs were prepared for each genotype at each sampling time point to observe each genotype of grapevine during B15 infection. Nine dpi of *P. viticola* were

picked and HR was observed at four times point (0, 3 , 6 and 9 days) and documented by photographing using an Olympus C-5060 camera. After two representative genotypes were screened, more detailed time points, 0, 12, 24, 48, 72, 96, 120 and 144 h after infection were set and the HR phenomenon was further observed by microscope (Leica, DM750, Switzerland) and photographed by a co-equipped camera (DFC400, Leica, Switzerland). Pictures were taken at 10x magnification and were recorded using the software Leica Application Suite V3.3.1. Two biological replicates were performed in the same reason of successive two years.

2.3.2 Quantification the degree of infection on infected leaf discs

The number of necrotic spots (only on *V. rupestris*) and sporangium spores (both cv. 'Müller-Thurgau' and *V. rupestris*) on infected leaf discs were separately documented to quantify the degree of infection. In the case of recording necrotic spots, infected drops were removed with sterile filter paper before each testing. All necrotic spots in the infection area were recorded and then counted and evaluated (see details in Appendix 5.7). Eight time points were set: from 0, 1, 2, 3 and 4 dpi in the early stage; to 6, 8 and 10 dpi in the later stage. According to the level of sporulation, infected drops were re-suspended up to 1 ml with distilled water and were then used to assess the spore concentration using a hemacytometer. Disease progress was monitored from 3, 4, 6, 8 to 10 dpi. All values were obtained using a Leica microscope and photographing system, as described above. Two biological replicates were performed for sporulation. Data were subsequently statistically analysed using Microsoft Excel.

2.3.3 Cell death detection by Evans blue staining

Evans blue staining was used to detect cell death; the principle of the method was described by Gaff and Okong'O-Ogola (1971). The detailed procedures are described as follows: a. infected leaf discs were first rinsed in distilled water and then placed in a 12-well plate; b. Let the entire leaf discs soak in a staining solution of 2.5 % (w/v) Evans blue (water as solvent); and c. the leaf discs were washed three more times and mounted in distilled water for examination via photographing using an Olympus C-5060 camera.

2.4 RNA extraction and cDNA synthesis

The leaves of *V. rupestris*, *V. vinifera* cv. 'Müller-Thurgau' were harvested, quick froze and stored at -80 ℃ at 0 hour, 12 hours, 24 hours, 48 hours, 72 hours, 96 hours, 120 hours and 144 hours after 1191-B15 infection as well as for distilled water-treated controls. The frozen leaf material was homogenized to a powder (Tissuelyser, Qiagen, frequency 22 Hz, duration 30 seconds). Then total RNA was extracted using the Spectrum™ Plant Total RNA Kit (Sigma, Deisenhofen) according to the instruction of the manufacturer. The extracted RNA was purified with the RNase-Free DNase Set (Qiagen, Hilden, Germany) to remove any potential contamination from genomic DNA. First-strand cDNA synthesis was performed by using M-MuLV cDNA Synthesis Kit (New England Biolabs; Frankfurt am Main, Germany) , using 1 µg of purified RNA as template for reverse transcription. All RNA related operations were performed on ice, and an RNase inhibitor (NEB, New England Biolab Company) was used as well, to protect the RNA from degradation.

For cell culture from *Vitis rupestris*, *Vitis vinifera* cv. Pinot Noir' and BY-2 tobacco cells, dry cell samples were harvested after different treatments (including solvent control) at 0h, 1h, 6h and 24h using a Büchner funnel via short-time vacuum (10s), and shock-frozen immediately in liquid nitrogen. After homogenizing, total RNA was extracted using Universal RNA Purification Kit (ROBOKLON, Berlin, Germany). The rest procedures as same as described in leaves above.

2.5 Semi-quantitative RT-PCR

Semi-quantitative RT–PCR was performed with ThermoPol buffer, dNTP and *Taq* polymerase (New England Biolabs) with 3 min of pre-denaturation at 94 ℃, followed by 32 cycles of 30 s denaturation at 94 ℃, 30 s annealing at 60 ℃, and 40 s extension at 68 ℃, conducted in a standard PCR-Thermocycler (Analytikjena, Jena, Germany) as described previously (Chang *et al.*, 2011; Chang and Nick, 2012; Duan *et al.*, 2015). The accession numbers and the primer sequences are given in Appendix 5.2 and were derived from the grapevine reference genome (*V. vinifera* cv. 'Pinot Noir'). Actin

(accession number: AF369524) was used as reference gene and the amplicons were separated and evaluated by electrophoresis on 2% agarose as described previously (Ismail *et al.*, 2012). The shown images are representative from three independent experimental series.

2.6 Quantitative Real-Time PCR

Quantitative real-time RT-PCR was carried out from both leaf and cell culture material on an CFX96 Touch™ Real-Time PCR Detection System (Bio-Rad, USA) for the two promising gene candidates cloned as described below: *VrMC2* (accession number KY069974) and *VrMC5* (cloned as described below, accession number KY069975) against actin (accession number AF369524) as reference gene using final concentrations of 200 nM for each primer, 200 nM for each dNTP, 1 x GoTaq colorless buffer supplemented with 2.5 mM $MgCl_2$, 0.5 U GoTaq polymerase (Promega, Mannheim, Germany), 1 x SYBR green I (Invitrogen, Darmstadt, Germany), and 1 µL of the cDNA template in a 1:10 dilution (50ng/ul). This protocol was adapted from (Svyatyna *et al.*, 2014). Amplicons for the two metacaspase genes and actin were generated by denaturation at 95 ℃ for 3 min, followed by 40 cycles of denaturation at two steps: 95 ℃ for 15 s, annealing at 61 ℃ for 40 s. To compare the mRNA expression levels between different samples, the C_t values from each sample were normalized to the value for the *actin* internal standard obtained from the same sample. For each triplicate, these normalized C_t values were averaged. Then the difference between the C_t values of the target gene X and those for the actin reference R were calculated as follows: The expression value on 0h of each genotype was set as control (ddH_2O control and infected samples shared). Then relative expression value was calculated: $\Delta\Delta Ct(X) = Avg.\Delta Ct(X) - Avg.\Delta Ct$ (control) (Livak and Schmittgen, 2001). The final result was expressed as $2^{-\Delta\Delta Ct}$ (X). The shown image was a representative from three independent experimental series.

2.7 Cloning the coding sequences of *VrMC2* and *VrMC5*

The entire open reading frames (ORF) of *VrMC2* (1351 bp) and *VrMC5* (1245 bp) were amplified from cDNA using Phusion High-Fidelity DNA polymerase (NEB,

Frankfurt, Germany) and the oligonucleotide primers given in Appendix 5.3 derived from the grapevine reference genome (*V. vinifera* cv. 'Pinot Noir') via PCR by 36 cycles of 98 ℃ for 10 s, annealing at 58 ℃ for 30 s, and synthesis at 72 ℃ for 90 s. PCR products were ligated with the pGEM®-T Easy Vector (Promega, Madison, PWl) and then transformed into Escherichia coli DH5α for DNA sequencing (GATC Biotech, Cologne, Germany). After verifying the sequence from several independent amplicons, the predicted protein sequences for *VrMC2* (accession number KY069974) and *VrMC5* (accession number KY069975) were submitted to Genebank. Afterwards, a phylogenetic tree was constructed with other 42 well-identified metacaspases in plant species and 2 putative metacaspases from *Chlamydomonas* algae as out-group using the neighbour-joining algorithm via the MEGA 5.0 software (www. megasoftware.net). Detail information of ORF sequence submission from this study can be found in Appendix 5.4. For gene structure analysis, Intron and exon organization of metacaspases was analysed by using FGENESH-C (http://linux1.softberry.com/berry.phtml?topic=fgenesc&group=programs&subgroup=gfs)

Then, each of the two isolated ORFs was verified by comparison with the reference genome (*V. vinifera* cv. Pinot Noir) and the predicted protein domains were analyzed using NCBI (https://www.ncbi.nlm.nih.gov/Structure/cod/ wrpsb.cgi). After alignment with ClustalW, specific primers for GATEWAY cloning were designed (Appendix 5.3) to amplify and clone the chosen sequence into the GATEWAY® entry vector (Invitrogen Corporation, Paisley, UK). From the two entry vectors for *VrMC2* and *VrMC5*, the inserts were further ligated into the vector pH7FWG2.0 (driving expression of a fusion of the insert with a C-terminal GFP under control of the CaMV 35S promoter and a hygromycin resistance upon expression in plants) by using GATEWAY LR recombination reactions. After a further verification of the sequence, these vectors were then used for stable transformation of tobacco BY-2 cells. A complete overview of both constructs generated from this study can be found in (Appendix 5.5).

2.8 Establishment of stable transformed on tobacco BY-2 cells using Agrobacterium-mediated transformation

To address cellular aspects of metacaspase function, two stable and overexpressing BY-2 cell lines *VrMC2*-GFP and *VrMC*5-GFP were need to be generated according to the method of agrobacterium-mediated transient transformation (Buschmann *et al.*, 2011) with minor modifications. Wild type (WT) tobacco BY-2 cells were used for investigations. Subcultivated condition of the cells was described above (see 2.1.2). Normally during 3-4 days after subcultivation, 90ml cells were collected and washed with Paul's medium (4.3 g l-1 MS salts with 1% sucrose, pH 5.8) for 3 times using a Scientific Nalgene® Filter Holder (Thermo Scientific, Langenselbold, Germany). It can filter cells by a Nylon mesh (diameter as 70 μm) and then suspended cell sediment as 20% of the starting volume. This 5ml of concentrated cells was ready for cocultivation with agrobacteria prepared as follows.

For *Agrobacterium* transformation, Chemo-competent *Agrobacteria* LBA4404 (Invitrogen Corporation, Paisley, UK) were prepared using a freeze-thaw transformation protocol: 100 μl LBA4404 competent cells were first thawed on ice for 10min, and then incubated with 100 ng of unique constructed binary expression vectors for further 20 min. After 37 ℃ heat shock transformation and 28 ℃ for 90 sec and incubation for 1.5~2h, bacteria were spread onto solid LB (Lennox Broth, Roth, Karlsruhe, Germany) medium containing corresponding antibiotics (50 $\mu g \cdot ml^{-1}$ rifampicin, 300 $\mu g \cdot ml^{-1}$ streptomycin, and 100 $\mu g \cdot ml^{-1}$ spectinomycin), and incubated for 3 days at 28 ℃ in the dark. Afterwards, single colonies were inoculated into liquid LB medium (5ml) with the same antibiotics and cultivated in a shaker (200 rpm) at 28 ℃ for further 24 hours. Then 1 ml suspended bacteria was transferred into 5 ml fresh LB medium without adding antibiotics until shaking up to get the OD600 value as 0.8. Next step, all 6 ml bacteria cells was transferred into a 50-ml Falcon and centrifuged at 8,000 rpm (Heraeus Pico 17 Centrifuge, Thermo Scientific, Langenselbold, Germany) for 8 min. Only sediment was stayed and further resuspended thoroughly with 180μl of Paul's medium. This liquid as inoculum, was well-mixed with prepared concentrated BY-2 suspension cells on shaker for 5 min at 100 rpm.

Following co-cultivation with *Agrobacterium*, The mixture of bacteria and BY-2 cells was pipetted onto Paul's agar plates (Paul's media with 0.5% Phytagel, without

antibiotics) as small drops with sterile cut tips. These plates were then incubated for 3 days at 22 ℃ in the dark. Cells were subsequently transferred on MS agar plates (MS media with 0.8% Danish agar) containing 300 $mg \cdot L^{-1}$ cefotaxime and 60 $mg \cdot L^{-1}$ hygromycin. After 14-21 days, resistant calli were pooled to obtain sufficient material for starting a suspension culture. In addition to overexpressing C-terminal GFP fusions of *VrMC2* and *VrMC5* using *pH7FWG2.0/VrMC2* and *pH7FWG2.0/ VrMC5* under control of a constitutive CaMV 35S promoter, one line was transformed in parallel with the empty vector *pH7FWG2.0* as negative control. Thus, the cells represent a population of several independent transformed genotypes. All these three transgenic cell lines were supplemented with 30 $mg.L^{-1}$ hygromycin as selective agent for expression of the transgene. As control for a non-specific cytosolic GFP signal, a BY2-line expressing free GFP cell line was (Nocarova and Fischer, 2009) kindly provided by Dr. J. Petrášek, Charles University, Prague, Czech Republic). Here, selective pressure was established by 25 $mg.L^{-1}$ kanamycin.

2.9 Subcellular localization of VrMC2 and VrMC5 using fluorescent microscopy

To observe and document the subcellular localization for the different transformants, GFP fluorescence was recorded via a AxioObserver Z1 (Zeiss, Jena, Germany) inverted microscope, equipped with a laser dual spinning disk scan head (Yokogawa CSU-X1 Spinning Disk Unit, Yokogawa Electric Corporation, Tokyo, Japan), a cooled digital CCD camera (AxioCam MRm; Zeiss), and a laser emission line of 488 nm (Zeiss, Jena, Germany). GFP-/Alexa-Fluor® 488-fluorescence were observed through 38 HE (excitation: 470 nm, beamsplitter: 495 nm, and emission: 525 nm) respectively (Zeiss). For ER tracker observation, first dilute the 1 mM stock solution of ER-Tracker™ Red dyes (Thermo Fisher Scientific, Germany) to 1μM in suspension cell as final working concentration. Then ER-tracker/RFP was observed under 561nm emission line of the Ar-Kr laser, through the filter sets 43 HE (excitation: 550 nm, beamsplitter: 570 nm, and emission: 605 nm). Images were acquired using Plan-Apochromat 63x/1.44 DIC (differential interference contrast) oil objective operated via the Zen 2012 software platform (Blue edition). Method of single section and Z stacks was used for representing localization images.

2.10 Identification of the expression of the VrMC2-GFP and VrMC5-GFP fusion protein

The overexpression of the VrMC2-GFP and VrMC5-GFP fusion (OxVrMC2-GFP, OxVrMC5-GFP) was verified firstly on an mRNA level. The correct size of full-length VrMC2 and VrMC5 was tested for the transcript by RT-PCR as described above. Secondly, Western blot using monoclonal GFP antibodies binding to the GFP tag was investigated to check the expression of VrMC2 and VrMC5 on the translational level. Samples from non-transformed WT BY-2 cell line and each transgenic cell line (OxVrMC2-GFP, OxVrMC5-GFP and Free GFP) were collected on the third day after subcultivation during the peak of proliferation activity. The extracts of soluble and microsomal proteins were then obtained from each cell line separately, according to the method of Nick *et al.* (1995), with some modifications. All the cells were homogenized in a precooled mortar and pestle with liquid nitrogen added continuously. Cell powder was mixed with the same volume of extraction buffer containing 25 mM morpholine ethanesulfonic acid, 5 mM EGTA, 5 mM $MgCl_2$, pH 6.9, supplemented with 1 mM dithiothreitol (DTT) and 1 mM phenylmethylsulphonyl fluoride (PMSF). Cell lysates were then centrifuged at 13000 g, at 4 ℃ for 5 min. The pellet was re-suspended with 200 uL extraction buffer and used as a microsomal fraction containing cell wall, plasma membrane, endomembrane and plastidic proteins. The supernatant was further ultracentrifuged at 100,000 g, at 4 ℃ for 15 min (rotor TLA 100.2, Beckman, Munich, Germany). This second supernatant was used as a soluble extract containing cytosolic proteins. All samples were finally dissolved in loading buffer (containing 50 mM Tris/HCl (pH 6.8), 30 % glycerol (v/v), 300 mM DTT, 6 % SDS, 0.01 % bromophenol blue) and heated at 95 ℃ for 5 min.

SDS-PAGE gel 10 % (w/v) was used to isolate the total protein and protein bands were subsequently probed by Western blotting, according to the method of Nick *et al.* (1995). Total protein was transferred onto PVDF membrane from SDS-PAGE separation gel, and then the PVDF membrane was blocked in TBST buffer (containing 20 mM Tris/HCl, 300 mM NaCl, 1 % Tween, pH 7.4) with 2 % milk powder (Sigma-Aldrich) and incubated overnight. Afterwards, primary antibody (Anti-Green Fluorescent Protein antibody, Sigma-Aldrich) was added in a dilution of

1:1000 and incubated for 1.5 h at room temperature, followed by washing three times with TBST buffer. The second antibody was then added and marked by alkaline phosphatase conjugated with goat anti-mouse IgG (Sigma-Aldrich) in a dilution of 1:2500, and further incubated for 1.5 h at room temperature. After washing three times in TBST buffer, the PVDF membrane was finally put into BCIP/NBT chromogenic reagent (Thermo Fisher Scientific, Germany) till the stripes appeared.

2.11 Mortality assay in response to Harpin, MeJA and DPI

The HR elicitor harpin (Pflanzenhilfsmittel, ProAct, Starnberg, Germany), derived from the phytopathogenic bacterium *Erwinia amylovora*, was used at a final concentration of 27 $\mu g \cdot ml^{-1}$ in BY-2 cell culture and 18 $\mu g \cdot ml^{-1}$ in grape cell culture (dissolved in distilled water) to activate cell death-related defence. In addition, MeJA (Sigma-Aldrich, Germany) was also used in this study at a final concentration of 100 µM (dissolved in enthanol) as an inducer of basal immunity. Lastly, to clarify whether induced cell death is correlated with oxidative burst, 200 nM of the inhibitor of NADPH oxidase, diphenyleneiodonium (DPI) (Cayman, USA) was investigated (dissolved in dimethylsulfoxide DMSO). All reagents were added at the time of subcultivation, except for the DPI+harpin treatment; in this case, the cells were initially pretreated for 30 min with 200 nM DPI. The maximal concentration of solvent used in the test samples was administered and did not exceed 0.1 %.

The VrMC2, VrMC5 overexpressor lines along with the non-transformed BY-2 WT cell cultures after subcultivation were analysed at 0, 24, 48 and 72 h after induction by the respective treatment, or without treatment for the response of mortality to score the mortality in response to each single factor treatment or combination treatment of two factors. For this purpose, 0.2-ml aliquots of each sample were transferred into custom-made staining chambers (Nick *et al.*, 2000) to remove the medium, and then incubated in 2.5 % (w/v) of the membrane impermeable dye Evans Blue for 3 – 5 min (Gaff and Okong'O-Ogola, 1971). After washing three times with sterilized water, the cells were mounted on a slide and observed under a light microscope (Zeiss-Axioskop 2 FS, DIC illumination, 20 x objectives). Mortality was calculated as the ratio of the number of dead cells (stained blue) over the total number of scored cells. Three

independent experiments were scored with 500 cells for each measurement for each time point.

2.12 Cloning and analysing the promoters of MC2 and MC5

The genomic DNA was extracted by cetyltrimethylammonium bromide (CTAB) method according to the protocol (Doyle and Doyle, 1987). Upstream promoter sequences of MC2 and MC5 were amplified from genomic DNA of both, *V. rupestris* and *V. vinifera* cv. 'Müller-Thurgau', using Q5® High-Fidelity DNA polymerase (NEB, Frankfurt, Germany) based on oligonucleotide primers derived from the grapevine reference genome (*V. vinifera* cv. 'Pinot Noir') and given in Appendix 5.3. The promoter fragments *pVvMC2* (accession number KY069976) comprising 1563 bp, and the fragment *pVvMC5*, (accession number KY069978) comprising 1631 bp upstream of the start codon were both cloned from *V. vinifera* cv. 'Müller-Thurgau', whereas fragments *pVrMC2* (1554 bp, accession number KY069977), and *pVrMC5* (1599 bp, accession number KY069979) were obtained from *V. rupestris*. Amplicons were obtained using 38 cycles of 30 sec annealing at 57 ℃, 120 sec elongation at 72 ℃, and 10 sec denaturation at 98 ℃, and eluted from the gel using the 0.1ug PCR products were ligated into the pGEM®-T Easy Vector (Promega, Madison, PWl) and then transformed into *Escherichia coli* DH5α for DNA sequencing (GATC Biotech, Cologne, Germany). The four promoter regions were further ligated into the luciferase vector pLuc of gateway version (containing attR sites), kindly provided by Prof. Dr. Jochen Bogs (DLR Neustadt) by using GATEWAY LR recombination reactions (Invitrogen Corporation, Paisley, UK), respectively.

After the resulting promoter vectors had been verified by sequencing, the presence of putative regulatory elements was analysed with the PlantCARE (http:// bioinformatics. psb.ugent.be/webtools/plantcare/html/) and PLACE (http://www.dna.affrc.go.jp/ PLACE/) databases. Then, the two promoters were aligned by DNAMAN software and differences between the two genotypes were plotted in a map.

2.13 Assay of promoter activity by using transient transfection and a dual-luciferase reporter

A well-established dual-luciferase system based on transient transformation (Czemmel *et al.*, 2009; Duan *et al.*, 2016; Merz *et al.*, 2015) was employed to measure promoter activation, using a suspension cell line from *V. vinifera* cv. 'Pinot Noir' as experimental material. The *Renilla* luciferase plasmid pRluc was transformed as an internal control in parallel to calibrate the firefly luciferase luminescence against variations of transformation (Horstmann *et al.*, 2004).

A transient transformation system was performed using biolistic bombardment: gold particles (1.5 – 3.0 µM; Sigma-Aldrich, Germany) were coated with plasmid DNA, including 50 ng of specific promoter DNA and 100 ng control plasmid pRluc, according to the standard manual of Bio-Rad (PDS-1000/He Particle Delivery System manual; Appendix 5.6 for details). DNA-coated particles were then loaded onto macrocarriers (Bio-Rad Hercules, CA USA) and transferred into a custom-made chamber for shooting cells. Three-day-old cells from *V. vinifera* cv. 'Pinot Noir' placed on solid MS medium (0.8 % Danish agar) were cultivated in liquid medium, as described above, and then transiently transformed through three shots at a pressure of 1.5 bar in a vacuum chamber of -0.8 bar, as described in Maisch *et al.* (2009).

Promoter activation was measured in response to elicitation by either 27 $\mu g \cdot ml^{-1}$ harpin or 100 µM MeJA, or a related solvent without elicitation administered 24 h after bombardment. Cells were harvested using a curette 24 h after elicitation and homogenised in 150 µL of 2 × passive lysis buffers (PLB, Promega, Madison, WI) by grinding on ice with a pestle and mortar for 1.5 min. After centrifugation of the lysates for 2 min at 10,000 rpm, measurement of the luciferase activities was performed with the dual-luciferase reporter assay system (PJK, Kleinbittersdorf, Germany), by sequential addition of 50 µL Beetle juice and Renilla Glow Juice to individual 20-µL samples of the lysate supernatant. Luminescence was measured using a Lumat LB9507 luminometer (Berthold Technologies, Bad Wildbad Germany). All experiments were performed in triplicate and all experiments were repeated in three independent series. Mean values of the ratios between firefly and *Renilla*

luciferase luminescence were recorded as a readout of luciferase activity, normalised for transformation efficiency, and relative changes of activity calculated over the values measured in the solvent-treated samples. Vectors pSTS29/pLuc (containing the promoter of stilbene synthesis gene STS29) and related pSTS29 activator MYB14/pART7 (Holl *et al.*, 2013) were used as positive controls and were kindly provided by Prof. Dr. Jochen Bogs (DLR Neustadt).

.

3. RESULTS

3.1 Resistance to *P. viticola* in *V. rupestris* correlates with HR-like necrosis

3.1.1 HR-like necrotic spots observed on *Rpv3*$^{+}$ grapevine induced by *P.viticola* 1191-B15

P. viticola, as a biotrophic pathogen, can suppress the innate immunity of native hosts such as *V. vinifera*. North American wild species of *Vitis* that have coevolved with this pathogen have developed resistance that is often linked with localised necrosis of infected cells, which is regarded as a classical HR. In the resistant *vinifera* genotype 'Bianca', harbouring the locus *Rpv3*, the resistance to *P. viticola* had been associated to HR (Bellin *et al.*, 2009). Since *Rpv3* is also present in the commercially important *vinifera* genotype 'Regent', the resistance might be based on HR, but this has not been directly addressed so far. Since the complex pedigree of 'Regent' comprises seven wild North American species of grapevine, the origin of the *Rpv3* locus is not clear (Fischer *et al.*, 2004). We investigated possible differences in the incidence of HR along with differences in susceptibility to *P. viticola* to clarify these open issues. We inoculated a panel of nine grape genotypes with the single sporangium pathogen strain 1191-B15 (Gomez-Zeledon *et al.*, 2013). The panel comprised the *Rpv3*-positive resistant vinifera variety 'Regent', along with *V. rupestris* and *V. riparia* as potential sources of *Rpv3*, three *Rpv3*-negative susceptible *vinifera* varieties, and three genotypes where pathogen resistance is independent of *Rpv3*. After controlled infection of leaf discs, we followed the local responses over time, starting from inoculation at day 0 over 6 and 9 dpi till inspection of sporulation at 9 dpi after infection (Fig 3.1). Necrotic spots indicative of HR became visible, even by the naked eye, from 3 dpi in *V. riparia* and *V. rupestris* and from 6 dpi in *V. vinifera cv.* 'Regent'. Interestingly, the *V. sylvestris* genotype Hoe29 also showed a few spots, but only after 9 dpi.

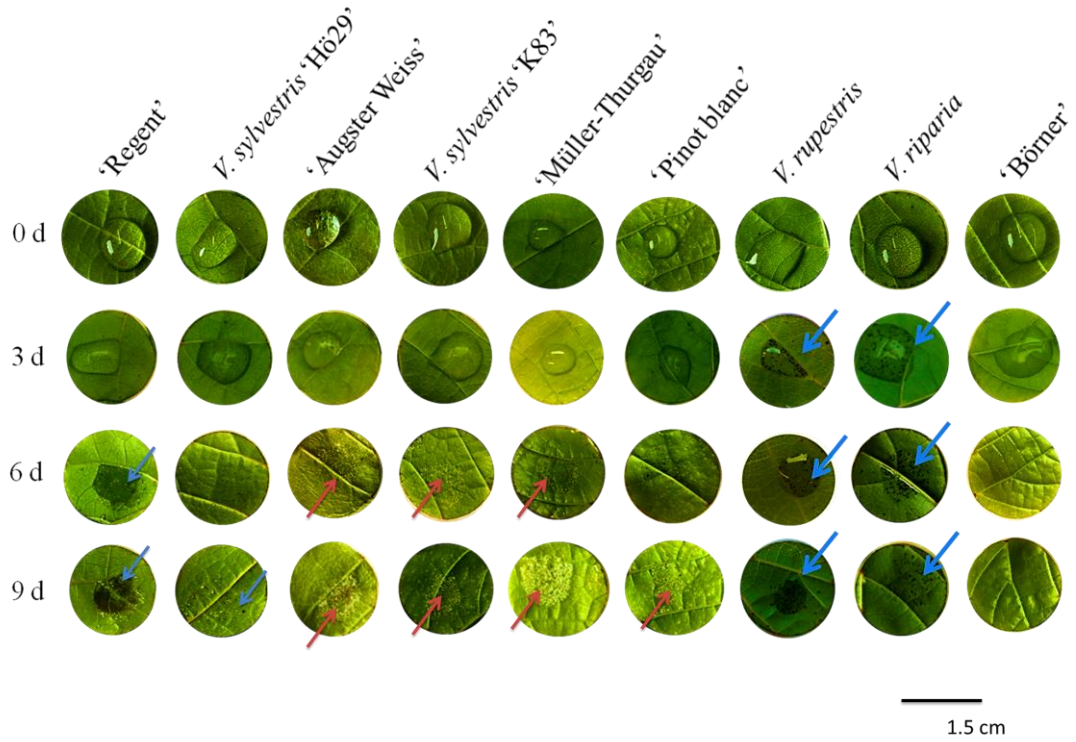

Figure 3.1 Leaf disc phenotype of 9 different grapevine varieties at 4 time points after *Plasmopara viticola* 1191-B15 infection

Pictures were taken at 0, 3, 6, 9 d (days) after infection. From left to right side: *V. vinifera Regent*, *V. vinifera* ssp. *sylvestris* Hoe29, *V. vinifera* Augster Weiss, *V. vinifera* ssp. *sylvestris* K 83, *V. vinifera* cv. Mueller Thurgau, *V. vinifera* cv. Pinot blanc, *V. rupestris*, *V. riparia* and *V. Boerner* (*V.*riparia x *V. cinerea*). Blue arrows, necrotic spots; Orange arrows, sporulation; Bar=1.5 cm

By contrast, no necrotic spots were observed on the susceptible *V. vinifera* genotypes 'Augster Weiss', 'Müller-Thurgau', or 'Pinot Blanc' even at 9 dpi. We further observed that the appearance of necrotic spots in *V. riparia*, *V. rupestris* and *V. vinifera* cv. 'Regent' correlated with a reduction of pathogen sporulation (Fig. 3.1). However, the *vinifera* genotypes which were not displaying HR-like lesions were seen to carry sporulations from 6 dpi. Three genotypes displayed different amplitudes of a third pattern: the *sylvestris* genotypes 'Hö29' and 'Ke83' (much less pronounced) supported only a reduced level of sporulation, but did not produce necrotic lesions till 6 dpi. The extreme expression of this third pattern was seen in the rootstock genotype 'Börner' (deriving from a cross between the North American wild species *V. riparia* and *V. cinerea*), where neither necrotic lesions nor sporulation were apparent.

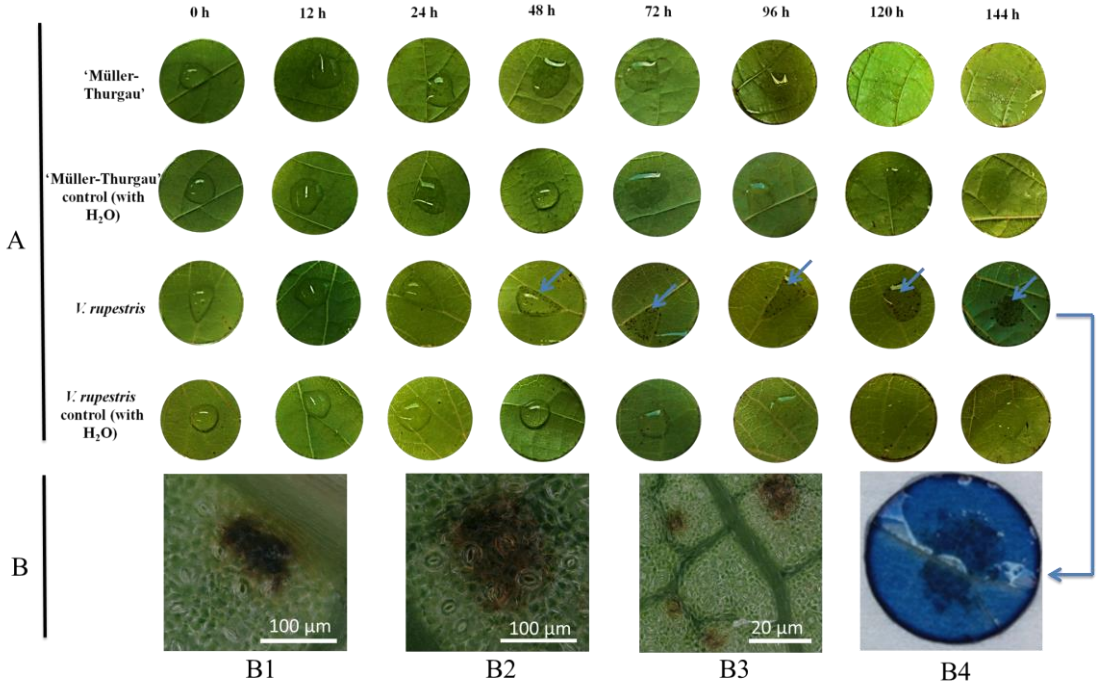

Figure 3.2 Necrotic spots in leaf discs of *V. vinifera* cv. Mueller Thurgau and *V. rupestris* at 8 time points after *Plasmopara viticola* 1191-B15 infection

A. Pictures were taken at 0 hour, 12 hours, 24 hours, 48 hours, 72 hours, 96 hours, 120 hours and 144 hours after *P. viticola* infection. Blue arrows indicate necrotic spots. These regions of local cell death could be observed only in *V. rupestris* from 48 hours post infection (hpi). Distilled H_2O treated samples are shown as negative control in parallel. B. Micrographs and staining after infection on *V. rupestris*. B1, necrotic spots under 20x magnification at 48 hpi; B2, necrotic spots under 20x magnification at 144 hpi; B3, necrotic spots under 10x magnification at 144 hpi; B4, Cell death appeared in areas showing a dark blue staining by Evans blue.

Based on this screening experiment, *V. vinifera* cv. 'Müller-Thurgau' was classified as susceptible, and *V. rupestris* as a resistant genotype. They were selected for a more detailed temporal analysis of cellular and molecular features of the necrotic lesion formation, including a mock inoculation as a negative control. Results showed necrotic lesion could be observed only on the infected leaves of *V. rupestris* (Fig. 3.2A). Every single necrotic spot developed around a stomata in the centre, surrounded by a continuous expanding area of dead cells, which could be verified by staining with Evans blue (Fig. 3.2B). These regions of local cell death could be observed from 48 h post infection (hpi), and were never seen in the mock controls and cv. 'Müller-Thurgau'. The frequency of the necrotic spots increased with the time after inoculation.

3.1.2 Continuous increase in number and size of necrotic sites on infected leaves in *V. rupestris*.

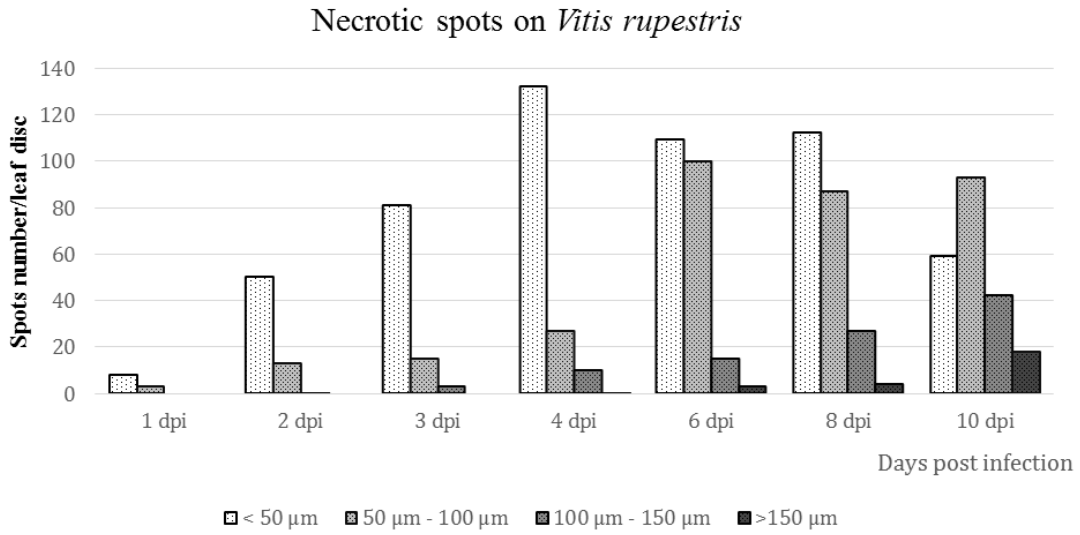

Figure 3.3 Number of necrotic spots at 7 time points after *P.viticola* 1191-B15 infection on *V. rupestris* leaf discs

The amounts of necrotic sites are displayed and classified for four size categories: <50 µm, 50-100 µm, 100-150 µm and> 150 µm; at 0, 1, 2, 3, and 4 dpi in the early stage, to 6, 8, and 10 dpi in the later stage.

The leaf discs were infected under same conditions to further quantify the HR of *V. rupestris* caused by *P. viticola*. All necrotic spots in the infection area were recorded and then counted and evaluated at regular intervals (Fig. 3.3). Four categories were created dependent on various diameters: < 50, 50 – 100, 100 – 150 and > 150 µm (details in Appendix 5.7) to evaluate the temporal course of these spots more precisely. This quantification revealed that necrotic lesions became detectable from 24 hpi, and first increased in number reaching a plateau from 72 hpi, while spot size rapidly increased after 96 hpi, indicative of a rapid initiation of lesions, followed by a slower expansion of necrosis. These results were also corroborated by staining with Evans blue, which steadily intensified with progressive time after inoculation (Fig. 3.4). By contrast, no lesions appeared after ddH_2O treatment as control.

3.1.3 The Formation of sporangia after *P. viticola* infection

Necrotic lesions of the host clearly indicated differences in the host-pathogen interaction. Therefore, variation of sporulation on the respective leaf surfaces between two genotypes can be analysed to reflect the resistance differences. For this purpose,

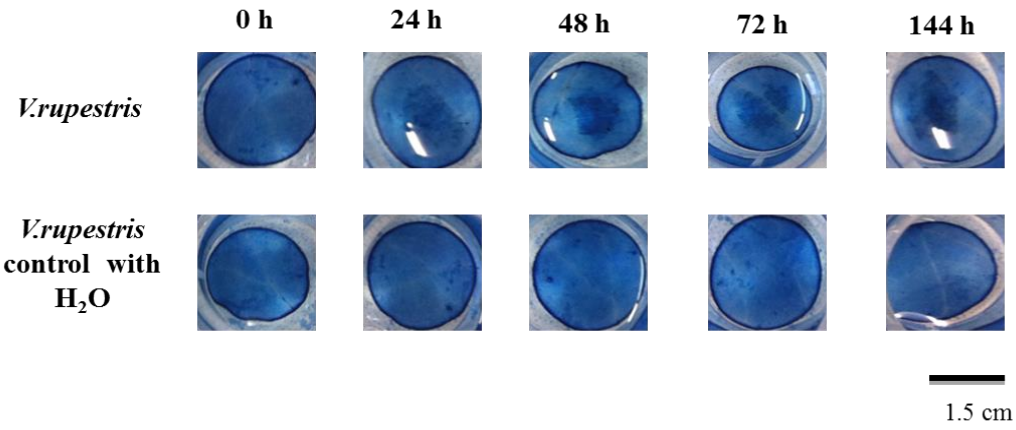

Figure 3.4 Representative leaf discs inoculated with *Plasmopara viticola* 1191-B15 and H_2O as control on *V. rupestris*. Leaf discs of V. rupestris were stained with Evans blue and pictures were taken at 0, 24, 48, 72 and 144 h (hours) after infection. Bar=1.5 cm. The result of a representative experiment is shown.

leaf discs were again infected with sporangia suspension under the same conditions described above. Afterwards, the concentration of sporangia was measured from the infected site of the leaf discs. Results showed that the sporangia density was progressively increasing in cv. 'Müller-Thurgau' from 4 dpi and had reached a level that was approximately thirtyfold compared to that seen in *V. rupestris* at 10 dpi (Fig. 3.5)

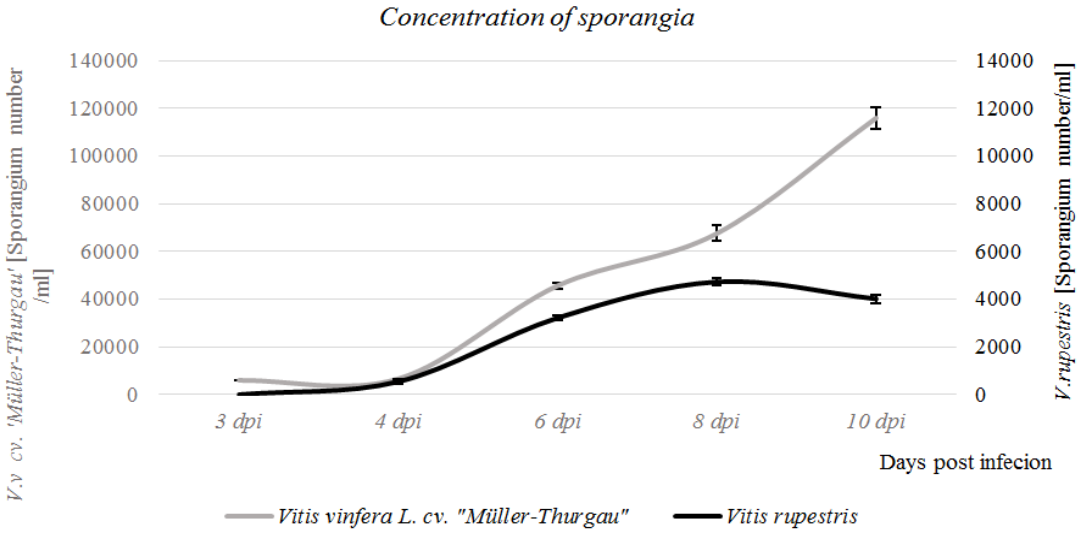

Figure 3.5 Sporulation of *P.viticola* 1191-B15 on leaf discs between *V. vinifera* cv. 'Mueller Thurgau' and *V. rupestris*.

Number of 1191-B15 sporangia grown on each grape leaf disc was counted and shown from 3 dpi up to 10 dpi after the infection. Two scaled Y-axis shows: left y-axis (light gray) results for *V. vinifera* cv. "Müller-Thurgau', right y-axis (black) results for *V. rupestris*. The respective line graphs follow the same color pattern. Two biological replicates were performed.

3.2 *VrMC2* and *VrMC5* are transcriptionally activated by infection with *P. viticola* correlating with cell death

We have shown previously that specific members of the grapevine metacaspase gene family were up-regulated during the key stage of ovule abortion in seedless grapes (Zhang *et al.*, 2013). The different temporal and spatial expression patterns of individual metacaspases implied that different processes involving PCD might be executed by different individual metacaspase members. This hypothesis leads to the question, whether the HR response to the biotrophic pathogen *P. viticola* might be associated with specific members of the metacaspase family. We therefore analysed the pathogen response of steady-state transcript levels for different metacaspase members under the same set-up as the development of necrotic lesions and sporulation (Fig. 3.6) in leaf discs of the susceptible *V. vinifera* 'Müller-Thurgau' versus the resistant *V. rupestris*.

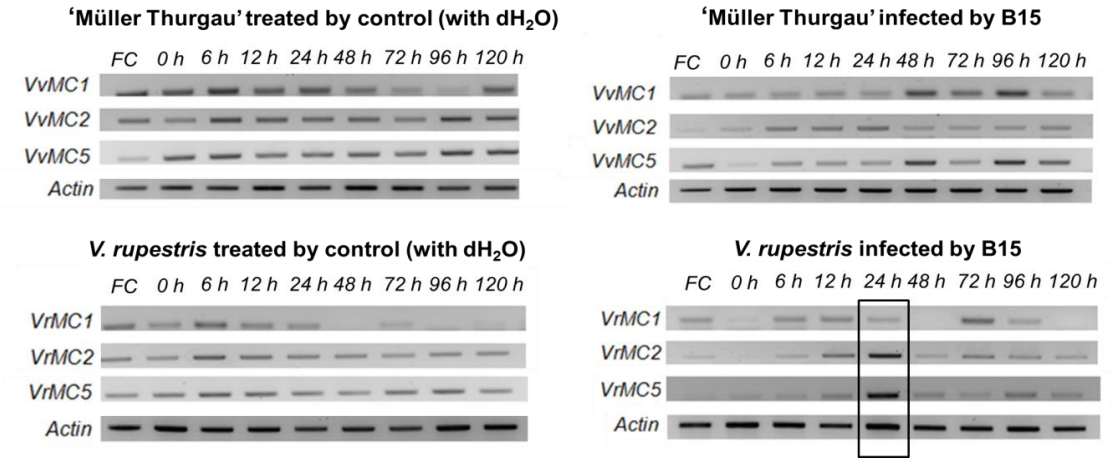

Figure 3.6 Semi-quantitative expression analysis of grape *MC1, MC2* and *MC5* genes during *P.viticola* 1191-B15 infection.

Representative agarose gels with the amplified transcripts of MC1, MC2 and MC5 on *V. vinifera* cv. 'Mueller Thurgau' and *V. rupestris* by semi-quantitative RT–PCR. FC (as fresh control), 0 hour, 6 hours 12 hours, 24 hours, 48 hours, 72 hours, 96 hours and 120 hours (corresponding time points with Fig 3) were set as time points after inoculation with 1191-B15. Actin was tested and compared as internal reference gene. Distilled H_2O treated samples were used as negative control in parallel.

All *Vitis* metacaspase members were measured by semi-quantitative RT-PCR using member-specific oligonucleotide primers that had been designed from the grapevine

reference genome. Candidates that are linked with pathogen-dependent HR should be specifically up-regulated in *V. rupestris* under infection, and this up-regulation should precede the manifestation of HR, i.e. it should be observed at 24 hpi. A further criterion qualifying a relevant MC member would be that this up-regulation was not seen in cv. 'Müller-Thurgau' and also not in *V. rupestris* in response to a mock control. To avoid background contamination by the wounding response resulting from the excision of leaf discs, the marginal zone was discarded immediately prior to freezing (so called "disc-in-disc" set-up).

While grapevine metacaspases *MC4* and *MC6* were apparently not expressed in leaf discs at all (see Appendix 5.8), we found that *MC3* was only up-regulated in infected cv. 'Müller-Thurgau', i.e. under conditions, where necrotic lesions were not observed. The same holds true for MC1 that was up-regulated in both host genotypes, but only at late time points (Fig. 3.6).

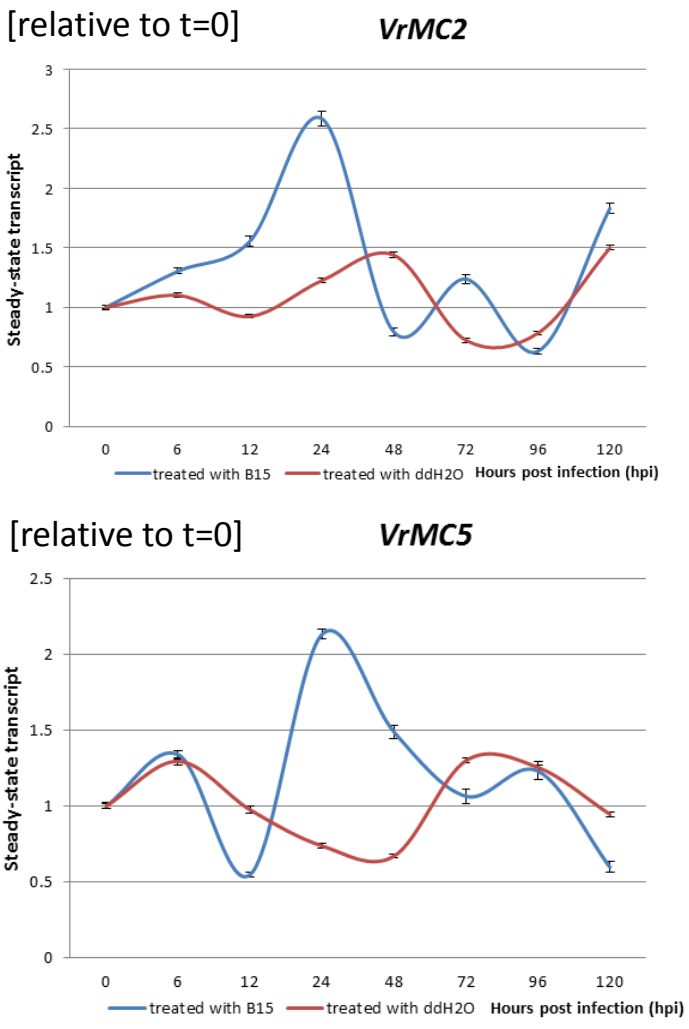

Figure 3.7 Quantitative PCR expression assays of *VrMC2* and *VrMC5* genes induced by 1191-B15 infection on *V. rupestris*

Quantification of transcripts of metacaspase2 (*VrMC2*) and metacaspase5 (*VrMC5*) at 0 hour, 6 hours 12 hours, 24 hours, 48 hours, 72 hours, 96 hours and 120 hours (consistant time points with Fig 3.7) after inoculation by quantitative real-time PCR. Actin was tested as internal reference gene. The result of a representative experiment is shown. Y-axis are scales of relative expression level (error bars indicate ±standard errors).

In addition to the metacaspases, a further well known plant-specific PCD regulator, Vacuolar Processing Enzyme (*VPE*) was investigated (Tang *et al.*, 2016). Under the three VPE members known for grapevine, only *VrγVPE* was specifically up-regulated by infection in *V. rupestris* from 24 hpi (see Appendix 5.8). In contrast to these genes, the grapevine metacaspases *MC2* and *MC5* met the criteria defined above (Fig. 3.6): In contrast to *MC1*, steady-state levels of *VrMC2 and VrMC5* transcripts were strongly and specifically up-regulated at 24 hpi, and this was neither seen in infected *V. vinifera* cv. 'Müller Thurgau' as a host, nor was it found in mock-inoculated leaf discs from *V. rupestris*.

The patterns of *VrMC2* and *VrMC5* in *V. rupestris* were then verified by quantitative real-time PCR using the same cDNA samples (Fig. 3.7). While steady-state transcript levels were not induced in the mock-control with expression values fluctuating between 0.5-1.5 compared to the levels prior to inoculation for both, *VrMC2* and *VrMC5,* the activity of both genes increased transiently to more than two-fold of the starting level at 24 hpi, and then dropped back at 48 hpi to the control level. Interestingly, there was a second peak for *VrMC2* from 4 dpi. However, this second increase was also seen in the mock control, and, thus, was not specifically linked with infection.

In addition, for further verifying our results, we tested two additional single sporangia strains of *P. viticola*: strain 1135-F2 was comparable to 1191-B15 with respect to infection behaviour, whereas strain 1137-C20 was able to break *Rpv3*-mediated resistance of the *vinifera* cultivar 'Regent' (Gomez-Zeledon *et al.*, 2013). We conducted a time course experiment and analysed *VrMC2* and *VrMC5* at 0 hpi, 24 hpi, 48 hpi and 96 hpi by semi-quantitative RT-PCR (Fig. 3.8). Again, steady-state transcript levels of *VrMC2* and *VrMC5* increased transiently at 24 hpi in both pathogen strains, whereas on *V. vinifera* cv. 'Müller-Thurgau', there was no obvious up-regulation. In comparison between the pathogen strains, it was noted that the up-regulation of *VrMC5* was more persistent upon infection with 1135-F2, whereas upon infection with the more virulent strain 1137-C20 it was rapidly declining and had returned to the level prior to infection at 48 hpi. Based on these expression patterns, these two genes, *VrMC2 and VrMC5,* were prioritized as central candidates

to clarify their gene structure, subcellular localization, cellular function, and the regulatory features of their promoters.

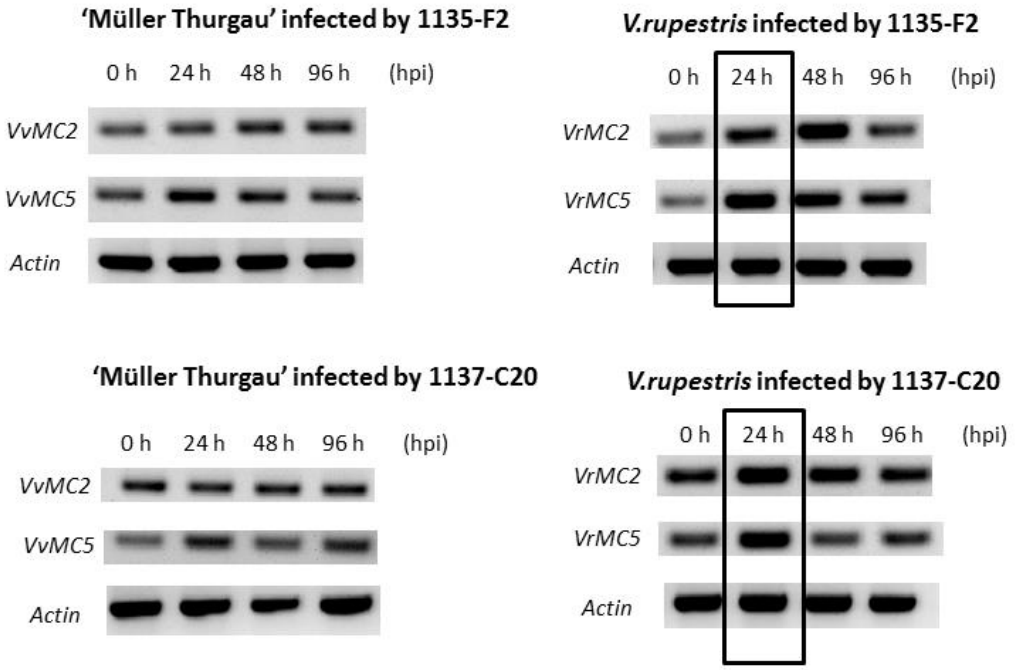

Figure 3.8 Regulation of *Vv(r)MC2* and *Vv(r)MC5* after infection by *P. viticola* strains 1135-F2, 1137-C20

Representative agarose gels with the amplifcated transcripts of *Vv(r)MC2* and *Vv(r)MC5* on *V. vinifera* cv. 'Mueller Thurgau' and *V. rupestris* by semi-quantitative RT–PCR. 0 hour, 24 hours, 48 hours and 96 hours after inoculation with strain 1135-F2 and 1137-C20, respectively. Actin was tested and compared as internal reference gene. Distilled H_2O treated samples were used as negative control in parallel.

3.3 Gene structure analysis of *VrMC2* and *VrMC5* and related putative proteins in *V. rupestris*

To reveal the intron and exon organization of those two central candidates, we aligned *VrMC2* and *VrMC5* cDNA sequences with the corresponding genomic DNA sequences (Fig. 3.9). Results showed that each gene possesses an individual, specific structure. *VrMC2* occupies 7211 bp on the genomic sequence including 5 exons, and 4 introns, whereas the structure of *VrMC5* was comparatively simple, consisting of 2 exons and 1 intron with a total length of only 1370 bp.

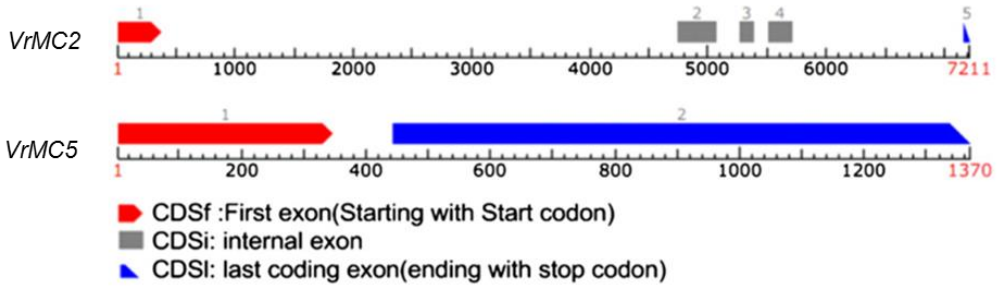

Figure 3.9 Introns and exons distribution of *VrMC2* and *VrMC5* in *V. rupestris*

The first exons are represented by red boxes. Internal exons are represented by grey boxes and the last exons are represented by blue boxes. Scales show the length of each gene's exons and introns in bp (base pair).

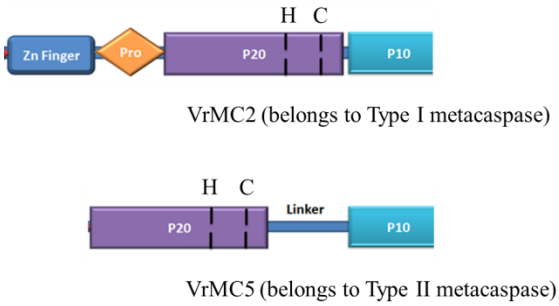

Figure 3.10 Conserved domains and catalytic site sequences in VrMC2 and VrMC5

VrMC2 belongs to Type I metacaspases, while VrMC5 is member of Type II metacaspases. P20 and p10: two caspase-like domain; H and C: two conservative amino acid residues, histidine (H) and cysteine (C), presented in the p20 subdomain; Zn Finger and pro: zinc finger motif and proline-rich repeat motif existing in N-terminal pro-domain of VrMC2; Linker: about 200 amino acid residues between the p20 and p10 subdomain existing in VrMC5.

Moreover, combined with previous research results, it was confirmed that the putative protein structure of VrMC2 had a similar conserved structure belonging to Type I metacaspase, consisting of a putative small (p10-like) subunit and a large (p20-like) subunit, containing the catalytic histidine in the H(Y/F) SGHG sequence and the catalytic cysteine in the active-site, pentapeptide DXCHS (where X is A or S) sequence, respectively (Figure 3.10). These two typical metacaspase secondary structural units determine their structures and enzyme activities (Rahman and Mahmudur, 2010). In addition, VrMC2 also contains a Pro/Gln-rich N-terminal prodomain of about 80–120 amino acids and a shorter linker region about 30 amino

acids between the putative large (p20-like) and small (p10-like) subunits. All features were in accordance with the characteristics of Type I metacaspases. VrMC5 possesses p10 and p20 subdomain as well, but lacks the Pro/Gln-rich N-terminal prodomain found in VrMC2. Besides, VrMC5 harbours a longer linker region of about 90-150 amino acids, which corresponds to the characteristics of Type II metacaspases.

Based on these features, the VrMC2 and VrMC5 were clearly qualified as one type I and one type II sub-family member of the *Vitis* metacaspases, as reflected by the position in the phylogenetic tree presented below (Figure 3.11).

3.4 Plant metacaspase diversity in different clades and taxa

Previously, we had identified and characterized the entire grape metacaspase family from the reference genome of *V. vinifera* cv. 'Pinot Noir' by a BLAST search based on the available sequences of *A. thaliana* metacaspase proteins *in silico* (Zhang *et al.*, 2013). To get further insight into the evolutionary history and phylogenetic relationships of the plant metacaspases, a Neighbour-Joining tree was constructed by using MEGA 5.0 software based on the protein sequence alignment of 42 *bona-fide* metacaspases from higher plants and 2 putative metacaspases from the algae *Chlamydomonas* (Fig 1). From the constructed tree, two major clusters (clades 1 and 2) emerged. Clade 1 comprised 20 type I metacaspases and was further divided into 3 subclades (I-III), while clade 2 comprised 22 type II metacaspases and was also divided into 3 subclades (IV-VI). The separation between subclade I versus subclades II/III was supported by a high bootstrap number (above 90%), whereas the separation between subclades II and III was not so significant (bootstrap values around 70%). Likewise, subclade IV was defined by high bootstrap support, whereas subclades V and VI were not so strictly delineated. While the two main clades (1 and 2) were found in all taxa, for which metacaspase sequences were available, there were taxa-specific differences with respect to the representation of the subclades: For instance, the grapevine metacaspases lacked members of subclades II and VI, whereas subclade I was diversified with three members.

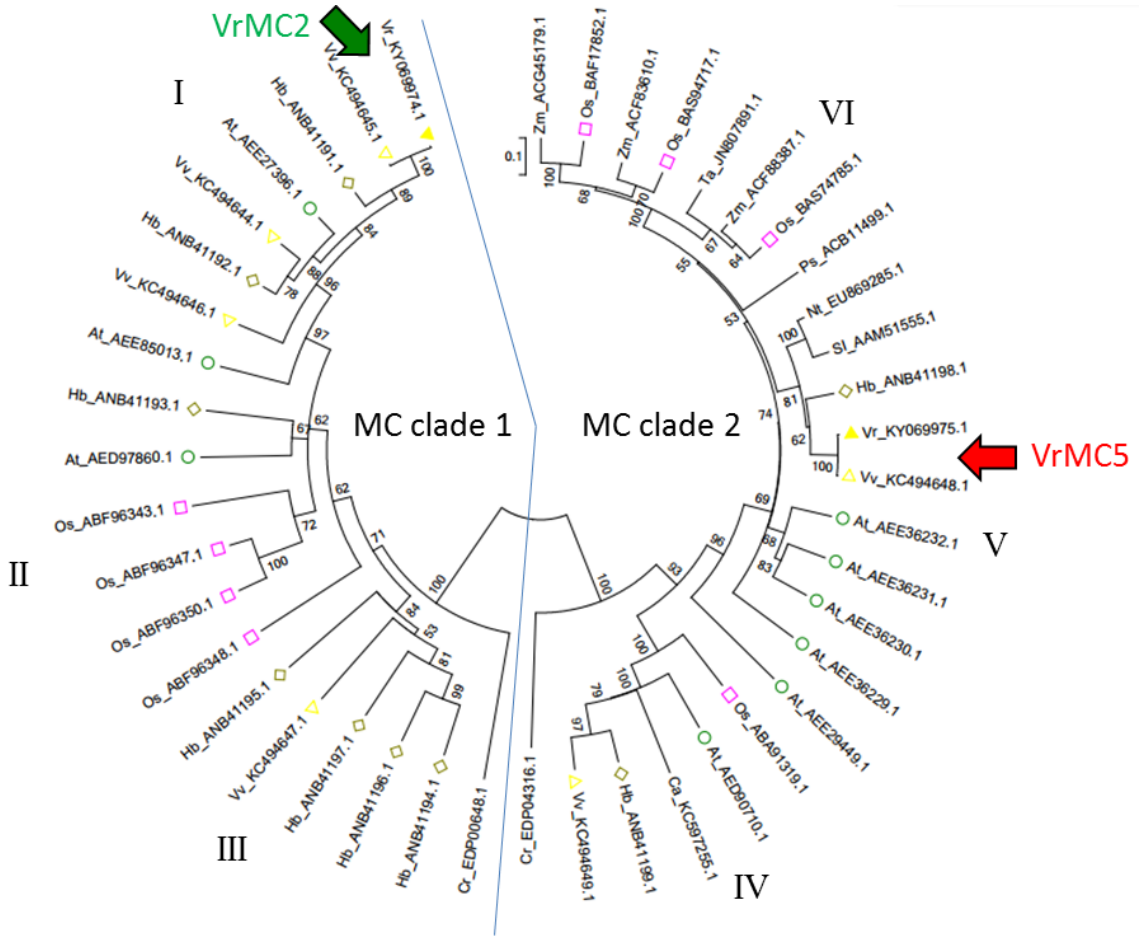

Figure 3.11 Molecular phylogeny constructed by the neighbour-joining algorithm on well-known 42 metacaspase genes

The position of the VrMC2 sequence from *V. rupestris* is indicated by a green arrow, and the position of the position of VrMC5 sequence from *V. rupestris* is indicated by a red arrow. Values next to the branches represent the percentage of replicate trees in which the associated taxa clustered together in the bootstrap test (based on 500 replicates). Green circles (○) indicated whole metacaspase family of *Arabidopsis*. Pink frame (□) indicated whole metacaspase famlily of *Oryza sativa*. Hollow yellow triangle (△) indicated whole metacaspase family of *Vitis vinifera.* Full-filled yellow triangle (▲) indicated metacaspase2 and metacaspase5 of *Vitis rupestris.* Hollow brown rhombus (◇) indicated whole metacaspase family of *Hevea brasiliensis.* None marked names are incomplete metacaspase family members from *Zea mays L.* (maize), *Triticum aestivum* (wheat), *Capsicum annuum L.* (pepper), *Lycopersicon esculentum Mill.* (Tomato), *Nicotiana tabacum* (Tobacoo), *Picea abies* (Norway spruce), separately. The acronym of metacaspase genes were named using the first letter of the genus followed by the first letter of the species, plus related Swiss-Prot accession numbers.

All sequences are well-identified and related references as follows: At (*Arabidopsis thaliana*) AEE27396.1, AEE85013.1, AED97860.1, AEE36232.1, AEE36231.1, AEE36230.1, AEE36229.1, AEE29449.1 and AED90710.1 (Tsiatsiani *et al.*, 2011); Ca (*Capsicum annuum*) KC597255.1 (Kim et al., 2013); Cr (*Chlamydomonas reinhardtii*) EDP04316.1 and EDP00648.1 (Merchant et al., 2007); Hb (*Hevea brasiliensis*) ANB41191.1, ANB41192.1, ANB41193.1, ANB41194.1, ANB41195.1, ANB41196.1, ANB41197.1, ANB41198.1 and ANB41199.1 (Liu et al., 2016); Sl (*Solanum lycopersicum*) AAM51555.1 (Hoeberichts et al., 2003); Nt (*Nicotiana tabacum*) EU869285.1 (Hao et al., 2007a); Os (*Oryza sativa*) ABF96343.1, ABF96350.1, ABF96347.1, BAF17852.1, BAS94717.1, BAS74785.1, ABA91319.1 and ABF96348.1 (Wang and Zhang, 2014); Ps (*Pinus sylvestris*) ACB11499.1 (Suarez et al., 2004); Ta (*Triticum aestivum*) JN807891.1 (Wang et al., 2012); Vr (*Vitis rupestris*) KY069974 and KY069975 (this paper); Vv (*Vitis vinifera*) KC494644.1, KC494645.1, KC494646.1, KC494647.1, KC494648.1 and KC494649.1 (Zhang *et al.*, 2013); Zm (*Zea mays*) ACG45179.1, ACF83610.1 and ACF88387.1(Ahmad et al., 2012).

In contrast, cluster 1 subclades II and III were found to be diversified in the cereals rice and barley, and cluster 2 subclade V in *Arabidopsis*. The two metacaspases predicted for the *Chlamydomonas* genome were found basal at the two clades, indicating that these clades are evolutionary ancient and might reflect different functions of the metacaspase family (Fig. 3.11).

Based on specific features of their regulation (see below), two metacaspase homologues named *VrMC2* (GenBank accession no. KY069974, Fig. 3.11, green arrow), and *VrMC5* (GenBank accession no. KY069975, Fig. 3.11, red arrow) were successfully cloned from the *V. rupestris*. Not surprisingly, the sequences from *V. rupestris* were almost identical to their already identified metacaspases from *V. vinifera* cv. 'Pinot Noir' (above 99% similarity, see Appendix 5.9). VrMC2 and its homologue VvMC2 belong to clade 1, whereas VrMC5 and its homologue VvMC5 are representatives of clade 2.

3.5 VrMC2 and VrMC5 exhibit differential subcellular localization

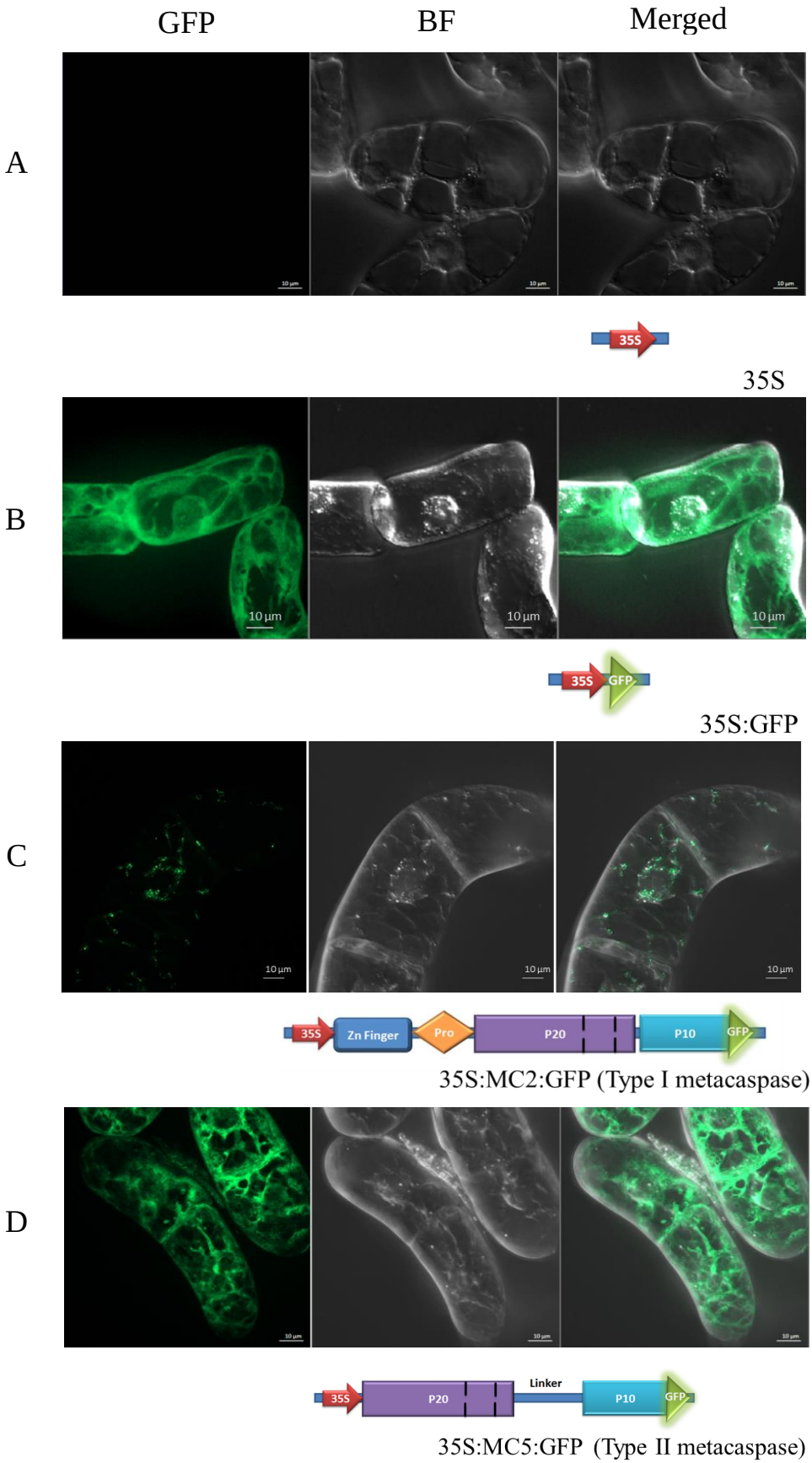

Figure 3.12 Subcellular localization of OxVrMC2-GFP (C-terminal) and OxVrMC5-GFP (C-terminal) transient transformation in BY-2 suspension cells

Left to right: GFP, The channel of green fluorescence signal; BF, Bright-field; Merged, combine channel of GFP and BF. (A). empty vector (35S :) as negative control; (B). Enhanced green fluorescence signal of free GFP (35S:GFP) as positive control; (C).VrMC2 localization (35S:VrMC2:GFP); (D).VrMC5 localization (35S:VrMC5:GFP); Scale bar represents 10 μm. All representative images are shown as the confocal sections from a z-stack along with a differential-interference contrast (DIC) image.

To get insight into potentially different functions of VrMC2 (belonging to clade 1) and VrMC5 (belonging to clade 2), subcellular localization was addressed after *Agrobacterium*-mediated transformation into tobacco BY-2 cells spinning-disc confocal microscopy (Fig. 3.12). VrMC2–GFP and VrMC5-GFP were expressed under the control of the CaMV 35S promoter in tobacco BY2 suspension cells. Subcellular localization of the fusion protein was visualized by imaging of green fluorescence.

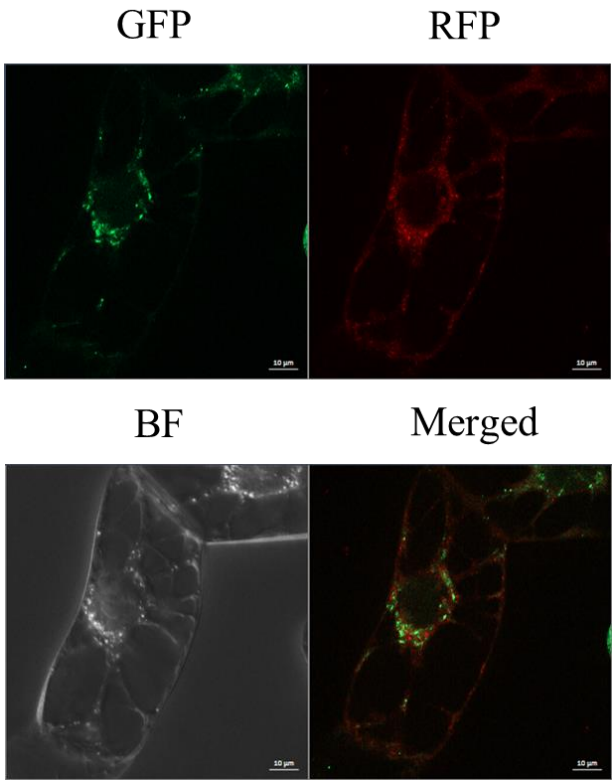

Figure 3.13 Duplex visualisation of OxVrMC2-GFP (C-terminal) and the endoplasmic reticulum (ER) marker ER-Tracker Red dye shown as overview

GFP, The channel where the HPL-GFP signal accumulates; RFP, The channel where ER (Endoplasmic reticulum) located; BF, Bright-field; Merged, combined channel of GFP , RFP and BF.

The free-GFP cell line was detected as positive control and located everywhere in both the cytoplasm and nucleus (Fig. 3.12B). Negative control was transformed in parallel with empty vector which only contain 35S promoter and no fluorescent signal

was detected (Fig. 3.12A). The results showed that *35S*::VrMC2-GFP was located exclusively around the nuclear zone. A faint fluorescent signals scattered around the plasma membrane (Fig. 3.12C).

We initially inferred VrMC2 was located on ER by their morphology and localization in cytoplasmic strands. To further confirm our inference, ER-Tracker red dye was used for co-localization with VrMC2. Results showed both fluorescence signals of RFP and GFP were almost entirely overlapped (Fig. 3.13). In contrast, *35S*::VrMC5-GFP was distributed homogeneously inside the cell which is similar with the free-GFP cell line , showing signals without obvious specificity, mainly in the cytoplasm, but also in the nucleus (Fig. 3.12D, details in Appendix 5.10). These differences suggested that the two different types of grape metacapases probably execute their PCD-related roles in different cell subcellular location.

3.6 The cell death executing function of *VrMC2* and *VrMC5* in HR signalling

3.6.1 Abundance of the VrMC2-GFP and VrMC5-GFP fusion proteins

Although GFP signals have been detected under a fluorescent microscope, it is still essential to verify whether the gene candidates *VrMC2* and *VrMC5* were completely expressed. Two approaches were used to detect the extent of each gene's expression on both a transcript and protein level. Firstly, after strong selection by hygromycin, high steady state levels for each candidate transcript were detectable in all the transgenic lines examined and all transcripts were of the size predicted. No transcript was detected from the WT cells (Fig. 3.14).

Moreover, Western blot was used to detect the presence of VrMC2 and VrMC5 using a monoclonal antibody binding the GFP tag to further identify the integrity of protein expression (Fig. 3.15). A GFP-free cell line was added as a positive control, which showed a strong signal at the expected size (28.6 KDa) in both microsomal and soluble fraction. Similarly, the fusion proteins in both transgenic cells were both the size predicted.

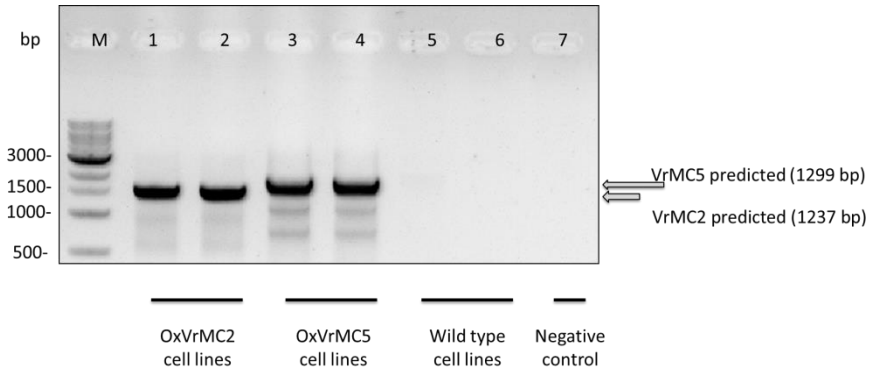

Figure 3.14 High-steady state levels of the transcript from OxVrMC2-GFP and OxVrMC5-GFP cells.

Steady-state levels of the *VrMC2* and *VrMC5* transcript were examined by RT-PCR with respective primers spanning full-length *VrMC2* or *VrMC5*. M: DNA marker; Lane 1-2: Overexpressed VrMC2-GFP lines; Lane 3-4: Overexpressed VrMC5-GFP lines; Lane 5-6: Wild type BY-2 lines (5 amplified by VrMC2 primers, 6 amplified by VrMC5 primers); Lane 7: Negative control without adding cDNA. Grey arrows show putative full-length of *VrMC2* and *VrMC5* transcript.

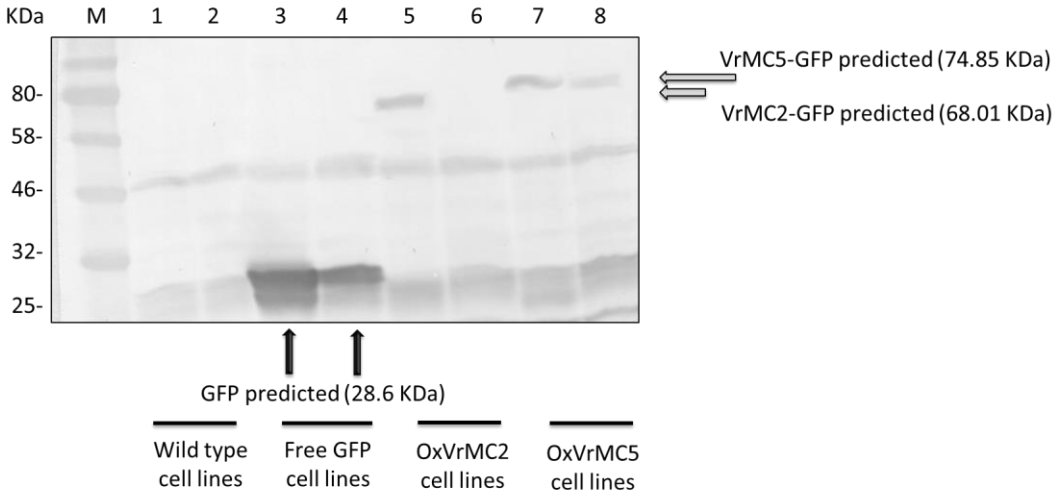

Figure 3.15 Immunodetection of OxVrMC2 and OxVrMC5 transgenic cell lines by Western-blot through total protein extract.

The GFP monoclonal antibody was used to bind to the GFP tag from each cell. All odd lanes are microsomal fractions, and the even lanes are cytosolic supernatant from protein extract of each cell line. M: Protein-Marker; Lane 1-2: Wild type BY-2 lines; Lane 3-4: Free GFP lines; Lane 5-6: Overexpressed VrMC2-GFP lines; Lane 7-8: Overexpressed VrMC5-GFP lines. Grey arrows show putative molecular weight of VrMC2-GFP and VrMC5-GFP. Black arrows show putative molecular weight of GFP

In the case of OxVrMC2, the hybridization signal was detected exclusively in microsomal fractions, whereas OxVrMC5 showed a signal in both the microsomal and soluble fraction. No signal was found from non-transformed BY-2 cells in any fraction. Results indicated that both VrMC2-GFP and VrMC5-GFP were properly expressed and accumulated to well-detectable levels.

3.6.2 Over-expression cell lines of VrMC2 and VrMC5 specifically elevates HR-like process by harpin induction

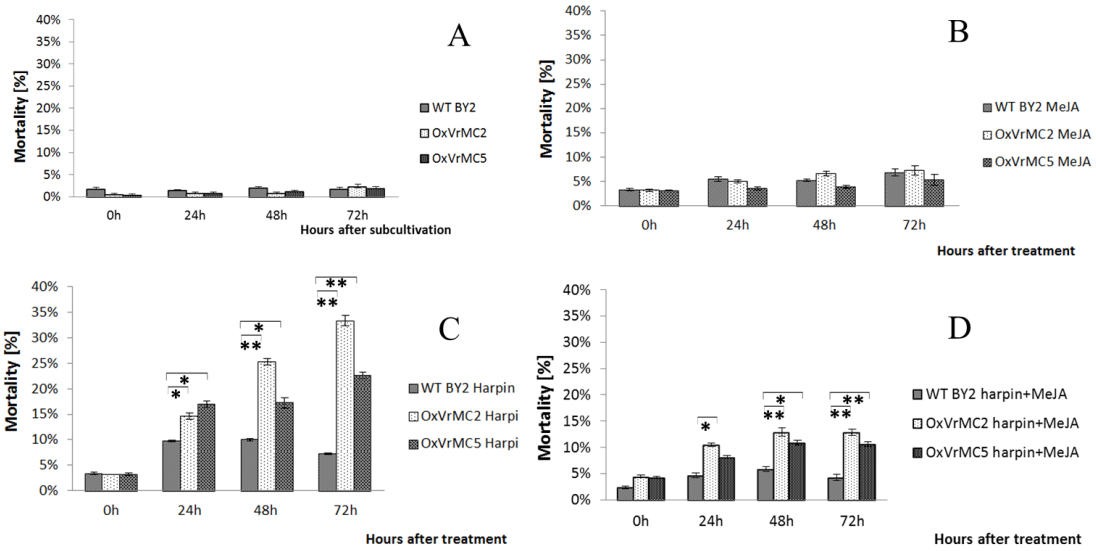

Figure 3.16 Cell mortality assays of suspension cell lines after Harpin and MeJA elicitation
The columns show the relative frequency of dead cells of Ox-*VrMC2* and Ox-*VrMC5* as compared to wild type BY2 control under normal condition (A) under normal cultivation, control, (B) after 100 µM MeJA (Methyl jasmonate) treatment, (C) after 27 $\mu g \cdot ml^{-1}$ harpin treatment, (D) after 100 µM MeJA +27 $\mu g \cdot ml^{-1}$ harpin treatment. * indicates differences that are statistically significant on the level $P < 0.05$. **indicate differences that are statistically significant on the level $P < 0.01$. Mean values and standard errors from three independent experimental series are shown.

Both overexpressing BY-2 cell lines *35S*::VrMC2-GFP and *35S*::VrMC5-GFP were exposed to a harpin treatment and mortality was evaluated three days after onset of the treatment using Evans Blue staining to get an insight into the cell death functions of *VrMC2* and *VrMC5* genes. Firstly, both untreated cell lines and WT BY2 as a

control were measured under normal growth condition after subcultivation (Fig. 3.16 A). Results during the first three days showed that the mortality percentage of WT BY2 was maintained at a very stable level around 2.5 %. There was no significant difference found between any time points of either transgenic cell line compared to WT under standard cultivation conditions. Since VrMC2 and VrMC5 were properly expressed, all three cell lines share a common viability, indicating that metacaspases were probably overexpressed in their inactive forms

An HR-like response in grapevine induced by exogenously added MeJA was observed in leaves and in suspension culture cells (Repka *et al.*, 2004). Although activation of the JA pathway is often correlated with HR, the actual evidence for a causal relationship has remained scarce (Chang *et al.*, 2017). An amount of 100 µM MeJA was treated on both overexpressor cell lines to further investigate the relationship between metacaspase-dependent cell death and jasmonate signalling (Fig. 3.16 B). The results showed that the mortality percentage of WT BY2 was slightly increased during 24 and 48 h, and up to 6.9 % at 72 h after treatment. However, this trend is quite similar to both *VrMC2* and *VrMC5* overexpressing cell lines, where the cell death rate was not significantly changed, even after incubation for 72 h.

Our previous studies have shown that harpin induced HR-like cell death in *V. rupestris* cell cultures and caused a strong increase up to almost 60 % at 72 h, but not in cell cultures of cv. 'Pinot Noir' (Chang and Nick, 2012). This result was regarded as a characteristic feature for mimicking the advanced immunity ETI level in a cell culture system. In our current test, two overexpressed cell cultures were treated with 27 $\mu g \cdot ml^{-1}$ harpin to induce HR to gain insight into the cell death executing functions of *VrMC2* and *VrMC5* (Fig. 3.16 C). At 24 h after treatment, the cell death of WT increased strongly to 9.7 %, whereas the mortality percentages in both overexpressing VrMC2 and VrMC5 cell lines, were significantly higher (14.6 and 17 %, respectively). At 48 h after elicitation, the WT was maintaining a steady state cell death rate of 10 %, but the cell death rate of Ox-VrMC2 and Ox-VrMC5 increased further until 72 h after elicitation and finally reached up to 33.3 and 26.6 %, respectively. However, the cell death rate in the WT at 72 h returned to even lower levels of 7.3 %. Moreover, we used 100 µM MeJA treatment prior to harpin treatment. The result showed that MeJA could prevent the strong activation of cell death by 27 $\mu g \cdot ml^{-1}$ harpin (Fig. 3.16 D).

MeJA pretreatment could also reduce harpin-induced mortality to an even lower level, even in the non-transformed WT, and cell death rate in both transgenic lines reached only about 50 % of the one observed with MeJA treatment.

This result implies that *VrMC2* and *VrMC5* certainly contribute a dominant role to execute HR under harpin-induced PCD, but not in response to MeJA. In addition, *VrMC2* was more effective in inducing cell death in response to harpin than *VrMC5*. In addition, MeJA was able to reduce harpin-triggered HR in both overexpression cell lines, indicating that jasmonate signalling might be a negative factor in HR regulation.

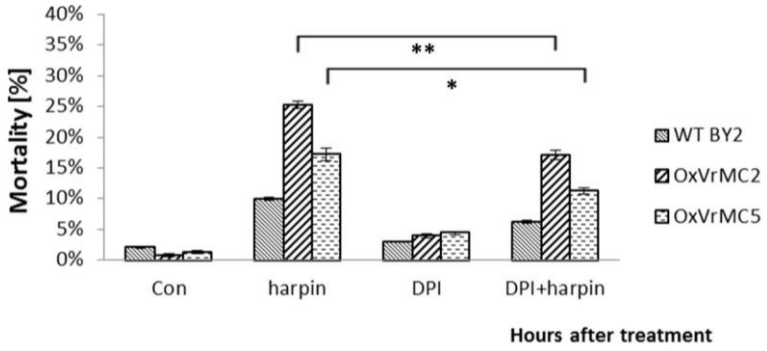

Figure 3.17 Effect of the NADPH-oxidase inhibitor Diphenyleneiodonium (DPI) on cell death of VrMC2 and VrMC5 overexpressors induced by harpin.

Mortality was scored after 48 h of treatment with DPI (0.2 µM), harpin (27 µgml¯1), or the combination of both in non-transformed BY-2 versus Ox-*VrMC2* and Ox-*VrMC5*. * indicate differences that are statistically significant on the $P < 0.05$ level. **indicate differences that are statistically extreme significant on the $P < 0.01$ level. Mean values and standard errors from three independent experimental series are shown.

The rapid generation of reactive oxygen species (ROS), termed oxidative burst triggered by the NADPH oxidase, is correlated with activation of cell death by harpin treatment in *V. rupestris* suspension cells (Chang and Nick, 2012). The NADPH oxidase inhibitor DPI was used to quell the increase of ROS abundance before cell death elicitation to test whether the oxidative burst is necessary for VrMC2/VrMC5-mediated cell death. As shown above (Fig. 3.17), after 48 h of the application of DPI with harpin, the cell mortality value was substantially suppressed in all three cell lines and the inhibitions were much more pronounced in OxVrMC2 cells. These data indicated that the NADPH oxidase participates in the mechanism responsible for the VrMC2/VrMC5 -dependence of harpin-triggered cell death.

3.7 *Cis*-element comparison of the pMC2 and pMC5 promotor between *V. vinifera* cv. 'Müller-Thurgau' and *V. rupestris*

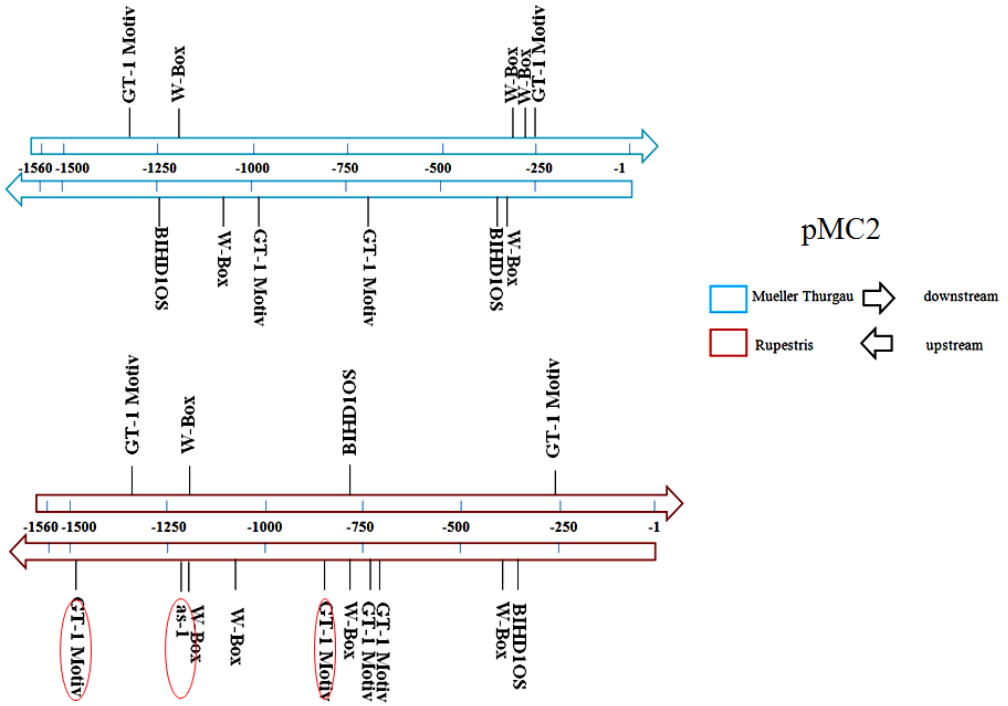

Figure 3.18 Cis-element distribution analysis of pMC2 in grapevine (pathogen response-related elements were showed)

Cis-element distribution in both upstream and downstream sequences of the MC2 promoter of *V. vinifera* cv. Mueller Thurgau (blue) and *V. rupestris* (red). The number scale refers to the base pairs before the initiation codon ATG of the respective gene from three independent experimental series are shown.

To get insight into the regulatory features of the two prime metacaspase candidates, we cloned for all 4 promoter regions (pMC2 and pMC5 from both *V. vinifera* cv. 'Müller-Thurgau and *V. rupestris*) 1500~1600 bp upstream of the translational start codon. The alignment of these putative promoter regions revealed a high degree of identity (around 95%) between the *pMC2* from *V. vinifera* cv. 'Müller-Thurgau' (abbreviated as *pVvMC2*, GenBank: KY069976) and *V. rupestris* (abbreviated as *pVrMC2*, GenBank: KY069977), as well as between the *pMC5* from *V. vinifera* cv. 'Müller-Thurgau' (abbreviated as *pVvMC5*, GenBank: KY069978) and *V. rupestris* KY069979).

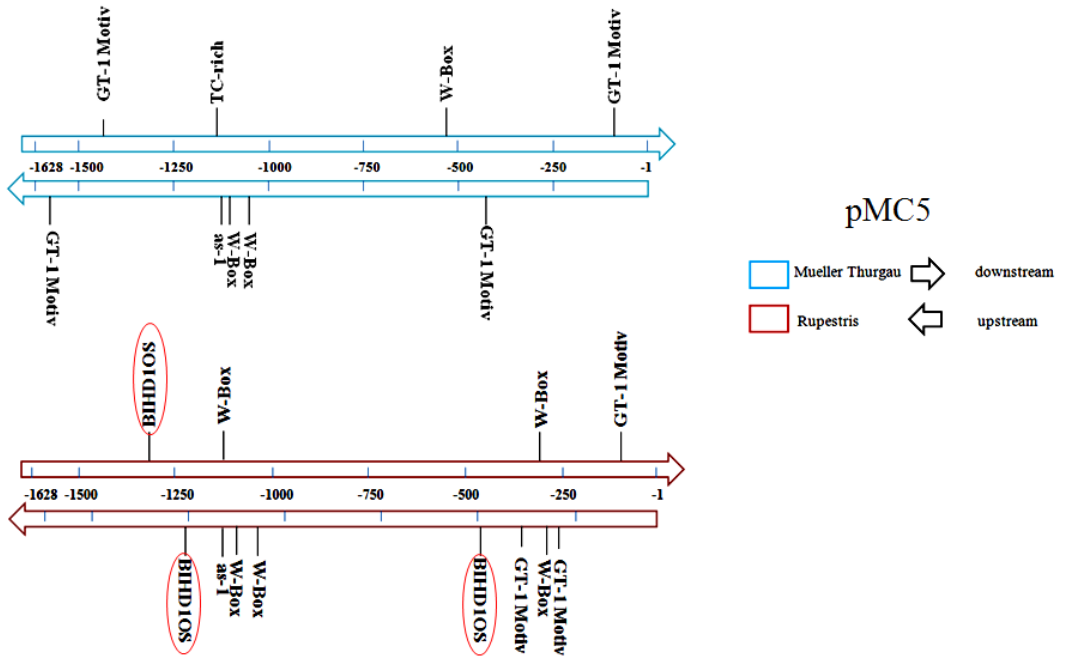

Figure 3.19 Cis-element distribution analysis of pMC5 in grapevine (pathogen response-related elements were showed)

Cis-element distribution in both upstream and downstream sequences of the MC2 promoter of *V. vinifera* cv. Mueller Thurgau (blue) and *V. rupestris* (red). The number scale refers to the base pairs before the initiation codon ATG of the respective gene from three independent experimental series are shown.

A scan for putative cis-regulatory elements using both the PlantCARE database (Lescot *et al.*, 2002) and the website PLACE (http://www.dna.affr c.go.jp/PLACE/), revealed that generally in the upstream sequences of *V. rupestris* the number of cis-elements is universally higher (see Appendix 5.11), and that the two *pMC2* regions harbour significantly more predicted cis-elements related to defence as compared to the respective *pMC5* regions (Figs. 3.18 and 3.19). In the case of *pMC2*, the allele of *V. rupestris* harbours two predicted GT-1 motives, predicted to be involved in the response to pathogen and salt stress, as well as one as-1/ocs element-like motif involved in defence (Chen *et al.*, 2002; Park *et al.*, 2004). These three predicted motives are not found in the *pMC2* allele from cv. 'Müller-Thurgau'. Likewise, the *pMC5* allele from *V. rupestris* contains three predicted BIHD1OS motives, proposed as regulator of disease resistance (Luo *et al.*, 2005). Again, this element is absent the *pMC5* allele from *V. vinifera* cv. 'Müller- Thurgau'. It should be mentioned that none

of the four putative promoter alleles contained any of the known jasmonate-related response elements or enhancer existed from any promoter sequence (detail see in Appendix 5.11).

3.8 Harpin activates promoter activity of both *pVrMC2 and pVrMC5*

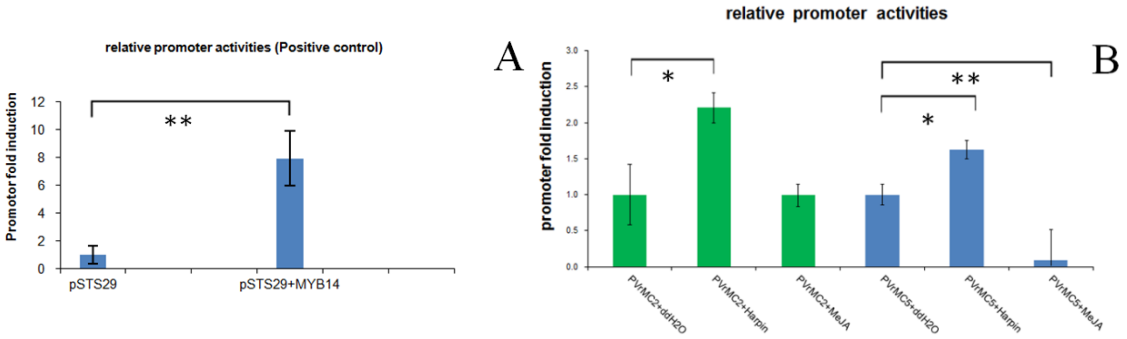

Figure 3.20 Dual luciferase assay for measuring pVrMC2, pVrMC5 promoter activity after Harpin and MeJA treatment

A: The columns show the relative activity values of pVvSTS29 promoter without treatment and fold induction level by MYB14 transcriptional factor activation. These vectors was transformed and set only as positive control to test the whole system. B: The columns show the relative activity values of pVrMC2, pVrMC5 promoters with sterile distill H_2O as negative control and fold induction level at 24 h after 27 ug/ml harpin and 100uM MeJA (Methyl jasmonate) treatment, respectively. * indicate differences that are statistically significant on the $P < 0.05$ level. **indicate differences that are statistically extreme significant on the $P < 0.01$ level.

The dual-luciferase reporter assay system (Holl *et al.*, 2013) was employed to investigate whether the activation of *VrMC2* and *VrMC5* in response to *P. viticola* is linked with the activation of the respective promoters in the context of cell death-related defence. We used the elicitor harpin to trigger cell death-related defence after using transient expression of the promoter-reporter system in a suspension culture of *V. vinifera* cv. 'Pinot Noir', which, by itself, shows only a low cell death activity (Chang and Nick, 2012). We used co-expression of a stilbene-synthase promoter, pSTS29/pLuc, and its transcriptional activator, MYB14/pART7, as a positive control to verify the stability of the system (Holl *et al.*, 2013). Compared to expression of pSTS29/pLuc alone, the co-expression with this transcriptional activator stimulated luciferase activity by a factor of 8 (Fig. 3.20 A), which is consistent with published results (Holl *et al.*, 2013).

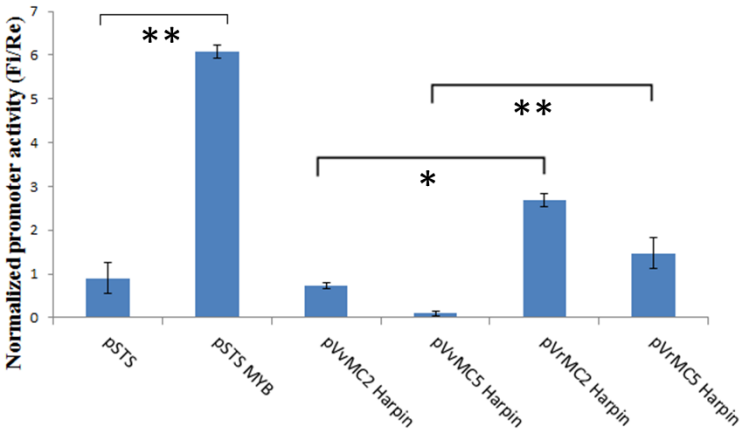

Figure 3.21 Dual luciferase assay for comparison of pMC2, pMC5 promoter activity between *V. vinifera* cv. 'Mueller Thurgau' and *V. rupestris* after 27 µg/ml harpin treatment

The columns show the relative activity values of *pVrMC2*, *pVrMC5*, *pVvMC2* and *pVvMC5* promoters with sterile distill H_2O as negative control and normalized induction level at 24 h after 27 µg/ml harpin. * indicate differences that are statistically significant on the $P < 0.05$ level. **indicate differences that are statistically extreme significant on the $P < 0.01$ level.

In the second step, we measured the activation of the *VrMC2 and VrMC5* promoters in response to the elicitor harpin (27 $\mu g \cdot ml^{-1}$) compared to a mock treatment with sterilized water as a solvent control, which did not produce any significant modulation of promoter activity, either for *pVrMC2* or for *pVrMC5* (Fig. 3.20 B). By contrast, the activity of *pVrMC2* in response to harpin was induced by 120 % and the activity of *pVrMC5* by 60 %. Since the analysis of putative cis-elements had not uncovered any of the known jasmonate-response elements, we also measured promoter activations in response to 100 µM MeJA. Neither the activity of *pVrMC2* nor that of *pVrMC5* was activated by MeJA. Surprisingly, the activity of pVrMC5 was completely repressed by MeJA.

We further measured the harpin response of the respective promoter alleles from *V. vinifera* cv. 'Müller-Thurgau'. No activity stimulation was found on *pVvMC2* and *pVvMC5*. The results further confirmed that *pVrMC2* was more responsive to harpin elicitation than *pVrMC5* (Fig. 3.21).

Overall, our promoter activity assay verified our former gene expression results: both pVrMC2 and pVrMC5 activities were approximately doubled after Harpin treatment. However, pVrMC2 showed no response for MeJA, and pVrMC5 activity even decreased after adding MeJA.

3.9 *VrMC2* and *VrMC5* expression induced after harpin treatment in grapevine cell culture

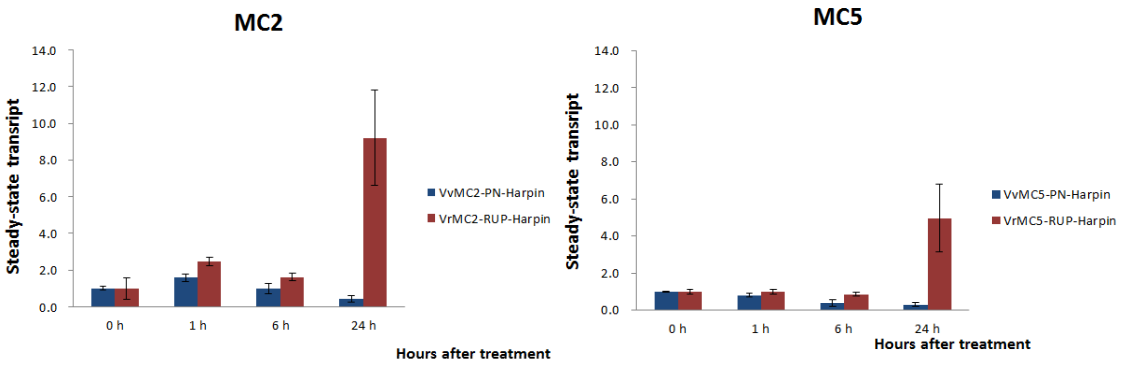

Figure 3.22 Quantitative PCR expression assays of *MC2* and *MC5* genes between *V. vinifera* cv. 'Pinot Noir' and *V. rupestris* cell culture after harpin treatment

Quantification of transcripts of metacaspase2 and metacaspase5 at 0 hour, 6 hours 12 hours and 24 hours after harpin (27 µg/ml) treatment by quantitative real-time PCR. Actin was used as internal reference gene. Data represent mean values from 3 independent experimental series. Y-axes are scales of relative expression level (error bars indicate ±standard errors).

The gene expression pattern has also been confirmed in grape cell culture systems, using harpin as an elicitor in two *Vitis* cell lines: *V. rupestris* as a resistant line and cv. 'Pinot Noir' as a susceptible line. Results showed that only *VrMC2* and *VrMC5* in *V. rupestris* were up-regulated 24 h after treatment with harpin (27 µg/ml). By contrast, the expression patterns of *VvMC2* and *VvMC5* from cv. 'Pinot Noir' confirmed that the genes from *V. vinifera* are not inducible by harpin.

3.10 Summary of results

For a better understanding of the roles of metacaspases on HR process, the grapevine - *Plasmopara viticola* interaction was included as a unique experimental model in this

study. Based on 8 time-points under same infection conditions by *P. viticola*, a screening system was established to filter out two genes as prime candidates amongst all *Vitis* metacaspase members, named *VrMC2* and *VrMC5*. Those two genes showed up-regulated expression in *V. rupestris* after 48h of infection using semi-quantitative RT-PCR and qPCR. After screening, *VrMC2* and *VrMC5* were cloned and further functional analyses were carried out by over-expressing each gene fused with GFP in tobacco BY-2 suspension cells. We found that VrMC2 and VrMC5 exhibited differential subcellular localization. Besides, results revealed harpin as a bacterial elicitor, that induced HR in overexpression cell lines of VrMC2 and VrMC5. MeJA could not induce HR, but clearly repress harpin-induced cell death. These findings provide more insight into the function of metacaspases in grapevine during HR process, and indicate their possible roles in ETI-related defence signalling.

To get insight into the gene regulation mechanism of metacaspases, promoters of *MC2* and *MC5* were cloned from both genotypes *V. rupestris* and *V. vinifera* (cv. ‘Müller-Thurgau’). Cis-element analysis showed there are more pathogen-responsive motives distributed on *pVrMC2* and *pVrMC5* than *pVvMC2* and *pVvMC5* respectively, such as GT-1 motives, BIHD1OS motives, as-1/ocs element-like motives. Using a promoter–reporter assay in grapevine suspension cells (Holl *et al.*, 2013), results revealed both *pVrMC2* and *pVrMC5* activities were doubled after harpin treatment, whereas no induction appeared in ‘Müller-Thurgau’. These findings not only correlated well with the transcriptional regulation of *VrMC2* and *VrMC5*, but also suggested that specific cis-elements regions in the promoter of *VrMC2* and *VrMC5* may harbour potential candidate targets for resistance breeding.

4. DISCUSSION

An increasing amount of research with mixed features has been described in regulating plant HR over the last decade. Simultaneously, an increasing number of HR-regulating genes have been identified and several lines of evidence have suggested a function for metacaspases in plant HR, such as *AtMC1*, *AtMC2*, *AtMCP2d* and *LeMCA1* (Coll *et al.*, 2010; Hoeberichts *et al.*, 2003; Watanabe and Lam, 2011a). The entire gene family of metacaspase in grapevine has already been uncovered, but there are still questions that remain unclear regarding HR-regulating gene members. Therefore, the aim in this study was to explore the metacaspase candidates responsible for mediating HR, and then try to get an insight into their function and further molecular mechanisms underpinning the role of HR in defence signalling.

VrMC2 and *VrMC5* were chosen based on a logical expression analysis filter. Both their ORFs were cloned and corresponding overexpressed lines were established in BY-2 cells to get insights into the cellular functions of these two members. We then focused on the cellular functions of VrMC2 and VrMC5 and answered the following main questions: Where are VrMC2 and VrMC5 localised, what is their cellular function and how do *VrMC2* and *VrMC5* function in response to factors related to HR signalling?

The first half of this study revealed that HR correlates with *VrMC2* and *VrMC5* transcripts in response to infection by *P. viticola*. Furthermore, we asked whether the induction of *VrMC2* and *VrMC5* transcripts might result from the upstream promoter regulation. In other words, does a promoter of *VrMC2* or *VrMC5* mediate their own gene as an HR-inducible promoter? To get insight into the question, promoters of *MC2* and *MC5* were isolated and distribution of cis-elements was analysed from both genotypes *V. rupestris* and cv. ‘Müller-Thurgau’. Lastly, promoter activity measurement revealed that the *pVrMC2* and *pVrMC5* were both responsive to harpin treatment, whereas *pVvMC2* and *pVvMC5* were not.

4.1 Characterization of disease outbreak and HR among 9 different grape varieties

Some downy mildew-resistant varieties in grapevine are highly associated with the ability of mounting a localized HR, whereas some are also resistant without HR, probably based on different resistance mechanisms. During the HR process, necrotic spots become apparent rapidly after the initiation of the infection. Hence, *P. viticola* was commonly used as an ideal experimental material for eliciting HR (JG. Zeledón *et al.*, 2016; Liu *et al.*, 2015). Although further reports revealed these varieties harbouring the locus *Rpv3* are capable of operating HR against downy mildew, the defence reactions differed among various genotypes. Hence, in this study, a set of nine host genotypes (three *Rpv3*$^{-}$-susceptible, three *Rpv3*$^{-}$-resistant, three *Rpv3*$^{+}$-resistant) were investigated to observe the possible differences in the incidence of HR to *P. viticola*. Because the origin of this oomycete is North America, it has been present throughout the evolutionary history of the *Vitis* varieties in the same region; therefore. as expected, all three North American varieties were highly resistant to *P. viticola* with the development of necrosis (Fig. 3.1). *V. rupestris* especially could completely block the sporulation of the strains selected and the necrotic spot symptoms were very obvious. Moreover, regarding timing, the appearance of necrotic spots from American grapes preceded visibly sporulation from susceptible European grapes, affirming that the HR phenomenon inhibits the spread of this pathogen and plays a positive role in disease resistance. In addition, sporulation in *V. riparia* has been found by others (JG. Zeledón *et al.*, 2016), but in our study, sporangium formation could not be observed on *V. riparia* inoculated leaf discs. Since the same stain 1191-B15 was used, it can be concluded that sporangia viability, inoculum concentration and environmental conditions are variable factors for the sporulation success on this highly resistant variety.

4.2 The potential role of the metacaspase gene family in (HR) biotic stress response in grapevine

Although the metacaspase activities are regulated mainly on a post-translational level in plants (Lam and Zhang, 2012; Vercammen *et al.*, 2004; Zhang and Lam, 2011), some studies showed that transcriptional regulation of the metacaspase expression is

also a major mechanism to regulate HR by a wide range of biotic stresses. *TaMCA4*, a Type II *metacaspase* gene in wheat, for instance, was expressed increasingly after 24 h under infection by the pathogen *Puccinia striiformis* f. sp. *tritici*. Enhancement of PCD was also detectable in wheat leaves overexpressing *TaMCA4*. Moreover, after knocking down *TaMCA4*, the susceptibility of wheat was enhanced and the necrotic area at infection sites was reduced under the same infection conditions (Wang *et al.*, 2012). Although the metacaspase family of grapevine has been previously characterized (Zhang *et al.*, 2013), none of the family members has yet been studied for the biological function in plant HR via the level of gene expression. In addition, previous results indicated that members of the *VvMC* family expressed quiet differentially in various tissues and organs, as well as during different stages of ovule development between seed and seedless cultivars. That implied responsiveness of the metacaspase family members might also vary under the HR process between *V. vinifera* and *V. rupestris* to some extent. Therefore, establishing a logical filter for screening *MC* candidates which respond most strongly during HR was a good approach to identify candidate genes for HR regulation in the metacaspase family of grapevine.

Since the expression of most MC genes was tissue- and organ-specific, the genes not expressed in leaves could be removed in the first step. These results were also consistent with our previous report. *VvMC4*, for instance, was specifically expressed in stem and *VvMC6* was dominantly expressed in flower (Zhang *et al.*, 2013). Meanwhile, both *βVPE* and *δVPE* have been reported as ovule-specific expressed genes. Our results further indicated that these genes are silent in leaves and not inducible after biotic stress (Appendix 5.8). We had an expectation that the candidate *MC* should be expressed increasingly before pathogen-dependent HR occurred. In addition, the candidate gene should be specifically up-regulated only in *V. rupestris* under infection. Under these criteria, *MC1* and *MC3* were further excluded due to their only weak response on the susceptible cultivar or up-regulation at a later time-point. By contrast, MC2 and MC5 in *V. rupestris* were detected weakly in the initial phase, but showed an obvious increase at 24 hpi, so only the expression of *VrMC2* and *VrMC5* matched the filter criteria (Fig. 3.6). These two genes were then regarded as HR-related genes in grape, and considered for further analysis.

MC function analysis in other plant species had revealed that the responsiveness of each member of the MC family varies in response to PCD-induced by different elicitors. AtMC8, for example, was required for UVC stress-induced cell death; AtMC4 mediates PCD activation by the fungal toxin FB1 and abiotic stress inducers; and McII-Pa was verified to be required for embryogenesis-associated PCD (He *et al.*, 2008; Suarez *et al.*, 2004; Watanabe and Lam, 2011a). Therefore, our results also implied that other MCs in grape which do not function in *P. viticola*-induced HR, probably play PCD-executor roles in other tissues or other developments requiring induced PCD processes.

Furthermore, qPCR assays revealed that there was a transient increase in the expression of both *VrMC2* and *VrMC5* at 24 hpi, due to the effect of infiltration (Fig. 3.7). However, each candidate's expression level declined immediately after 48 hpi, back to a level fluctuating around the expression level at 0 hpi. That indicated that there might be no need for *VrMC2* and *VrMC5* to sustain high expression in a prolonged time period on the transcript level. Instead, just a transient up-regulation before HR occurs might be sufficient for activating an HR cascade. The reason behind it might be that MC is initially formed as inactive form. The activity of MC can be achieved later by self-processing of the protein in the case of PCD induction (Lam and Zhang, 2012). In animals, the initiator caspase proprotein is activated by auto-proteolytical cleaving, while the executor caspase is further cleaved by activated initiator caspase. This hierarchical structure allows an amplifying chain reaction or cascade for degrading cellular components during controlled cell death (Slee *et al.*, 1999). The MCs are structurally related to caspases. Thus, combined with our results, it implied there would be a more complex regulation mechanism of MC existing to activate PCD on a translated or post-translated level in grapevine.

4.3 Phylogenetic analysis of MCs in plant species

The construction of phylogenetic trees allows the analysis of the evolutionary history and relationships among individuals or groups of organisms. Previously, a small scale tree has been constructed containing only *Arabidopsis* and grapevine metacaspases in order to identify the gene family in *Vitis* (Zhang *et al.*, 2013). In this study, to further obtain insight into the evolutionary history and phylogenetic relationships of more

comprehensive metacaspases in plant, a more systematic tree has been constructed using Neighbour-Joining method (Fig. 3.11). Based on dividing all members into six main branches, we also observed that some representatives from the same plant species formed sub-clusters inside the class, such as OsMC1, OsMC2 and OsMC3; or AtMC4, AtMC5 and AtMC6. This observation suggests that duplication events might have occurred after the formation of species. Furthermore, putative metacaspases from the algae *Chlamydomonas*, as ancient representatives, are presented as out-group from the principal six clusters formed by plant metacaspases, either indicating the classification of metacaspases originated in the early stages of plant evolution.

4.4 VrMC2 and VrMC5 exhibit differential subcellular localization

To explore the subcellular localization of the VrMC2 and VrMC5 proteins, secondary structure of these deduced amino acid sequences was analysed firstly by PSORT (http://psort.ims.u-tokyo.ac.jp/). It predicted that VrMC2 possesses a zinc finger domain Znf_LSD1 in the N-terminus. Although no targeting signals could be found in the VrMC2 protein sequence (some I type metacaspase contain nuclear located sequences, NLS), the presence of the zin finger domain suggested VrMC2 might be capable of the interaction with LSD proteins, which were reported as negative regulators of PCD, via repressing the activity of LSD protein by binding of VrMC2 on the Znf_LSD1 domain, like in the case of AtMC1 and AtLSD1 *in Arabidopsis* (Coll *et al.*, 2010). In addition, we found there is an ER membrane retention signals, termed KKXX-like motif: KPFI in the C-terminus of VrMC2, implying this protein is probably present in the ER. However, in the case of VrMC5, no obvious signal peptide or organelle-targeting signal was found, implying that VrMC5 protein is probably located in the cytoplasm. All these predictions are consistent with our actual observation.

Not all of the metacaspases of the same type share the same subcellular localization pattern. For instance, the homologous gene OsMC1 was reported that solely localized to the nucleus probably because it contains an NLS in the N-terminal region (Huang *et al.*, 2015). There was no NLS found in VrMC2, but containing ER membrane retention signal instead. This is the possible reason that causes VrMC2 such specific localization (Fig. 3.12). On the other hand, VrMC5-GFP fusion protein was observed

mainly in the cytoplasm, although weak fluorescence was also detectable in the nucleus (Fig. 3.12). This result was corresponding with the localization of homologous genes OsMC5 and OsMC6 in rice and AtMC4 in *Arabidopsis* (Huang *et al.*, 2015; Watanabe and Lam, 2011a).

In addition, Arabidopsis AtMC9 has been reported to be located in the nucleus, cytoplasm and apoplast (Tsiatsiani *et al.*, 2013). But its subcellular localization can be changed from evenly distributed in cytoplasm of living cells to patches or aggregates of various sizes in cells during late autolysis (Bollhoner *et al.*, 2013). Hence, it needs to be examined further, whether dynamics in subcellular localization upon different death stages would be observed in the case of VrMC2 and VrMC5 proteins. The subcellular localization was further confirmed by a Western blot approach (Fig. 3.15). Consistently with microscopical studies, VrMC2-GFP was exclusively detected in the microsomal fraction by Western blot, but not in cytosolic proteins. In contrast, VrMC5-GFP was found in both microsomal and soluble fraction.

4.5 Harpin and MeJA: elicitor and repressor of HR

Constructing a heterologous over-expression system and using various cell death elicitors for treatment, is a common assay system for evaluating the cell death function of metacaspases in plants. For instance, using overexpression via transient or stable transformation into tobacco plants, a pepper metacaspase gene called *Camc9* has been reported to positively influence bacterial pathogen-induced cell death after infection with *Xanthomonas campestris* pv. *Vesicatoria*, (Kim *et al.*, 2013). However, it is not clear whether this Camc9-induced cell death is correlated with ETI-triggered HR. For this purpose, a specific HR-elicitor applied to metacaspase overexpressing plants is needed.

Harpin, as a trigger for HR-like cell death, has acquired a considerable interest since a long time (Baker *et al.*, 1993). Moreover, harpin protein has been used in our group in previous work to mimic various aspects of ETI in grapevine suspension cells, including activation of rapid oxidative burst, delaying calcium influx and following induced cell death (Chang and Nick, 2012; Chang *et al.*, 2017). In this study, the mortality in response to harpin was strongly promoted from 24h and keeps increasing till 72h after treatment in both *VrMC2* and *VrMC5* overexpressors (Fig. 3.16).

Therefore, this unique quick cell death response to harpin could also be seen as HR-like phenomenon. It indicated more precisely that VrMC2 and VrMC5 are responsible for regulating ETI-like triggered HR process. However, beside the VrMC2 or VrMC5, tobacco has endogenous MCs as well which potentially may function as cell death regulator. There is a type II metacaspase named *NbMCA1*, which has been reported from *Nicotiana benthamiana* and showed a peak in expression at 72 h after *Colletotrichum destructivumi* inoculation (Hao *et al.*, 2007). In this study, the cell death fluctuation in WT probably implied that the metacaspase homologues in tobacco may have synergistic effect with VrMC2 and VrMC5 during harpin induction. In future it would be further addressed which MC family homologues exist in tobacco BY-2 cells and how their expression would be regulated during HR.

JA as a well-known plant hormone also has reported to play a role associated with HR in responses to pathogens. On the one hand, in both tobacco plants and *Arabidopsis* protoplasts, accumulation of JA could be observed during defence-related cell death (Kenton *et al.*, 1999; Zhang and Xing, 2008). On the other hand, JA negatively regulates cell death in *A. thaliana* under oxidative stress caused by ozone treatment (Tamaoki, 2008). It has also been found that hijacking of the jasmonate pathway by the mycotoxin fumonisin B1 (FB1) could initiate PCD in *Arabidopsis* (Zhang *et al.*, 2015). Therefore, although regulation of the JA pathway is often correlated with HR, the actual evidence for a causal relationship has remained scarce. The differences of JA with respect to cell death still need to be elucidated. According to our results, sole MeJA treatment did not induce cell death rate in any type of cell lines, indicating that it possesses no positive effect as HR inducing compound in BY-2 cell lines (Fig. 3.16). Furthermore, harpin-induced mortality was decreased when cells were treated with MeJA in both overexpressors. That implies that jasmonate signalling might be a negative regulator of the HR process.

It is worth mentioning, that under the same conditions, values of mortality of *VrMC2* were induced stronger and showed more significance as compared to WT under either harpin or MeJA/harpin treatment, suggesting *VrMC2* probably demonstrates a more pronounced ability to perform cell death than *VrMC5*.

4.6 Relationship between promoter activity and inducible gene expression

The expression of plant genes at the transcriptional level is mainly due to the coordination of multiple cis-acting elements and trans-acting factors. The plant gene promoter, as an important cis-acting element, is a cluster of functional DNA located on 5' upstream sequences of transcription initiation site. It triggers initiation of gene transcription and regulates transcriptional activity (Allison, 2007). An entire promoter normally includes 3 parts: core promoter element (located around -35 bp), proximal promoter element (around -250 bp) and distal regulatory element (> -300 bp). Among them, the core promoter element is most important functional area and can be recognized by RNA polymerase II and other subunits to initiate transcription (Smale and Kadonaga, 2003). According to the characteristics of promoter, it can be further divided into three types: constitutive promoter, tissue-specific promoter activated via specific growth stage or tissues, and inducible promoter. Among them, only inducible promoter's activity is influenced by the presence or absence of biotic or abiotic factors. Then we can accurately understand the related inducible gene function via its promoters because natural expression mode is driven by this type of promoter activities under different stress conditions. Moreover, inducible promoters could also drive other reporter genes to carry out self-regulated expression under different environmental conditions (Reynolds, 1999). That allowed activity of promoter assay could be tested precisely by using quantifiable marker.

Stress-inducible gene expression generally requires the interaction between transcriptional or environmental factors and cis-elements in their upstream promoter region. In planta, promoter activity assays have revealed that many promoters are activated and then further regulate their downstream expression of ORF by variable biotic and abiotic stress elicitors. For example, *Vitis pseudoreticulata* VpSTS promoter from the stilbene synthase gene in grapevine responds to defence signalling molecules, abiotic stresses and *Erysiphe necator* (powdery mildew) infection (Xu *et al.*, 2010; Xu *et al.*, 2011). Promoter activity of VpSTS could be qualified further by a dual-luciferase reporter system (Jiao *et al.*, 2016). We have found that *VrMC2* and *VrMC5* presented different expression profiles in resistant and susceptible cultivars after inoculation with *P. viticola*, but there is no ORF sequence difference between *V.*

rupestris and cv. 'Mueller Thurgau'. That suggested differential expression might be regulated by specific cis-elements located in the upstream region. Therefore, to elucidate the main mechanisms of metacaspase gene activation in response to HR-like elicitors' treatment, cis-elements involved in pathogen responsiveness and their distribution on promoter sequences must be identified first. Then the corresponding activities of specific promoter would be measured under the same elicitors' treatment. Our previous *in silico* cis-element analysis from NCBI genomic DNA sequences showed that there are a wide range of cis-elements playing various roles in either normal development of grape, or mediating responses to biotic or abiotic stresses (Zhang *et al.*, 2013). In our current study, we further found that there are 5 different kinds of defence related key cis-elements distributed on both *MC2* and *MC5* gene promoter region, such as W-box, TC-rich repeats, BIHD1OS, as-1/ocs element and GT-1 motif (Fig. 3.18; 3.19). Moreover, total number of each cis-element from *pVrMC2* and *pVrMC5* are higher than the numbers from *pVvMC2* and *pVvMC5*. The extra elements in *V. rupestris* promoters might be part of the reason to cause the higher response of transcripts in response to downy mildew. By using dual-luciferase system to detect the promoter activity, we found that specifically *pVrMC2* and *pVrMC5* promoters displayed increased activity in response to harpin treatment, but not promoters of *pVvMC2* and *pVvMC5* (Fig. 3.21). Since harpin is capable to mimicking ETI-like process and induce HR, these findings indicated that *VrMC2* and *VrMC5* gene expression trend were partially regulated by their corresponding promoter activities. All promoter activity assays suggested that specific cis-elements regions in the promoter of *VrMC2* and *VrMC5* may harbour a potential as a candidate target for resistance breeding.

4.7 A model for the signalling pathway of metacaspase-induced cell death

Pathogen effectors recognition via NLRs in animals and NB-LRRs in plants leads to inhibition of pathogen growth, which is often, but not always, accompanied by the HR in plants (Coll *et al.*, 2011). From the beginning of infection to the end, culminating in cell death, we found that there are various factors participating and contributing their functions to mediate HR successfully. Therefore, to describe an overall picture of cell

death mediated via active VrMC2 and VrMC5 in resistant grape *V. rupestris*, we will in the following, present a signature model of HR cell death signalling that can explain most and covered all our observations in this study (Fig. 4.1).

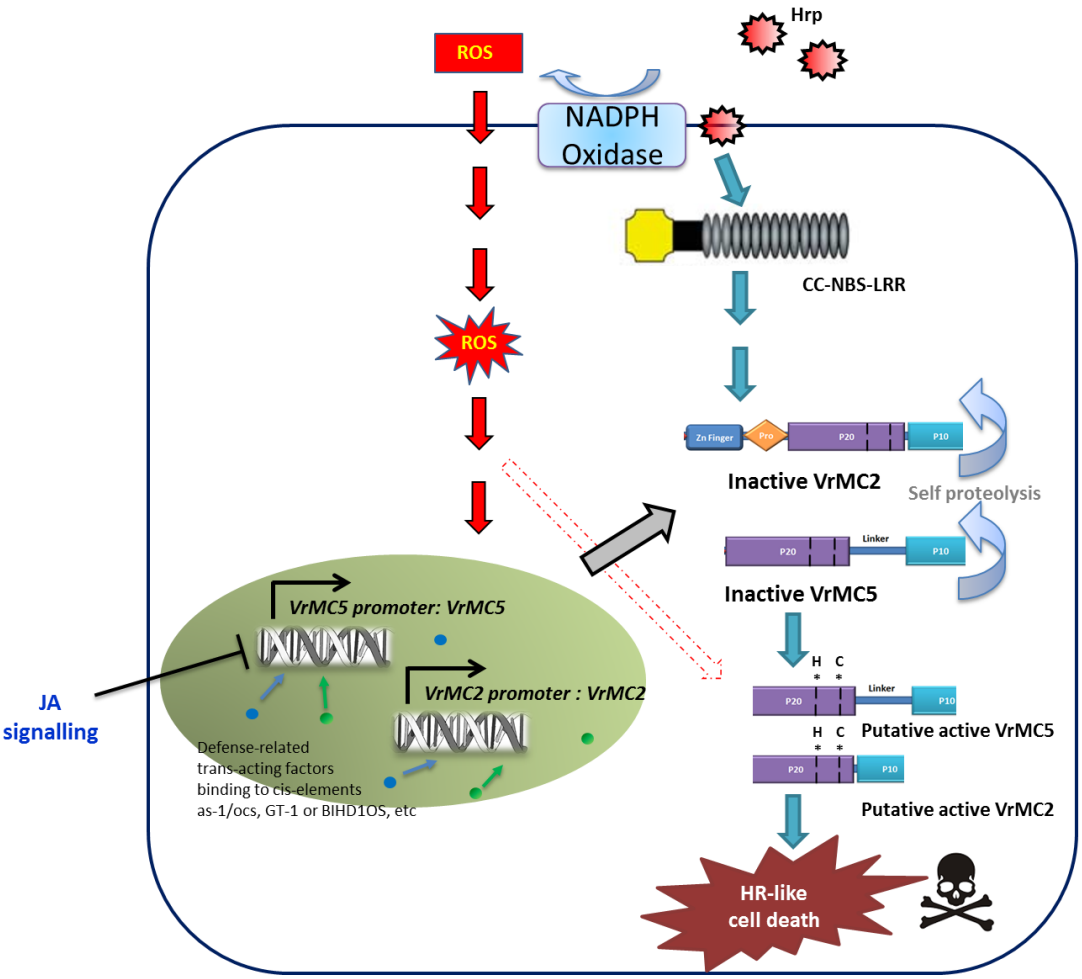

Figure 4.1 Model for VrMC2- and VrMC5-mediated HR-like cell death related signalling induced by harpin as effector-like elicitor.

The diagram represents some of the characteristic features of VrMC2 and VrMC5-mediated HR-like cell death that could occur in response to HR elicitor stimulation in plants. Details are explained in the discussion. Hrp, harpin as bacteria elicitor; CC-NBS-LRR, N-terminal coiled- coil domain, nucleotide-binding site, leucine-rich repeats, as R receptors to recognize elicitor; NADPH, Nicotinamide adenine dinucleotide phosphate hydrogen; ROS, reactive oxygen species; JA/MeJA, jasmonic acid/methyljasmonate; HR, hypersensitive response

Firstly, recognition of the bacterial elicitor harpin by the CC-NBS-LRR (R receptors) will lead to the stimulation of the membrane-bound NADPH oxidase-RboH, causing an increased production of ROS. Subsequently, the ROS burst signal activates the

expression of HR genes *VrMC2* and *VrMC5*. The activation depends on specific cis-elements in the VrMC2 and VrMC5 promoter regions, such as as-1/ocs, GT-1 or BIHD1OS. However, the activity of the VrMC5 promoter can be prevented by exogenous jasmonate application, suggesting a possible repressor function of jasmonate. Afterwards, inactive VrMC2 and VrMC5 pro-proteins will be synthesized and converted to an active protease by self-proteolysis after ROS stimulation. Consequently, active VrMC2 and VrMC5 act as executors to mediate HR-like cell death.

As we showed above, increased ROS levels induced by stimulation of the membrane-bound NADPH oxidase appeared as a hallmark of HR. Afterwards, increased ROS could act as a cell death signal into the nucleus, leading to induction of metacaspase gene expression. However, according to gene expression results from various plant species and our own results, this transcript change is mild and ephemeral. In addition, metacaspase is synthesized in the form of proprotein in the beginning, and the active form emerges via self-hydrolysis (Tsiatsiani *et al.*, 2011). Recent biochemical and molecular characterizations have shown that the formation of active metacaspase requires more sophisticated regulation, such as calcium and pH environment (Lam and Zhang, 2012). That implies post-translational regulation of metacaspase proteases would take more responsibility for regulating the execution of HR in plants.

4.8 Conclusion

In this dissertation, we wanted to elucidate the link between HR and metacaspase during the stimulation of the biotrophic pathogen *P. viticola* or bacteria effector harpin in grapevine. The whole project resulted in the following main findings:

1. HR-like necrosis is relative to *Rpv3*$^{+}$ grapevine resistance (especially in *V. rupestris*) induced by *P. viticola*.

2. *VrMC2* and *VrMC5* were expressed increasingly during the infection of *P. viticola*, correlating with cell death.

3. Based on features of conserved domains and molecular phylogeny, the VrMC2 and VrMC5 were clearly qualified as one type I and one type II sub-family member of the *Vitis* metacaspases.

4. VrMC2 and VrMC5 exhibit differential subcellular localization: VrMC2 is exclusively present on ER, whereas VrMC5 is located mainly in the cytoplasm.

5. Harpin can induce HR-like cell death on both VrMC2 and VrMC5 overexpressed cell lines. MeJA cannot induce cell death, but clearly repressed harpin-induced cell death.

6. Total numbers of defence-related cis-elements from *pVrMC2* and *pVrMC5* are higher than the numbers in *pVvMC2* and *pVvMC5*.

7. Promoters *pVrMC2* and *pVrMC5* displayed increased activity in response to harpin treatment, but not the promoters isolated from Müller-Thurgau, *pVvMC2* and *pVvMC5*.

4.9 Outlook: Two different cell death modes by the induction of harpin or MeJA treatment in grapevine cell culture

In the grape cell culture system, Xiaoli Chang has worked out defence signalling in two grapevine cell lines using the same harpin elicitor to induce HR-like cell death in the resistant cell line *V. rupestris*, but not in the susceptible 'Pinot Noir' (Chang and Nick, 2012). In addition, as we discussed above, JA and related conjugates, as a well-known plant hormone, not only play a role in basal immunity, but has also been reported to play a role associated with cell death. Intriguingly, in the case of *Vitis* suspension cells, we found exogenous MeJA could induce cell death on susceptible cv. 'Pinot Noir', but not on the resistant line *V. rupestris* (Fig 4.2).

We initially measured the detailed time-course of cell patterns produced by these two different elicitors via Evans Blue assay on six time points from 0 to 48 h. As we

expected, the results showed two opposite cell death modes induced by 9 µg/ml harpin and 100 µM MeJA treatment, respectively. The cell culture of the cv. 'Pinot Noir' is very responsive to MeJA, but is not responsive to the elicitor harpin, while *V. rupestris* is very responsive to the elicitor harpin, but not to MeJA.

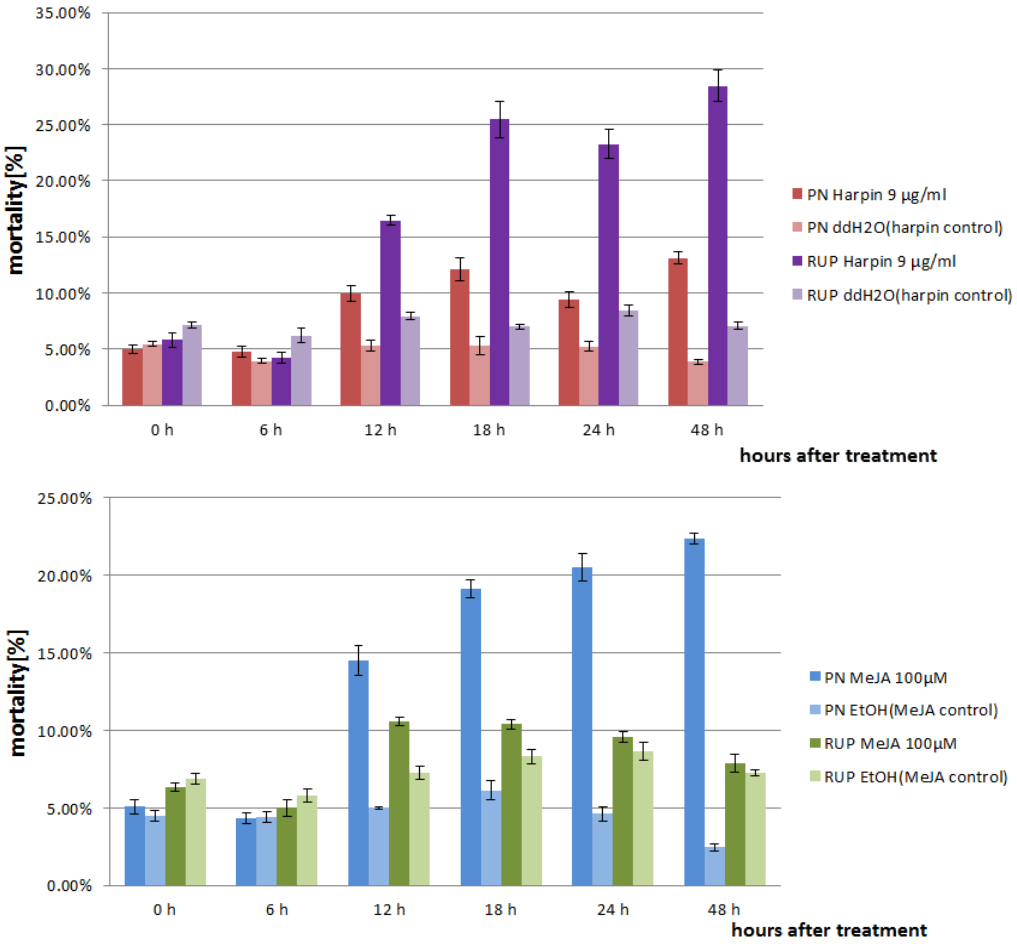

Figure 4.2 Time course of cell mortality in response to MeJA and Harpin.

The relative frequency of dead cells after treatment with MeJA (100 µM, blue and green bars, lighter blue and green bars as solvent control) or Harpin (9 µg/ml, red and purple bars, light red and purple bars as solvent control in *V. vinifera cv. 'Pinot Noir'* and *V. rupestris*, was followed over time scoring samples of 1500 cells for each data point. Mean values and standard errors from three independent experimental series are shown.

Future work will be directed to understand the mechanism behind these two modes of cell death. Since we know harpin-induced cell death in *V. rupestris* was regulated by VrMC2 and VrMC5, it will be interesting to elucidate whether metacaspases also play a role in MeJA-induced cell death in cv. 'Pinot Noir', and how the expression will be

regulated in response to MeJA treatment. Whether MeJA-induced cell death is of the PCD type or not will also be answered by gene expression analysis of metacaspases.

In addition, there will be a focus on potential PCD-related signals for manipulating the underlying signalling pathway of PCD in more detail, such as signals actin, reactive oxygen species, sphingolipids, MAPK cascades, phytoalexin (stilbene) induction, PR5 and PR10 proteins, and more caspase-like proteins. We want to further clarify the cellular function of these events and understand their interaction in the signal-specific context of plant PCD.

The second plan will include functional studies, where more genes of interest related to the signalling pathway of cell death will be overexpressed in BY-2 WT cells or loss-of-function T-DNA mutants will be obtained via the Crisp-cas technique. Alternatively, some of the players will be activated by chemical engineering (ROS pathway using mitochrondria-targeted Trojan Peptoids) or inhibition (blocking ceramide synthase by fumonisin B1 via competing structural sphingosine d18:1 analogues) additionally in the grapevine system. Actin bundling will be followed to ensure the relationship between these phenomena and PCD. We expect to be able to assign specific functions to individual events preceding PCD and to understand the context specificity of the respective signals as an important step to also manipulate plant immunity in the context of application.

5. APPENDIX

5.1 Table 1. List of suspension cell cultures and related cultivation conditions

Name of cell line	Antibiotics	Volume for Subcultivation	Reference
Vitis vinifera cv. 'Pinot Noir'	None	6ml	(Seibicke T, 2002)
Vitis Rupestris	None	8ml	(Seibicke T, 2002)
Wild Type BY-2	None	1ml	(Nagata et al., 1992)
Free GFP BY-2	25 $mg \cdot L^{-1}$ kanamycin	1.5ml	(Nocarová and Fischer, 2009)
VrMC2-GFP	45 $mg \cdot L^{-1}$ hygromycin	1.5ml	This paper
VrMC5-GFP	45 $mg \cdot L^{-1}$ hygromycin	1.5ml	This paper

5.2 Table 2. Primers sequences information for semi-quantitative and quantitative PCR analysis

Primer	Primer sequence (5'→3')	Primer	Primer sequence (5'→3')	Accession number
***QVv*MC1-F:**	ACCTCTTCCTCA TGGGGTTAAG	***QVv*MC1-R:**	TGTCCACTCC TGCTCATTCT G	KC494644
***QVv*MC2-F:**	TGGGGAGGTCA TTTCCTTTAG	***QVv*MC2-R:**	GGTTGATCGC ATTGAATTTA GC	KC494645
***QVv*MC3-F:**	CCCTACTCCTCC GCTTACCA	***QVv*MC3-R:**	GCGTCATTTA CAGACCCCTT C	KC494646
***QVv*MC4-F:**	CTCGGAAAAGG GCAAGCATA	***QVv*MC4-R:**	GGTTGAAGC ATCTCCCTCG TA	KC494647
***QVv*MC5-F:**	GAGGGTTGCCG CATTACGA	***QVv*MC5-R:**	GCACCTTGC ACGGTTTGGT	KC494648
***QVv*MC6-F:**	GACATGAATCCA ATGATGACCG	***QVv*MC6-R:**	CCGACTGCT GCTTGAAAA CC	KC494649
QRT-γVPE-F	ATCTATGCCACC ACAGCCGC	**QRT-*αVPE*-R**	TGTCCTCCAT CCAAGCAAC AC	KU240051
QRT-βVPE-F	TTCTACTTGGAC CAGAAAACGG	**QRT-*βVPE*-R**	ATTGGCGAA AGCCCTCATA	KC136352.1
QRT-δVPE-F	CTGGTTGGAGG ACAGTGAAATG	**QRT-*δVPE*-R**	GGATTTGTGC CCATGTAGGT GA	KU240052
QACT-F:	CTCTATATGCCA GTGGGCGTAC	**QACT-R:**	CTGAGGAGC TGCTCTTTGC AG	AF369524

5.3 Table 3. Primers information for *VrMC2, VrMC5* gene and corresponding promoter sequences cloning and related vector construction

Name of Primers	Sequence（5'→3'）	Purpose or vector
RUP-MC2-F	*CAGGCTTCATGATGATGCTGGTGGACTG*	*cDNA cloning pGEM®-T Easy*
RUP-MC2-R	*CTGGGTCGAGGATGAAAGGCTTTGAGT*	*cDNA cloning pGEM®-T Easy*
RUP-MC5-F	*AGGCTTCATGGGGAAGAAGGCAGTGTT*	*cDNA cloning pGEM®-T Easy*
RUP-MC5-R	*TGGGTCAATGTCGCAGATGAATGGAG*	*cDNA cloning pGEM®-T Easy*
pMC2-F	*AGGCTTCAGTGTGGCTTGGGTTAGGTT*	*gnomic DNA cloning pGEM®-T Easy*
pMC2-R	*TGGGTCTTCAAAAGCTGAAAGCACTT*	*gnomic DNA cloning pGEM®-T Easy*
PMC5-F	*AGGCTTCGCTAGCATTATCCGCTTGCA*	*gnomic DNA cloning pGEM®-T Easy*
PMC5-R	*TGGGTCGATTTGCTGTGTGTTTCCCT*	*gnomic DNA cloning pGEM®-T Easy*
GWRUP-MC2-F	*GGGGACAAGTTTGTACAAAAAAGCAGGCT TCATGATGATGCTGGTGGACTG*	*Gateway cloning PK7WGF2,0*
GWRUP-MC2-R	*GGGGACCACTTTGTACAAGAAAGCTGGGT CGAGGATGAAAGGCTTTGAGT*	*Gateway cloning PK7WGF2,0*
GWRUP-MC5-F	*GGGGACAAGTTTGTACAAAAAAGCAGGCT TCATGGGGAAGAAGGCAGTGTT*	*Gateway cloning PK7WGF2,0*
GWRUP-MC5-R	*GGGGACCACTTTGTACAAGAAAGCTGGGT CAATGTCGCAGATGAATGGAG*	*Gateway cloning PK7WGF2,0*
GW-pMC2-F	*GGGGACAAGTTTGTACAAAAAAGCAGGCT TCAGTGTGGCTTGGGTTAGGTT*	*Gateway cloning PLUC vetor*
GW-pMC2-R	*GGGGACCACTTTGTACAAGAAAGCTGGGT CTTCAAAAGCTGAAAGCACTT*	*Gateway cloning PLUC vetor*
GW-PMC5-F	*GGGGACAAGTTTGTACAAAAAAGCAGGCT TCGCTAGCATTATCCGCTTGCA*	*Gateway cloning PLUC vetor*
GW-PMC5-R	*GGGGACCACTTTGTACAAGAAAGCTGGGT CGATTTGCTGTGTGTTTCCCT*	*Gateway cloning PLUC vetor*

5.4 ORF sequence information from genebank submission on this study

***VrMC2* (accession number KY069974)**

[*Vitis Rupestris* metacaspase-2 *VrMC2*, complete cds.] 1237 bp mRNA linear

BASE COUNT: 294 a; 304 c; 308 g; 331 t

ORIGIN SEQ (Highlight part shows ORF sequence)

1 caactccttc cccgctatct ttacatatta gctttcagct ttcagctttc agttttcagt
61 tttcagtttt cagttttcac atttatttcc taagtgcttt cagcttttga aatgatgatg
121 ctggtggact gctcaaactg ccgcattccg ctgcagcttc cgccgggggc ccgggcaatc
181 cgctgctcgg tctgtcatgc cgtcacccgg atcgcggatc cccgggctct ccctacgccg
241 gcgtactcgt ccacccaaag ccaccacgct gtgcctccgg ctcctcccgt tccgtctccg
301 tacgggcaga tgccggcggg gcagccggcg ggggtccacg gcaggaagaa ggcgttggtg
361 tgcggcgtgt cgtacaccag ctcgcggtat gagctgaagg ggtgtgtgaa cgatgccaag
421 tgtatgaagt atttgctggt gaatcggttc aagtttcccg aggcttccgt tctcatgctt

481 actgaagaag aaatcgatcc ttacaagaag ccaaccaaac acaacatgag aatggcaatg
541 ttttggctag tacaagggtg tcaaccagga gactccctgg tgttccattt ttctggtcat
601 ggttcgcaac agagaaacta cactggagat gaggtagatg gatatgatga gacactttgc
661 cccttggact ttgaaactca gggaatgatt gtcgatgatg aaatcaatgc agcaattgtt
721 aggcctcttc ctcatggagt taagcttcat gcaatcattg atgcatgcca tagtggcact
781 gtgttagatt taccattcct ctgtagaatg aacaggagcg gacagtatat atgggaggac
841 catcgccccc catcaggtat atggaaagga acaagtggtg gggaggtcat ttcctttagt
901 ggctgtgatg ataatcaaac ctctgctgat acgtcggctc tatcaaagat cacttcaaca
961 ggtgcaatga cttattcttt catccaagca atagaggttg gaaatgcaac tacatatggg
1021 aacatgctaa attcaatgcg atcaaccatc cgtaatacag acaatcttgg gggtggtgtt
1081 gtgacatctc ttctcaccat gcttttgaca ggacagagtc ttagtggtgg gttgaggcag
1141 gaaccacaac taactgccaa cgaaccattt gacgtgtact caaagccttt catcctctga
1201 ctgagagctc aattgctcaa tgctccatcc tgtggct

translation="MMMLVDCSNCRIPLQLPPGARAIRCSVCHAVTRIADPRALPTPAYSSTQS
HHAVPPAPPVPSPYGQMPAGQPAGVHGRKKALVCGVSYTSSRYELKGCVNDAKCMK
YLLVNRFKFPEASVLMLTEEEIDPYKKPTKHNMRMAMFWLVQGCQPGDSLVFHFSG
HGSQQRNYTGDEVDGYDETLCPLDFETQGMIVDDEINAAIVRPLPHGVKLHAIIDAC
HSGTVLDLPFLCRMNRSGQYIWEDHRPPSGIWKGTSGGEVISFSGCDDNQTSADTSA
LSKITSTGAMTYSFIQAIEVGNATTYGNMLNSMRSTIRNTDNLGGGVVTSLLTMLLTG
QSLSGGLRQEPQLTANEPFDVYSKPFIL"

VrMC5 (accession number KY069975)

[*Vitis Rupestris* metacaspase-5 *VrMC5*, complete cds.] 1299 bp mRNA linear

BASE COUNT: 339 a; 333 c; 372 g; 255 t

ORIGIN SEQ (Highlight part shows ORF sequence)

1 gcaaatcatg gggaagaagg cagtgttgat aggatgcaat taccagggaa ccaaggctga
61 gctcaagggc tgcatcaacg atgtcaaccg aatgtacaac tccctcgtca atcgcttcgg
121 cttctcccag gacgacatca ccgtcctcat cgacaccgat cccgatggcg ttcagcctac
181 cggcaagaac attcgccgcg ccctccttaa tctcatccga tctgccgaac ccggcgacat
241 cctcttcgtc cactacagcg gccacggcac tcgactccct gccgagaccg gagaggacga
301 cgacaccggc tacgacgagt gcatcgtccc tactgacatg aatctcatta ccgatgacga
361 tttcaggtct tttgtggaca aggttccgga gggttgccgc attacgatag tgtcggattc
421 gtgccacagc ggtggcctga tcgatgaggc taaagagcag atcggggaga gcaccaggct
481 gcaacaagag caagaatcgg gatctggatt cggattcaaa agcttcctgc accaaaccgt
541 gcaaggtgcg attgaatctc gcggaattca gctcccttcg gccttgcaac accaccacca
601 ccaccgccgc cgccaccacg aggaggatgt ggatgaggga ggagtggatg cggagtacgg
661 agatcgcggc tatgtgaaga gcagatctct gccgctttca actcttatcg agatactcaa
721 gcagaaaact ggtaaagatg acattgatgt cgggaaactg aggccaacgc tttttgatgt
781 tttcggtgaa gatgcgagtc ccaaggtgaa gaagttcatg aatgttgtta tgaacaagct
841 ccaacaaggc ggcgagggtg gaggcgaggg cggagggttc ttgggaatgg ttgggagcct
901 ggcgcaggat ttcctgaagc aaaagcttga agaaaacaac gaagactatg cgaaacctgc
961 gttggagaca gaagtgggaa gcaagcaaga ggtttatgca ggatccggga agagggcact
1021 gccagataat gggattctga tcagcggctg ccagactgac cagacatccg cggatgccag
1081 cccatctgga aactctgctg aagcttatgg ggctctgagc aacgccattc aaaccataat
1141 tgaagaatcg gacggaagta ttcggaacca ggagcttgtt ttgaaggcca gggagacgct
1201 gaagcgccag ggcttcaccc agcgccctgg actctactgc agcgatcacc atgctgatgc
1261 tccattcatc tgcgacattt aaaacgaggg cagtggatt

translation="MGKKAVLIGCNYQGTKAELKGCINDVNRMYNSLVNRFGFSQDDITVLI
DTDPDGVQPTGKNIRRALLNLIRSAEPGDILFVHYSGHGTRLPAETGEDDDTGYDECI
VPTDMNLITDDDFRSFVDKVPEGCRITIVSDSCHSGGLIDEAKEQIGESTRLQQEQESG
SGFGFKSFLHQTVQGAIESRGIQLPSALQHHHHHRRRHHEEDVDEGGVDAEYGDRG
YVKSRSLPLSTLIEILKQKTGKDDIDVGKLRPTLFDVFGEDASPKVKKFMNVVMNKL
QQGGEGGGEGGGFLGMVGSLAQDFLKQKLEENNEDYAKPALETEVGSKQEVYAGSG
KRALPDNGILISGCQTDQTSADASPSGNSAEAYGALSNAIQTIIEESDGSIRNQELVLKA
RETLKRQGFTQRPGLYCSDHHADAPFICDI"

5.5 Overview of Gateway® constructed destination vectors

Overview of PH7FWG /GWRUP-MC2 and PH7FWG /GWRUP-MC5 vector, which were used to overexpress VrMC2 and VrMC5 fused with GFP

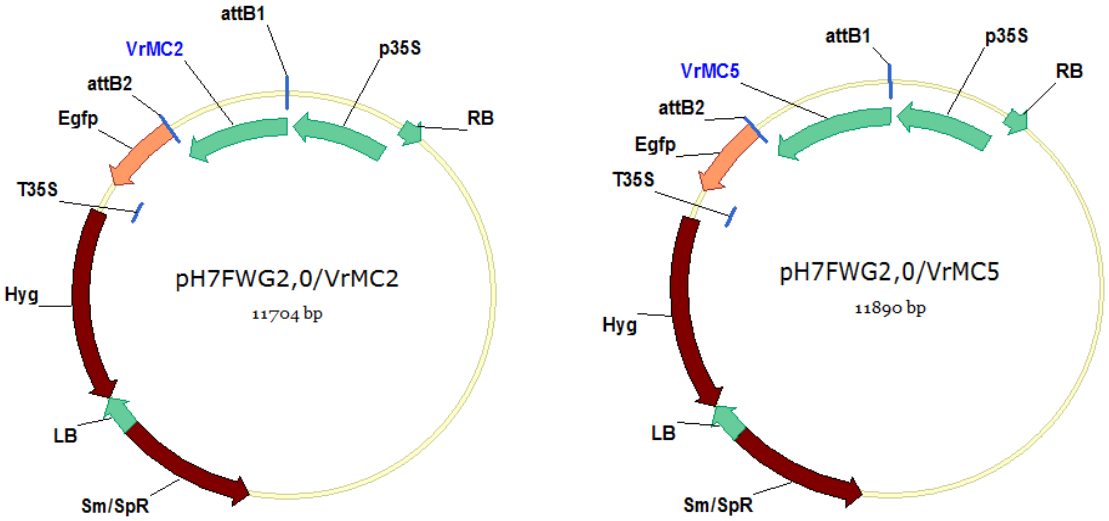

Overview pLUC and pRLUC vector, which were used in this experiment to measure luciferase activity of firefly (drove by specific promoter) and renilla (drove by 35S promoter).

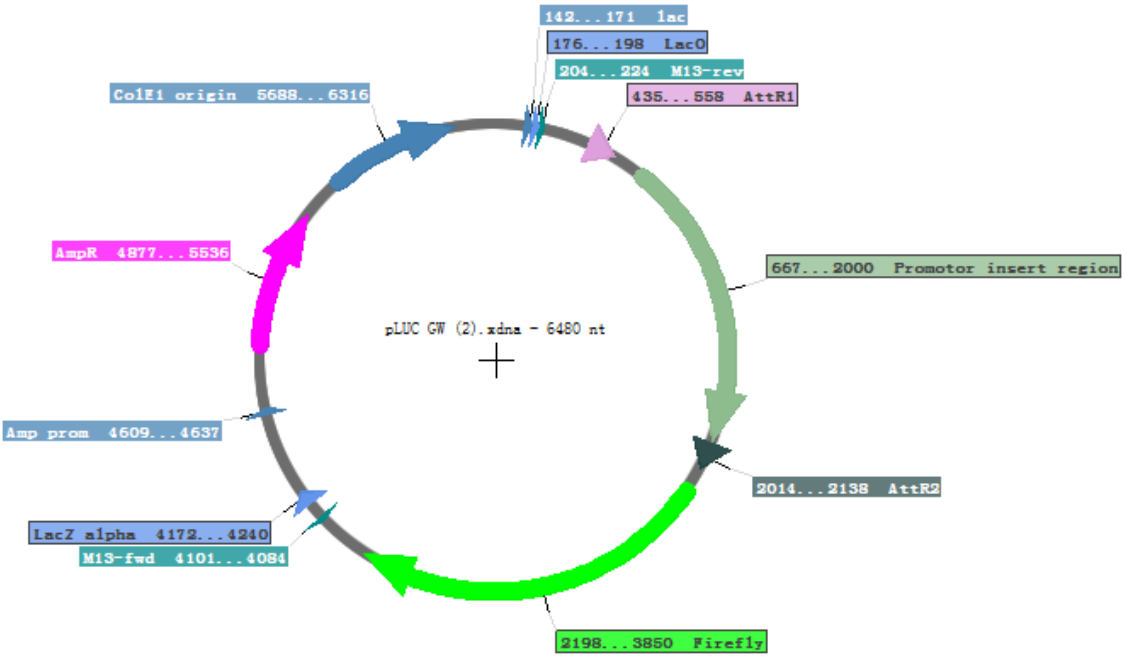

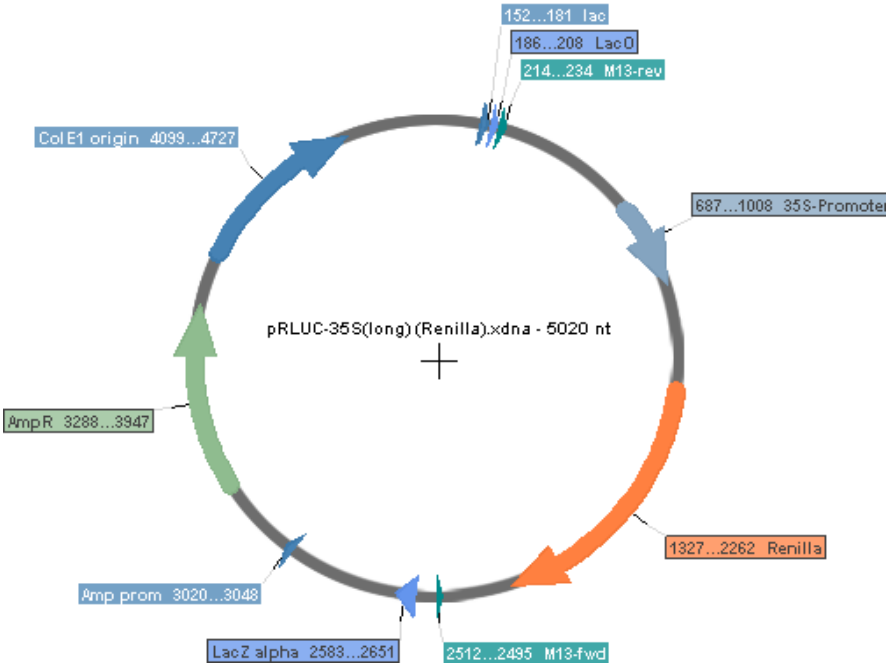

5.6 The promoter region of *MC2* and *MC5* from *V. vinifera* cv. 'Müller-Thurgau' and *V. rupestris*

Alignment of *PVvMC2* (upper line) and *PVvMC5* (lower line)
Identity=94.38 %(1579/1673) Gap=4.07 % (71/1744)

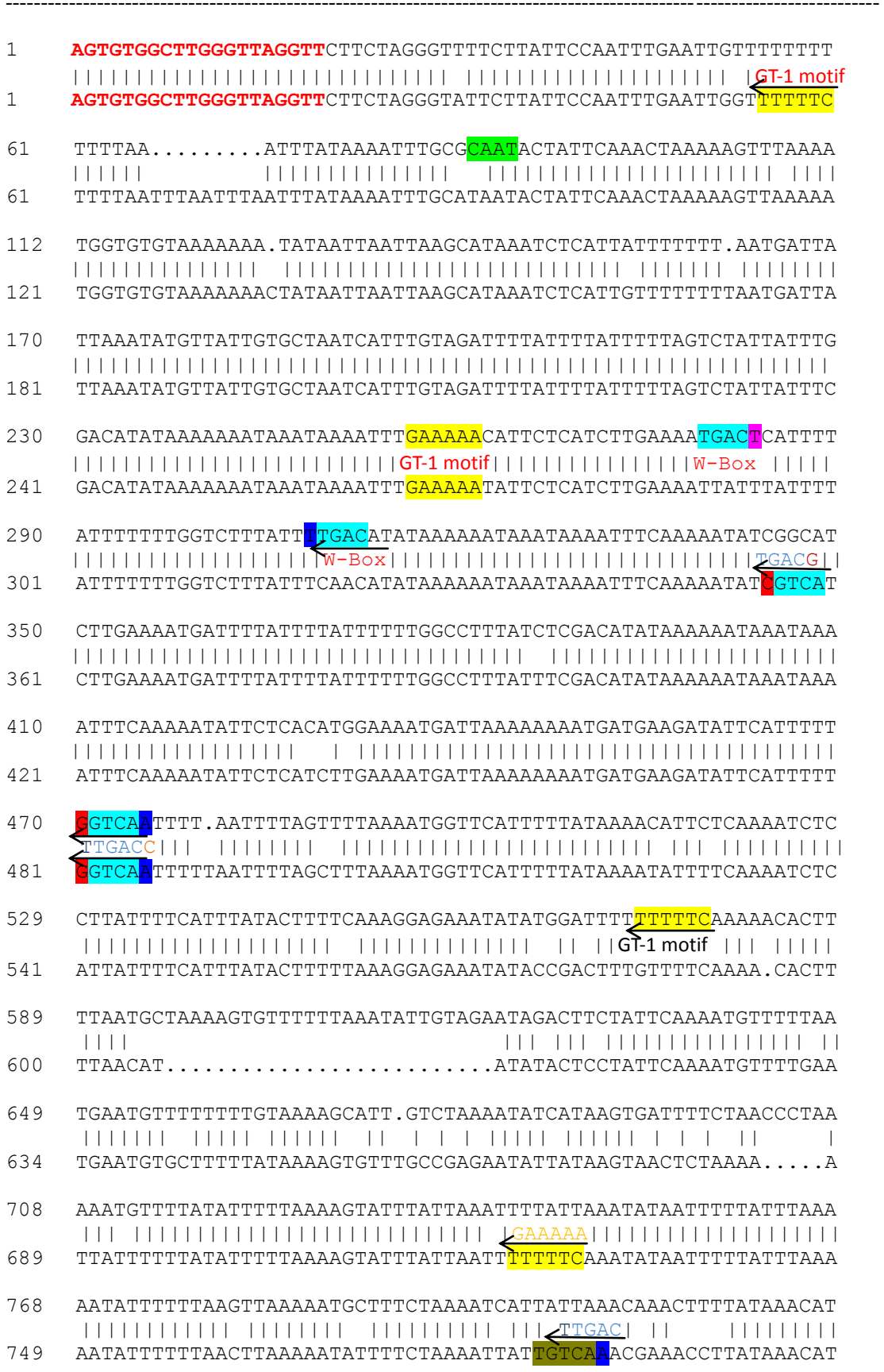

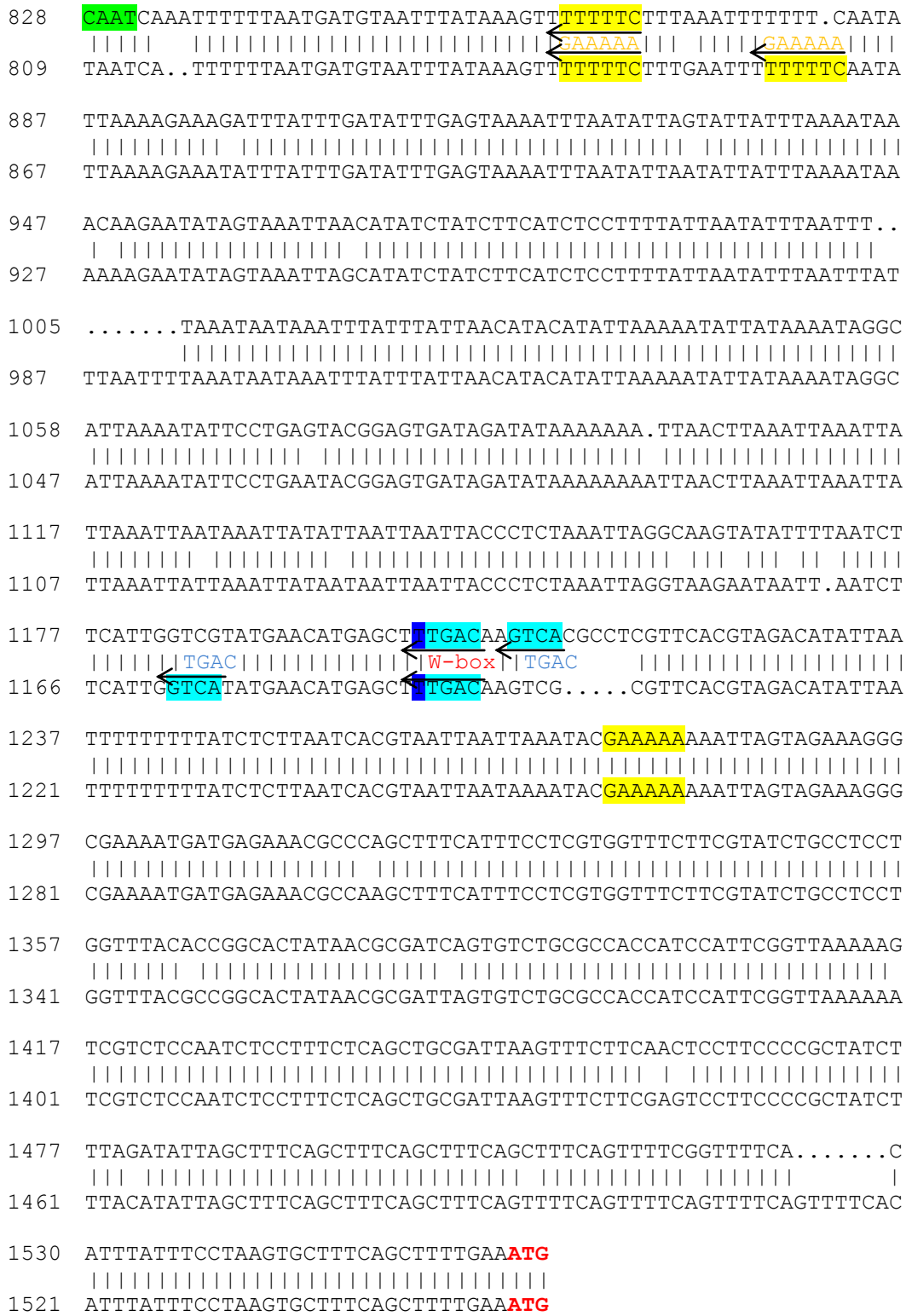
828 CAATCAAATTTTTTAATGATGTAATTTATAAAGTTTTTTTCTTTAAATTTTTTT.CAATA
GAAAAA GAAAAA
809 TAATCA..TTTTTTAATGATGTAATTTATAAAGTTTTTTTCTTTGAATTTTTTTTCAATA
887 TTAAAAGAAAGATTTATTTGATATTTGAGTAAAATTTAATATTAGTATTATTTAAAATAA
867 TTAAAAGAAATATTTATTTGATATTTGAGTAAAATTTAATATTAATATTATTTAAAATAA
947 ACAAGAATATAGTAAATTAACATATCTATCTTCATCTCCTTTTATTAATATTTAATTT..
927 AAAAGAATATAGTAAATTAGCATATCTATCTTCATCTCCTTTTATTAATATTTAATTTAT
1005 .......TAAATAATAAATTTATTTATTAACATACATATTAAAAATATTATAAAATAGGC
987 TTAATTTTAAATAATAAATTTATTTATTAACATACATATTAAAAATATTATAAAATAGGC
1058 ATTAAAATATTCCTGAGTACGGAGTGATAGATATAAAAAAA.TTAACTTAAATTAAATTA
1047 ATTAAAATATTCCTGAATACGGAGTGATAGATATAAAAAAAATTAACTTAAATTAAATTA
1117 TTAAATTAATAAATTATATTAATTAATTACCCTCTAAATTAGGCAAGTATATTTTAATCT
1107 TTAAATTATTAAATTATAATAATTAATTACCCTCTAAATTAGGTAAGAATAATT.AATCT
1177 TCATTGGTCGTATGAACATGAGCTTTGACAAGTCACGCCTCGTTCACGTAGACATATTAA
TGAC W-box TGAC
1166 TCATTGGTCATATGAACATGAGCTTTGACAAGTCG.....CGTTCACGTAGACATATTAA
1237 TTTTTTTTTATCTCTTAATCACGTAATTAATTAAATACGAAAAAAAATTAGTAGAAAGGG
1221 TTTTTTTTTATCTCTTAATCACGTAATTAATAAAATACGAAAAAAAATTAGTAGAAAGGG
1297 CGAAAATGATGAGAAACGCCCAGCTTTCATTTCCTCGTGGTTTCTTCGTATCTGCCTCCT
1281 CGAAAATGATGAGAAACGCCAAGCTTTCATTTCCTCGTGGTTTCTTCGTATCTGCCTCCT
1357 GGTTTACACCGGCACTATAACGCGATCAGTGTCTGCGCCACCATCCATTCGGTTAAAAAG
1341 GGTTTACGCCGGCACTATAACGCGATTAGTGTCTGCGCCACCATCCATTCGGTTAAAAAA
1417 TCGTCTCCAATCTCCTTTCTCAGCTGCGATTAAGTTTCTTCAACTCCTTCCCCGCTATCT
1401 TCGTCTCCAATCTCCTTTCTCAGCTGCGATTAAGTTTCTTCGAGTCCTTCCCCGCTATCT
1477 TTAGATATTAGCTTTCAGCTTTCAGCTTTCAGCTTTCAGTTTTCGGTTTTCA.......C
1461 TTACATATTAGCTTTCAGCTTTCAGCTTTCAGTTTTCAGTTTTCAGTTTTCAGTTTTCAC
1530 ATTTATTTCCTAAGTGCTTTCAGCTTTTGAAATG
1521 ATTTATTTCCTAAGTGCTTTCAGCTTTTGAAATG

Alignment of *PVvMC5* (upper line) and *PVrMC5* (lower line) Identity=95.82 % (1491/1556) Gap=9.43 % (162/1718)

```
1     GCTAGCATTATCCGCTTGCACTTCCATGATTGTGCCGTTAGGGTAAGTTTTTCTTTCTCT
      ||||||||||||||||||||||||||||||||||||||||||||||||||GAAAAA    ||||
1     GCTAGCATTATCCGCTTGCACTTCCATGATTGTGCCGTTAGGGTAAGT........CTCT

61    CTCTCTAACATCTATCTTCATTGTGAAAAAAATCAATCTCTACAAATTAATCTAGCTAAC
       |||||||||||| ||||||||| |||||||||||||||| ||||||||||||||||||||
53    CTCTCTAACATCCATCTTCATTATGAAAAAAATCAATC.CTACAAATTAATCTAGCTAAC

121   AATATATATTATATAAAGCTTAAGTAATGGGCGATAATGTATATTAAAATAGTACAACAT
       |||||||||||||||||||| |||||||| |||||||||||    ||| | | || |
112   AATATATATTATATAAAGCTTGAGTAATGGGTGATAATGTATACACTAATGGAATAATA.

181   GACACTAATGGAATAATAATAATAATGTATAACTAAAAGATTCGATGAAACCATAAAATG
                |||||||||||||||||||||||||||||| ||||||||||||||||
171   .........ATAATAATAATAATAATGTATAACTAAAAGATTCAATGAAACCATAAAATG

241   CATTGCAGGGATGCGATGCATCGATTTTGCTAAATCATGCAGGGAGTGAGAGGAGGGCTG
       ||||||||||||||||||||||||||||||||||||||||||||||||||||||||||||
222   CATTGCAGGGATGCGATGCATCGATTTTGCTAAATCATGCAGGGAGTGAGAGGAGGGCTG

301   AGGCCAGCAAGACACTGAGGGGATTCCAGGTGATAGAGGAGATCAAAGCAGAGGTTGAGA
       ||||||||||||||||||||||||||||||||||||||||||||||||||||||||||||
282   AGGCCAGCAAGACACTGAGGGGATTCCAGGTGATAGAGGAGATCAAAGCAGAGGTTGAGA

361   AGAGGTGTCCCGGAAGAGTCTCATGTGCGGACATTCTCACAGCTGCTGCAAGAGATGCCA
       |||||||||||||||||||| |||||TGTCA||||||||||||||||||||||||||||
342   AGAGGTGTCCCGGAAGAGTCTCGTGTGCTGACATTCTCACAGCTGCTGCAAGAGATGCCA

421   CCGTCCTCATTGGAGGTCCGTTCTGGGAAGTCCCTTTCGGGAGGAAAGATGGGAAGGTCT
       |||||||||||||||||| ||||||||||||||||||||||||||||||||||||||||
402   CCGTCCTCATTGGAGGTCCATTCTGGGAAGTCCCTTTCGGGAGGAAAGATGGGAAGGTCT

481   CCATTGCCAGAGAAGCCAACAGGGTTCCTCAGGGCCACGAAAACGTCACTGACTTGATCC
       ||||||||||||||||||||||||||||||||||||||||||TGACG ||||||||||||
462   CCATTGCCAGAGAAGCCAACAGGGTTCCTCAGGGCCACGAAAACGTCACCGACTTGATCC

541   AATTCTTCCAAGCTCGAGGCTTGAACATACTGGATCTGGTCATCCTCTCAGGCTCACACA
       |||||||||||||||||||||||||||||| |||||TGAC||||||||||||||||||
522   AATTCTTCCAAGCTCGAGGCTTGAACATACTCGATCTGGTCATCCTCTCAGGCTCACACA


601   CCATCGGCAGGAGCACCTGCCATTCCATTCAACACAGGCTCTCCAACTTTAATGGGACAT
       |||| ||||||||||||||||||||||||||||||||||||||||||||||||||||||
582   CCATTGGCAGGAGCACCTGCCATTCCATTCAACACAGGCTCTCCAACTTTAATGGGACAT

661   ACAAGCCCAATCCCTCACTCAATGCCACATACCTGAGGGTGCTGAAGGGGAAATGTGGGA
       |||||||| ||||||||||||||||||||||||||||||||||||||||||||||||||||
642   ACAAGCCCGATCCCTCACTCAATGCCACATACCTGAGGGTGCTGAAGGGGAAATGTGGGA

721   GGAGGTACAACTACGTGGATCTAGATGGTACAACTCCGAGGAAATTTGATACAGAATACT
       |||||||||||||||||||||||||||||||||||||||||||| ||| |||||||||
702   GGAGGTACAACTACGTGGATCTAGATGGTACAACTCCGAGGAAATTCGATGCAGAATACT

781   ACAAGAATCTAGGGAAGAAGATGGGGTTGCTGTCGACGGATCAAGGACTGTATAGGGATT
       |||||||||| |||||||||||||||||||||||||||||||| ||||||||||||||
762   ACAAGAATCTTGGGAAGAAGATGGGGTTGCTGTCGACGGATCAAGGGCTGTATAGGGATT
```

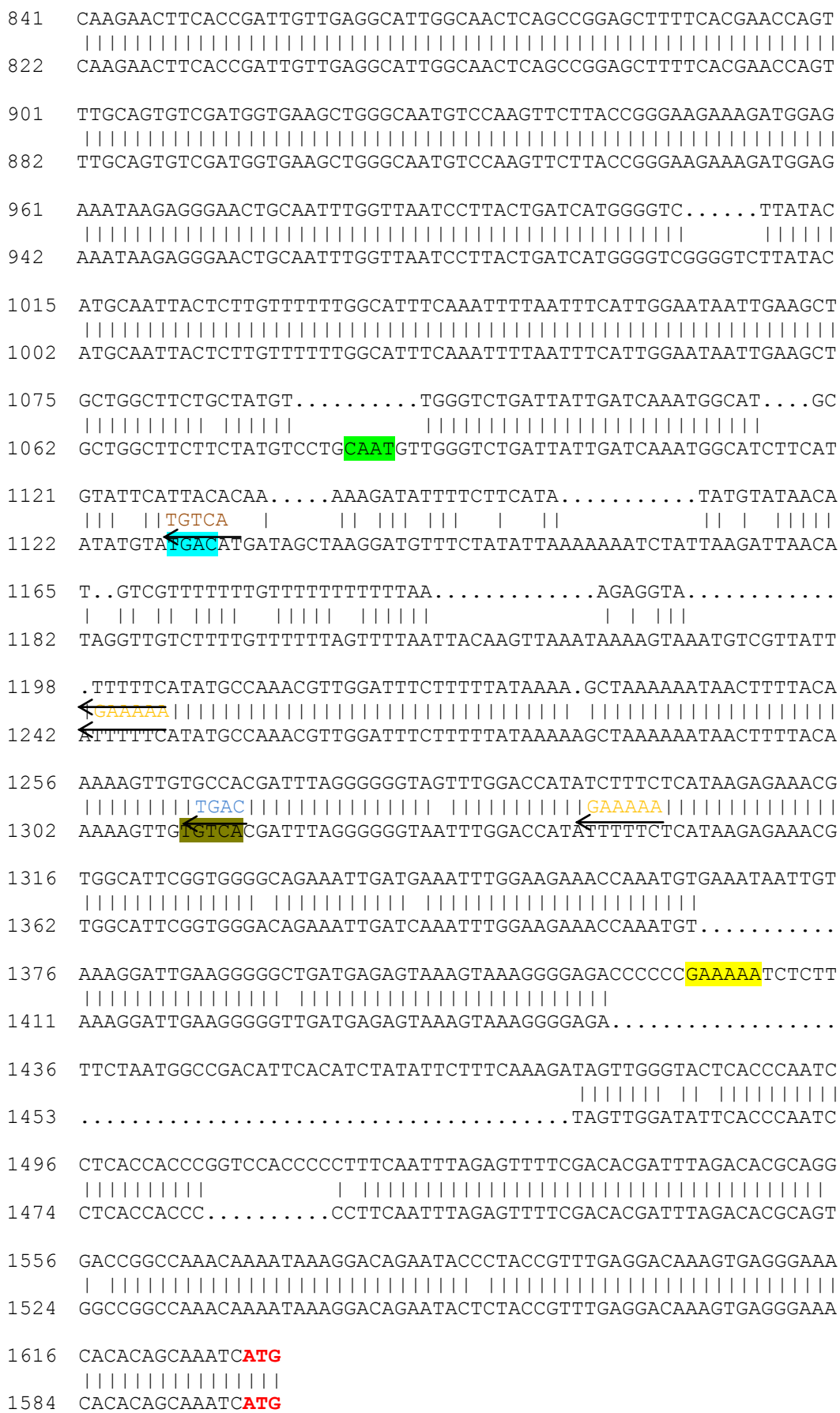
841 CAAGAACTTCACCGATTGTTGAGGCATTGGCAACTCAGCCGGAGCTTTTCACGAACCAGT
822 CAAGAACTTCACCGATTGTTGAGGCATTGGCAACTCAGCCGGAGCTTTTCACGAACCAGT
901 TTGCAGTGTCGATGGTGAAGCTGGGCAATGTCCAAGTTCTTACCGGGAAGAAAGATGGAG
882 TTGCAGTGTCGATGGTGAAGCTGGGCAATGTCCAAGTTCTTACCGGGAAGAAAGATGGAG
961 AAATAAGAGGGAACTGCAATTTGGTTAATCCTTACTGATCATGGGGTC......TTATAC
942 AAATAAGAGGGAACTGCAATTTGGTTAATCCTTACTGATCATGGGGTCGGGGTCTTATAC
1015 ATGCAATTACTCTTGTTTTTTGGCATTTCAAATTTTAATTTCATTGGAATAATTGAAGCT
1002 ATGCAATTACTCTTGTTTTTTGGCATTTCAAATTTTAATTTCATTGGAATAATTGAAGCT
1075 GCTGGCTTCTGCTATGT..........TGGGTCTGATTATTGATCAAATGGCAT....GC
1062 GCTGGCTTCTTCTATGTCCTGCAATGTTGGGTCTGATTATTGATCAAATGGCATCTTCAT
1121 GTATTCATTACACAA.....AAAGATATTTTCTTCATA...........TATGTATAACA
1122 ATATGTATGACATGATAGCTAAGGATGTTTCTATATTAAAAAAATCTATTAAGATTAACA
1165 T..GTCGTTTTTTTGTTTTTTTTTTTAA.............AGAGGTA.....
1182 TAGGTTGTCTTTTGTTTTTTAGTTTTAATTACAAGTTAAATAAAAGTAAATGTCGTTATT
1198 .TTTTTCATATGCCAAACGTTGGATTTCTTTTTATAAAA.GCTAAAAAATAACTTTTACA
1242 ATTTTTTCATATGCCAAACGTTGGATTTCTTTTTATAAAAAGCTAAAAAATAACTTTTACA
1256 AAAAGTTGTGCCACGATTTAGGGGGGTAGTTTGGACCATATCTTTCTCATAAGAGAAACG
1302 AAAAGTTGTGTCACGATTTAGGGGGGTAATTTGGACCATATTTTTCTCATAAGAGAAACG
1316 TGGCATTCGGTGGGGCAGAAATTGATGAAATTTGGAAGAAACCAAATGTGAAATAATTGT
1362 TGGCATTCGGTGGGACAGAAATTGATCAAATTTGGAAGAAACCAAATGT.....
1376 AAAGGATTGAAGGGGGCTGATGAGAGTAAAGTAAAGGGGAGACCCCCCGAAAAATCTCTT
1411 AAAGGATTGAAGGGGGTTGATGAGAGTAAAGTAAAGGGGAGA.....
1436 TTCTAATGGCCGACATTCACATCTATATTCTTTCAAAGATAGTTGGGTACTCACCCAATC
1453 .....TAGTTGGATATTCACCCAATC
1496 CTCACCACCCGGTCCACCCCCTTTCAATTTAGAGTTTTCGACACGATTTAGACACGCAGG
1474 CTCACCACCC.....CCTTCAATTTAGAGTTTTCGACACGATTTAGACACGCAGT
1556 GACCGGCCAAACAAAATAAAGGACAGAATACCCTACCGTTTGAGGACAAAGTGAGGGAAA
1524 GGCCGGCCAAACAAAATAAAGGACAGAATACTCTACCGTTTGAGGACAAAGTGAGGGAAA
1616 CACACAGCAAATCATG
1584 CACACAGCAAATCATG

5.7 Four categories to classify all necrotic spots in the infection area after 1191 B15 inoculation

In order to quantify the HR of *V. rupestris* caused by *P. viticola* 1191-B15, leaf discs of the genotype were infected with the pathogen and the occurrence of necrotic sites on these leaf discs was documented at regular time intervals. All necrotic spots in the infection area were recorded and then counted and evaluated in certain temporal course. In order to better evaluate the development and modification of these spots, four size categories were created using 4 diameter regions, in which all the identified spots were then classified. The selected size categories are shown as following with example figures: <50 µm, 50-100 µm, 100-150 µm and> 150 µm (Fig. 5.1).

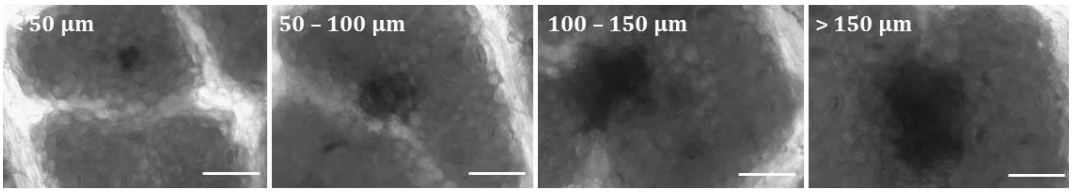

Figure 5.1 Size categories for evaluation of the necrotic sites on *V. rupestris.* The categories were determined by the 4 diameter regions of the necrotic sites and are defined as follows: (from left to right) <50 µm, 50-100 µm, 100-150 µm,> 150 µm. The scale shown as size of 100 µm.

5.8 Expression analysis of grape caspase-like genes (except *MC1, MC2, MC5*) during *P.viticola* 1191-B15 infection

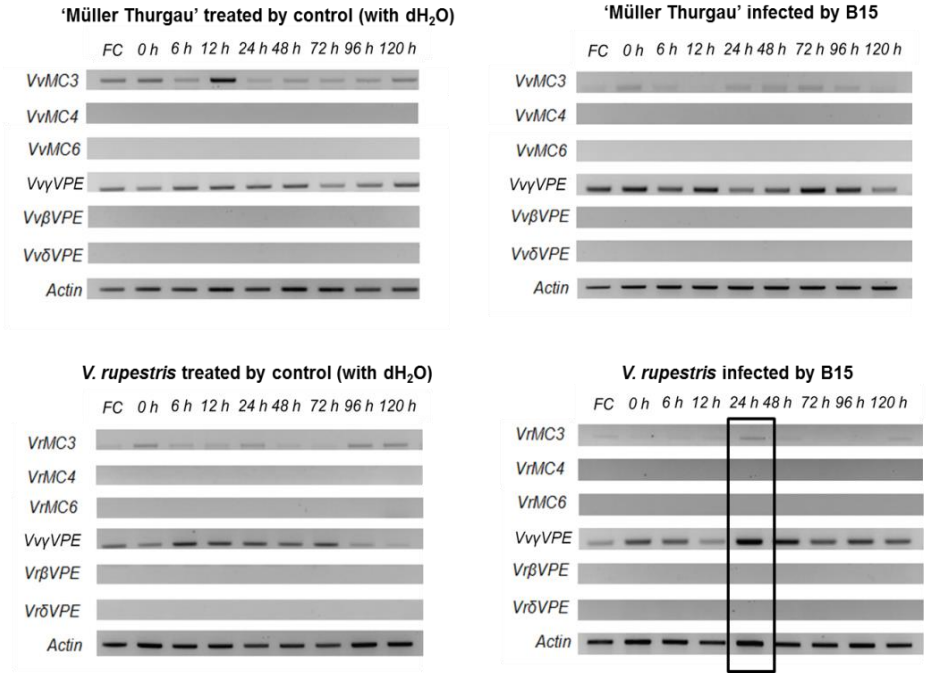

Figure 5.2 Semi-quantitative expression analysis of grape caspase-like genes (except *MC1, MC2, MC5*) during *Plasmopara viticola* 1191-B15 infection

Representative agarose gels with the amplifcated transcripts of MC1, MC2 and MC5 on *V. vinifera* cv. Mueller Thurgau and *V. rupestris* by semi-quantitative RT–PCR. FC (as fresh control), 0 hour, 6 hours 12 hours, 24 hours, 48 hours, 72 hours, 96 hours and 120 hours (corresponding time points with Fig 3) were set as time points after inoculation with 1191-B15. Actin was tested and compared as internal reference gene. Dist H_2O treated samples as negative control in parallel.

5.9 Sequences alignment of MC2 and MC5 putative protein between cv. 'Pinot Noir' and *V. rupestris*

Quary: sequence from *V.rupestirs*
Sbjct: sequence from *V. vinifera* cv. 'Pinot Noir'

MC2

Range 1: 1 to 362 Graphics ▼ Next Match ▲ Previou

Score	Expect	Method	Identities	Positives	Gaps
751 bits(1938)	0.0	Compositional matrix adjust.	358/362(99%)	360/362(99%)	0/362(0%)

```
Query  1    MMMLVDCSNCRIPLQLPPGARAIRCSVCHAVTRIADPRALPTPAYSSTQSHHAVPFAPFV  60
            MMMLVDCSNCRIPLQLPPGARAIRCSVCHAVTRIADPRA+PTP YSSTQSHHAVPFAPFV
Sbjct  1    MMMLVDCSNCRIPLQLPPGARAIRCSVCHAVTRIADPRAVPTPFYSSTQSHHAVPFAPFV  60

Query  61   PSPYGQMPAGQPAGVHGRKKALVCGVSYTSSRYELKGCVNDAKCMKYLLVNRFKFPEASV  120
            PSPYGQMPAGQPAGVHGRKKALVCGVSYTSSRYELKGCVNDAKCMKYLLVNRFKFPEASV
Sbjct  61   PSPYGQMPAGQPAGVHGRKKALVCGVSYTSSRYELKGCVNDAKCMKYLLVNRFKFPEASV  120

Query  121  LMLTEEEIDPYKKPTKHQMRMAMFWLVQGCQPGDSLVFHFSGHGSQQRNYTGDEVDGYDE  180
            LMLTEEEIDPYKKPTKHQMRMAMFWLVQGCQPGDSLVFHFSGHGSQQRNYTGDEVDGYDE
Sbjct  121  LMLTEEEIDPYKKPTKHQMRMAMFWLVQGCQPGDSLVFHFSGHGSQQRNYTGDEVDGYDE  180

Query  181  TLCPLDFETQGMIVDDEINAAIVRPLPMGVKLHAIIDACHSGTVLDLPFLCRMNRSGQYI  240
            TLCPLDFETQGMIVDDEINA IVRPLP+GVKLHAIIDACHSGTVLDLPFLCRMNRSGQYI
Sbjct  181  TLCPLDFETQGMIVDDEINATIVRPLPYGVKLHAIIDACHSGTVLDLPFLCRMNRSGQYI  240

Query  241  WEDHRPPSGIWKGTSGGEVISFSGCDDNQTSADTSALSKITSTGAMTYSFIQAIEVGNAT  300
            WEDHRPPSGIWKGTSGGEVISFSGCDDNQTSADTSALSKITSTGAMTYSFIQAIEVGNAT
Sbjct  241  WEDHRPPSGIWKGTSGGEVISFSGCDDNQTSADTSALSKITSTGAMTYSFIQAIEVGNAT  300

Query  301  TYGNMLNSMRSTIRNTDNLGGGVVTSLLTMLLTGQSLSGGLRQEPQLTANEPFDVYSKPF  360
            TYGNMLNSMRSTIRNTDNLGGGVVTSLLTMLLTGQSLSGGLRQEPQLTANEPFDVYSKPF
Sbjct  301  TYGNMLNSMRSTIRNTDNLGGGVVTSLLTMLLTGQSLSGGLRQEPQLTANEPFDVYSKPF  360

Query  361  IL  362
            IL
Sbjct  361  IL  362
```

MC5

Range 1: 1 to 424 Graphics ▼ Next Match ▲ Previ

Score	Expect	Method	Identities	Positives	Gaps
867 bits(2240)	0.0	Compositional matrix adjust.	422/424(99%)	423/424(99%)	0/424(0%)

```
Query  1    MGKKAVLIGCNYQGTKAELKGCINDVNRMYNSLVNRFGFSQDDITVLIDTDPDGVQPTGK  60
            MGKKAVLIGCNYQGTKAELKGCINDVNRMYNSLVNRFGFSQDDITVLIDTDPDGVQPTGK
Sbjct  1    MGKKAVLIGCNYQGTKAELKGCINDVNRMYNSLVNRFGFSQDDITVLIDTDPDGVQPTGK  60

Query  61   NIRRALLNLIRSAEPGDILFVHYSGHGTRLPAETGEDDDTGYIDECIVPTDMNLITDDDFR  120
            NIRRALLNLIRSA+PGDILFVHYSGHGTRLPAETGEDDDTGYIDECIVPTDMNLITDDDFR
Sbjct  61   NIRRALLNLIRSAQPGDILFVHYSGHGTRLPAETGEDDDTGYIDECIVPTDMNLITDDDFR  120

Query  121  SFVDKVPEGCRITIVSDSCHSGGLIDEAKEQIGESTRLQQEQESGSGFGFKSFLHQTVQG  180
            SFVDKVPEGCRITIVSDSCHSGGLIDEAKEQIGESTRLQQEQESGSGFGFKSFLHQTVQG
Sbjct  121  SFVDKVPEGCRITIVSDSCHSGGLIDEAKEQIGESTRLQQEQESGSGFGFKSFLHQTVQG  180

Query  181  AIESRGIQLPSALQHHHHHRRRHHEEDVDEGGVDAEYGDRGYVKSRSLPLSTLIEILKQK  240
            AIESRGIQLPSALQHH HHRRRHHEEDVDEGGVDAEYGDRGYVKSRSLPLSTLIEILKQK
Sbjct  181  AIESRGIQLPSALQHHRHHRRRHHEEDVDEGGVDAEYGDRGYVKSRSLPLSTLIEILKQK  240

Query  241  TGKDDIDVGKLRPTLFDVFGEDASPKVKKFMNVVMNKLQQGEGGGEGGGFLGMVGSLAQ  300
            TGKDDIDVGKLRPTLFDVFGEDASPKVKKFMNVVMNKLQQGEGGGEGGGFLGMVGSLAQ
Sbjct  241  TGKDDIDVGKLRPTLFDVFGEDASPKVKKFMNVVMNKLQQGEGGGEGGGFLGMVGSLAQ  300

Query  301  DFLKQKLEENNEDYAKPALETEVGSKQEVYAGSGKRALPDNGILISGCQTDQTSADASPS  360
            DFLKQKLEENNEDYAKPALETEVGSKQEVYAGSGKRALPDNGILISGCQTDQTSADASPS
Sbjct  301  DFLKQKLEENNEDYAKPALETEVGSKQEVYAGSGKRALPDNGILISGCQTDQTSADASPS  360

Query  361  GNSAEAYGALSNAIQTIIEESDGSIRNQELVLKARETLKRQGFTQRPGLYCSDHMADAPF  420
            GNSAEAYGALSNAIQTIIEESDGSIRNQELVLKARETLKRQGFTQRPGLYCSDHMADAPF
Sbjct  361  GNSAEAYGALSNAIQTIIEESDGSIRNQELVLKARETLKRQGFTQRPGLYCSDHMADAPF  420

Query  421  ICDI  424
            ICDI
Sbjct  421  ICDI  424
```

Fig 5.3 Sequences alignment of MC2 and MC5 putative protein between cv. 'Pinot Noir' and *V. rupestris*

5.10 VrMC5 mainly in the cytoplasm, but also existing in nuclear

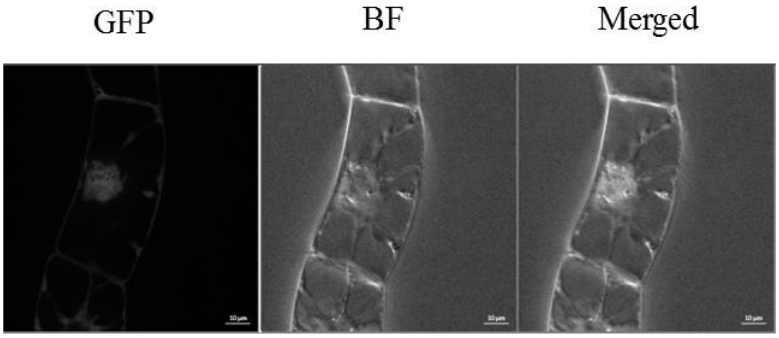

Figure 5.4 Localisation of the VrMC5 isolated from *Vitis rupestris* as zoom-in of the nuclear region. Left to right: GFP, The channel of green fluorescence signal; BF, Bright-field; Merged, combine channel of GFP and BF.

5.11 Table 4 Cis-element distribution analysis of PMC2 and PMC5 promoters related on pathogen or stress defence response

Name	**sequence**	**numbers**		**Function**	**Reference**
		pMC2 MT-RUP	*pMC5* MT-RUP		
GT-1 motif	GAAAAA	4 – 6	4 – 3	Pathogen and salt stress	Rao et al. (2010)
W-Box	TGAC	5 – 5	3 – 5	Wound and defence response	Euglem et al. (2000)
W-Box	TGACT	1 – 0	1 – 0	Wound and defence response	Maleck et al. (2000)
W-Box	TTGAC	3 – 4	0 – 0	Stress response to environmental influences	Chen et al. (2002)
W-Box	TTGACC	1 – 1	0 – 0	fungal elicitor responsive element	Guguloth et al. (2009)
as-1/ocs element-like	TGACG	0 – 1	1 – 1	Pathogen response	Chen et al. (2002)
BIHD1OS	TGTCA	0 – 1	0 – 3	Disease resistance response	Luo et al. (2005)
TC-rich repeats	ATTTTCT TCA	0 – 0	1 – 0	Defence and stress responsiveness	Diaz-De-Leon *et al.*, (1993)

Table 5 Cis-element distribution analysis of PMC2 and PMC5 promoters related on hormone response

Name	Sequence	Amount in		Function	Reference
		MC2 MT-Rup	MC5 MT-Rup		
ASF1MOTIFCAMV	TGACG	0-1	1-1	Gene activation by Auxin and SA	Despres *et al*. (2003)
ELRECOREPCRP1	TTGACC	1-1	0-0	Activation of PR- and WRKY-genes	Laloi *et al.* (2004)
GT1CONSENSUS	GRWAAW	16-15	8-7	SA-inducible gene expression	Zhou (1999)
MARABOX1	AATAAAYAAA	4-4	0-0	A-box in SAR	Gasser *et al.* (1989)
MARARS	WTTTATRTTTW	1-1	0-0	Found in SAR	Gasser *et al.* (1989)
MARTBOX	TTWTWTTWTT	8-5	1-0	T-Box; found in SAR	Gasser *et al*. (1989)
WBOXATNPR1	TTGAC	2-3	0-0	Part of SA-answer	Xu *et al*. (2006)

REFERENCES

Ahmad R, Zuily-Fodil Y, Passaquet C, Bethenod O, Roche R, Repellin A. 2012. Ozone and aging up-regulate type II metacaspase gene expression and global metacaspase activity in the leaves of field-grown maize (*Zea mays* L.) plants. *Chemosphere*.

Allison A. 2007. Tools for analyzing gene expression. **US: Blackwell Publishing Ltd.**

Aravind L, Koonin EV. 2002. Classification of the caspase–hemoglobinase fold: Detection of new families and implications for the origin of the eukaryotic separins. *Proteins: Structure, Function, and Bioinformatics* **46**, 355-367.

Baker CJ, Orlandi EW, Mock NM. 1993. Harpin, an Elicitor of the Hypersensitive Response in Tobacco Caused by Erwinia-Amylovora, Elicits Active Oxygen Production in Suspension Cells. *Plant Physiology* **102**, 1341-1344.

Bellin D, Peressotti E, Merdinoglu D, Wiedemann-Merdinoglu S, Adam-Blondon A-F, Cipriani G, Morgante M, Testolin R, Di Gaspero G. 2009. Resistance to Plasmopara viticola in grapevine 'Bianca' is controlled by a major dominant gene causing localised necrosis at the infection site. *Theoretical and Applied Genetics* **120**, 163-176.

Bent AF, Mackey D. 2007. Elicitors, effectors, and R genes: The new paradigm and a lifetime supply of questions. *Annual Review of Phytopathology* **45**, 399-436.

Berrocal-Lobo M, Molina A, Solano R. 2002. Constitutive expression of ETHYLENE-RESPONSE-FACTOR1 in Arabidopsis confers resistance to several necrotrophic fungi. *Plant Journal* **29**, 23-32.

Boller T, He SY. 2009. Innate Immunity in Plants: An Arms Race Between Pattern Recognition Receptors in Plants and Effectors in Microbial Pathogens. *Science* **324**, 742-744.

Bollhoner B, Zhang B, Stael S, Denance N, Overmyer K, Goffner D, Van Breusegem F, Tuominen H. 2013. Post mortem function of AtMC9 in xylem vessel elements. *New Phytologist* **200**, 498-510.

Brown I, Trethowan J, Kerry M, Mansfield J, Bolwell GP. 1998. Localization of components of the oxidative cross-linking of glycoproteins and of callose synthesis in papillae formed during the interaction between non-pathogenic strains of Xanthomonas campestris and French bean mesophyll cells. *Plant Journal* **15**, 333-343.

Buschmann H, Green P, Sambade A, Doonan JH, Lloyd CW. 2011. Cytoskeletal dynamics in interphase, mitosis and cytokinesis analysed through Agrobacterium-mediated transient transformation of tobacco BY-2 cells. *New Phytologist* **190**, 258-267.

Carmona-Gutierrez D, Frohlich KU, Kroemer G, Madeo F. 2010. Metacaspases are caspases. Doubt no more. *Cell Death and Differentiation* **17**, 377-378.

Casagrande K, Falginella L, Castellarin SD, Testolin R, Di Gaspero G. 2011. Defense responses in Rpv3-dependent resistance to grapevine downy mildew. *Planta* **234**, 1097-1109.

Chang X, Heene E, Qiao F, Nick P. 2011. The Phytoalexin Resveratrol Regulates the Initiation of Hypersensitive Cell Death in <italic>Vitis</italic> Cell. *Plos One* **6**, e26405.

Chang XL, Nick P. 2012. Defense Signalling Triggered by Flg22 and Harpin Is Integrated into a Different Stilbene Output in Vitis Cells. *Plos One* **7**.

Chang XL, Seo M, Takebayashi Y, Kamiya Y, Riemann M, Nick P. 2017. Jasmonates are induced by the PAMP flg22 but not the cell death-inducing elicitor Harpin in Vitis rupestris. *Protoplasma* **254**, 271-283.

Chen WQ, Provart NJ, Glazebrook J, Katagiri F, Chang HS, Eulgem T, Mauch F, Luan S, Zou GZ, Whitham SA, Budworth PR, Tao Y, Xie ZY, Chen X, Lam S, Kreps JA, Harper JF, Si-Ammour A, Mauch-Mani B, Heinlein M, Kobayashi K, Hohn T, Dangl JL, Wang X, Zhu T. 2002. Expression profile matrix of Arabidopsis transcription factor genes suggests their putative functions in response to environmental stresses. *Plant Cell* **14**, 559-574.

Clarke A, Desikan R, Hurst RD, Hancock JT, Neill SJ. 2000. NO way back: nitric oxide and programmed cell death in Arabidopsis thaliana suspension cultures. *The Plant Journal* **24**, 667-677.

Cohen GM. 1997. Caspases: the executioners of apoptosis. *Biochem. J.* **326**, 1-16.

Coll NS, Epple P, Dangl JL. 2011. Programmed cell death in the plant immune system. *Cell Death and Differentiation* **18**, 1247-1256.

Coll NS, Vercammen D, Smidler A, Clover C, Van Breusegem F, Dangl JL, Epple P. 2010. Arabidopsis type I metacaspases control cell death. *Science* **330**, 1393-1397.

Czemmel S, Stracke R, Weisshaar B, Cordon N, Harris NN, Walker AR, Robinson SP, Bogs J. 2009. The grapevine R2R3-MYB transcription factor VvMYBF1 regulates flavonol synthesis in developing grape berries. *Plant Physiology* **151**, 1513-1530.

Danon A, Delorme V, Mailhac N, Gallois P. 2000. Plant programmed cell death: A common way to die. *Plant Physiology and Biochemistry* **38**, 647-655.

De Jong AJ, Hoeberichts FA, Yakimova ET, Maximova E, Woltering EJ. 2000. Chemical-induced apoptotic cell death in tomato cells: involvement of caspase-like proteases. *Planta* **211**, 656-662.

del Pozo O, Lam E. 1998. Caspases and programmed cell death in the hypersensitive response of plants to pathogens. *Current Biology* **8**, 1129-1132.

Dodds PN, Rathjen JP. 2010. Plant immunity: towards an integrated view of plant–pathogen interactions. *Nat Rev Genet* **11**, 539-548.

Doyle J, Doyle J. 1987. A rapid DNA isolation procedure from small quantities of fresh leaf tissues. *Phytochemical Bulletin* **19**, 11–15.

Duan D, Fischer S, Merz P, Bogs J, Riemann M, Nick P. 2016. An ancestral allele of grapevine transcription factor MYB14 promotes plant defense. *Journal of Experimental Botany* **67**, 1795-1804.

Duan D, Halter D, Baltenweck R, Tisch C, Troster V, Kortekamp A, Hugueney P, Nick P. 2015. Genetic diversity of stilbene metabolism in Vitis sylvestris. *Journal of Experimental Botany* **66**, 3243-3257.

Durrant WE, Dong X. 2004. Systemic acquired resistance. *Annual Review of Phytopathology* **42**, 185-209.

Earnshaw WC, Martins LM, Kaufmann SH. 1999. MAMMALIAN CASPASES: Structure, Activation, Substrates, and Functions During Apoptosis. *Annual review of biochemistry* **68**, 383-424.

Enoksson M, Salvesen G. 2010. Metacaspases are not caspases – always doubt. *Cell Death and Differentiation* **17**, 1221.

Fischer BM, Salakhutdinov I, Akkurt M, Eibach R, Edwards KJ, Topfer R, Zyprian EM. 2004. Quantitative trait locus analysis of fungal disease resistance factors on a molecular map of grapevine. *TAG. Theoretical and applied genetics. Theoretische und angewandte Genetik* **108**, 501-515.

Freeman BC, Beattie GA. 2008. An Overview of Plant Defenses against Pathogens and Herbivores. *The Plant Health Instructor*.

Fu ZQ, Dong XN. 2013. Systemic Acquired Resistance: Turning Local Infection into Global Defense. *Annual Review of Plant Biology*, **64**, 839-863.

Gadjev I, Stone JM, Gechev TS. 2008. Chapter 3: Programmed Cell Death in Plants: New Insights into Redox Regulation and the Role of Hydrogen Peroxide. In: Kwang WJ, ed. *International Review of Cell and Molecular Biology*, **270**, 87-144.

Gaff DF, Okong'O-Ogola O. 1971. The Use of Non-permeating Pigments for Testing the Survival of Cells. *Journal of Experimental Botany* **22**, 756-758.

Getz S, Fulbright DW, . CTS. 1983. Scanning electron microscopy of infection sites and lesion development on tomato fruit infected with Pseudomonas syringae pv. tomato. *Phytopathology*, 39–43.

Gomez-Gomez L, Boller T. 2000. FLS2: An LRR receptor-like kinase involved in the perception of the bacterial elicitor flagellin in Arabidopsis. *Molecular Cell* **5**, 1003-1011.

Gomez-Zeledon J, Zipper R, Spring O. 2013. Assessment of phenotypic diversity of Plasmopara viticola on Vitis genotypes with different resistance. *Crop Protection* **54**, 221-228.

Gorczyca W, Tuziak T, Kram A, Melamed MR, Darzynkiewicz Z. 1994. Detection of apoptosis-associated DNA strand breaks in fine-needle aspiration biopsies by in situ end labeling of fragmented DNA. *Cytometry* **15**, 169-175.

Greenberg JT, Ausubel FM. 1993. Arabidopsis mutants compromised for the control of cellular damage during pathogenesis and aging. *The Plant Journal* **4**, 327-341.

Greenberg JT, Yao N. 2004. The role and regulation of programmed cell death in plant–pathogen interactions. *Cellular Microbiology* **6**, 201-211.

Gruis D, Selinger DA, Curran JM, Jung R. 2002. Redundant Proteolytic Mechanisms Process Seed Storage Proteins in the Absence of Seed-Type Members of the Vacuolar Processing Enzyme Family of Cysteine Proteases. *The Plant Cell Online* **14**, 2863-2882.

Gunawardena AHLAN. 2008. Programmed cell death and tissue remodelling in plants. *Journal of Experimental Botany* **59**, 445-451.

Hammond-Kossack K, Jones J. 2000. Responses to Plant Pathogens. *in Biochemistry and molecular biology of plants (eds)* B Buchanan, et al. (American Society of Plant Physiologists), pp 1102–1146.

Hao L, Goodwin PH, T.Hsiang. 2007. Expression of a *metacaspase* gene of *Nicotiana benthamiana* after inoculation with *Colletotrichum destructivum* or Pseudomonas syringae pv. *tomato*, and the effect of silencing the gene on the host response. *Plant Cell Rep* **26**, 1879–1888.

Hara-Nishimura I, Nishimura M. 1987. Proglobulin Processing Enzyme in Vacuoles Isolated from Developing Pumpkin Cotyledons. *Plant Physiology* **85**, 440-445.

Haranishimura I, Takeuchi Y, Nishimura M. 1993. Molecular Characterization of a Vacuolar Processing Enzyme Related to a Putative Cysteine Proteinase of Schistosoma-Mansoni. *Plant Cell* **5**, 1651-1659.

Hatsugai N, Kuroyanagi M, Yamada K, Meshi T, Tsuda S, Kondo M, Nishimura M, Hara-Nishimura I. 2004. A Plant Vacuolar Protease, VPE, Mediates Virus-Induced Hypersensitive Cell Death. *Science* **305**, 855-858.

He P, Shan L, Lin NC, Martin GB, Kemmerling B, Nurnberger T, Sheen J. 2006. Specific bacterial suppressors of MAMP signaling upstream of MAPKKK in Arabidopsis innate immunity. *Cell* **125**, 563-575.

He R, Drury GE, Rotari VI, Gordon A, MartinWiller, TabasumFarzaneh, EJW, Galloi P. 2008. Metacaspase-8 Modulates Programmed Cell Death Induced by Ultraviolet Light and H2O2 in *Arabidopsis*. *The Journal of biological chemistry* **283**, 774–783.

Heath MC. 2000. Hypersensitive response-related death. *Plant Molecular Biology* **44**, 321-334.

Hoeberichts FA, Have At, Woltering EJ. 2003. A tomato metacaspase gene is upregulated during programmed cell death in Botrytis cinerea-infected leaves. *Planta* **217**, 517–522.

Hoisington., M.G.Neuffer, V. Walbot. 1982. Disease lesion mimic in maize *Dev. Biol* **93,**, 381-388.

Holl J, Vannozzi A, Czemmel S, D'Onofrio C, Walker AR, Rausch T, Lucchin M, Boss PK, Dry IB, Bogs J. 2013. The R2R3-MYB Transcription Factors MYB14 and MYB15 Regulate Stilbene Biosynthesis in Vitis vinifera. *Plant Cell* **25**, 4135-4149.

Horstmann V, Huether CM, Jost W, Reski R, Decker EL. 2004. Quantitative promoter analysis in Physcomitrella patens: a set of plant vectors activating gene expression within three orders of magnitude. *BMC Biotechnology* **4**, 13.

Huang J-s. 1986. Ultra structure of bacterial penetration in plants. *Annu. Rev. Phytopathol*, 141–157.

Huang L, Zhang H, Hong Y, Liu S, Li D, Song F. 2015. Stress-Responsive Expression, Subcellular Localization and Protein-Protein Interactions of the Rice Metacaspase Family. *International journal of molecular sciences* **16**, 16216-16241.

Iakimova ET, Atanassov A, Woltering EJ. 2005. Chemical- and pathogen-induced programmed cell death in plants. *Biotechnology and Biotechnological Equipment* **19**, 124-138.

Ismail A, Riemann M, Nick P. 2012. The jasmonate pathway mediates salt tolerance in grapevines. *Journal of Experimental Botany* **63**, 2127-2139.

Jacobson MD, Weil M, Raff MC. 1997. Programmed cell death in animal development. *Cell* **88**, 347-354.

Jeworutzki E, Roelfsema MRG, Anschutz U, Krol E, Elzenga JTM, Felix G, Boller T, Hedrich R, Becker D. 2010. Early signaling through the Arabidopsis pattern recognition receptors FLS2 and EFR involves Ca2+-associated opening of plasma membrane anion channels. *Plant Journal* **62**, 367-378.

JG. Zeledón, M. Kaiser, Spring O. 2016. An Extended Leaf Disc Test for Virulence Assessment in Plasmopara viticola and Detection of Downy Mildew Resistance in Vitis. . *J Plant Pathol Microbiol* **7:**353.

Jiao YT, Xu WR, Duan D, Wang YJ, Nick P. 2016. A stilbene synthase allele from a Chinese wild grapevine confers resistance to powdery mildew by recruiting salicylic acid signalling for efficient defense. *Journal of Experimental Botany* **67**, 5841-5856.

Jones JDG, Dangl JL. 2006. The plant immune system. *Nature* **444**, 323-329.

Kenton P, Mur LAJ, Draper J. 1999. A requirement for calcium and protein phosphatase in the jasmonate-induced increase in tobacco leaf acid phosphatase specific activity. *Journal of Experimental Botany* **50**, 1331-1341.

Kiefer B, Riemann M, Buche C, Kassemeyer HH, Nick P. 2002. The host guides morphogenesis and stomatal targeting in the grapevine pathogen Plasmopara viticola. *Planta* **215**, 387-393.

Kim SM, Bae C, Oh SK, Choi D. 2013. A pepper (Capsicum annuum L.) metacaspase 9 (Camc9) plays a role in pathogen-induced cell death in plants. *Molecular Plant Pathology* **14**, 557-566.

Kinoshita T, Nishimura M, Hara-Nishimura I. 1995. Homologues of a vacuolar processing enzyme that are expressed in different organs in Arabidopsis thaliana. *Plant Molecular Biology* **29**, 81-89.

Kinoshita T, Yamada K, Hiraiwa N, Kondo M, Nishimura M, Hara-Nishimura I. 1999. Vacuolar processing enzyme is up-regulated in the lytic vacuoles of vegetative tissues during senescence and under various stressed conditions. *The Plant Journal* **19**, 43-53.

Kitanaka C, Kuchino Y. 1999. Caspase-independent programmed cell death with necrotic morphology. *Cell Death and Differentiation* **6**, 508-515.

Lam E. 2004. Controlled cell death, plant survival and development. *Nat Rev Mol Cell Biol* **5**, 305-315.

Lam E, Zhang Y. 2012. Regulating the reapers: activating metacaspases for programmed cell death. *Trends in Plant Science* **17**, 487-494.

Langford AN. 1948. AUTOGENOUS NECROSIS IN TOMATOES IMMUNE FROM CLADOSPORIUM FULVUM COOKE. *Canadian Journal of Research* **26c**, 35-64.

Lebel E, Heifetz P, Thorne L, Uknes S, Ryals J, Ward E. 1998. Functional analysis of regulatory sequences controlling PR-1 gene expression in Arabidopsis. *The Plant journal : for cell and molecular biology* **16**, 223-233.

Lescot M, Dehais P, Thijs G, Marchal K, Moreau Y, Van de Peer Y, Rouze P, Rombauts S. 2002. PlantCARE, a database of plant cis-acting regulatory elements and a portal to tools for in silico analysis of promoter sequences. *Nucleic Acids Research* **30**, 325-327.

Liu R, Wang L, Zhu J, Chen T, Wang Y, Xu Y. 2015. Histological responses to downy mildew in resistant and susceptible grapevines. *Protoplasma* **252**, 259-270.

Livak KJ, Schmittgen TD. 2001. Analysis of Relative Gene Expression Data Using Real-Time Quantitative PCR and the 2−ΔΔCT Method. *Methods* **25**, 402-408.

Lockshin RA, Williams CM. 1964. Programmed Cell Death .2. Endocrine Potentiation of the Breakdown of the Intersegmental Muscles of Silkmoths. *Journal of Insect Physiology* **10**, 643-649.

Luna E, Bruce TJA, Roberts MR, Flors V, Ton J. 2012. Next-Generation Systemic Acquired Resistance. *Plant Physiology* **158**, 844-853.

Luo H, Song F, Goodman RM, Zheng Z. 2005. Up-regulation of OsBIHD1, a rice gene encoding BELL homeo-domain transcriptional factor, in disease resistance responses. *Plant Biology* **7**, 459-468.

Maisch J, Fišerová J, Fischer L, Nick P. 2009. Tobacco Arp3 is localized to actin-nucleating sites in vivo. *Journal of Experimental Botany* **60**, 603-614.

Merz PR, Moser T, Höll J, Kortekamp A, Buchholz G, Zyprian E, Bogs J. 2015. The transcription factor VvWRKY33 is involved in the regulation of grapevine (Vitis vinifera) defense against the oomycete pathogen Plasmopara viticola. *Physiologia Plantarum* **153**, 365-380.

Munson T. 1909. Foundations of American grape culture. *T.V. Munson & Son Denison*, 252.

Muthamilarasan M, Prasad M. 2013. Plant innate immunity: An updated insight into defense mechanism. *Journal of Biosciences* **38**, 433-449.

Nagata T, Nemoto Y, Hasezawa S. 1992. Tobacco BY-2 Cell Line as the "HeLa" Cell in the Cell Biology of Higher Plants. *International Review of Cytology* **132**, 1-30.

Nick P. 2014. Schützen und nützen - von der Erhaltung zur Anwendung. Fallbeispiel Europäische Wildrebe. *Handbuch Genbank WEL* **Hoppea Denkschr Regensb Bot Ges Sonderband**, 159-173.

Nick P, Heuing A, Ehmann B. 2000. Plant chaperonins: a role in microtubule-dependent wall formation? *Protoplasma* **211**, 234-244.

Nick P, Lambert AM, Vantard M. 1995. A microtubule-associated protein in maize is expressed during phytochrome-induced cell elongation. *Plant Journal* **8**, 835-844.

Nocarova E, Fischer L. 2009. Cloning of transgenic tobacco BY-2 cells; an efficient method to analyse and reduce high natural heterogeneity of transgene expression. *Bmc Plant Biology*,**9**.

Nomura H, Komori T, Kobori M, Nakahira Y, Shiina T. 2008. Evidence for chloroplast control of external Ca2+-induced cytosolic Ca2+ transients and stomatal closure. *Plant Journal* **53**, 988-998.

Nurnberger T. 1999. Signal perception in plant pathogen defense. *Cellular and Molecular Life Sciences* **55**, 167-182.

Olmo H. 1976. Grapes: Vitis, Muscadinia (Vitaceae). In: Simmonds NW, ed. . *Evolution of crop plants*. **London: Longman,**, 294-298.

Ouyang L, Shi Z, Zhao S, Wang FT, Zhou TT, Liu B, Bao JK. 2012. Programmed cell death pathways in cancer: a review of apoptosis, autophagy and programmed necrosis. *Cell Proliferation* **45**, 487-498.

Park HC, Kim ML, Kang YH, Jeon JM, Yoo JH, Kim MC, Park CY, Jeong JC, Moon BC, Lee JH, Yoon HW, Lee SH, Chung WS, Lim CO, Lee SY, Hong JC, Cho MJ. 2004. Pathogen- and NaCl-induced expression of the SCaM-4 promoter is mediated in part by a GT-1 box that interacts with a GT-1-like transcription factor. *Plant Physiology* **135**, 2150-2161.

Pennell RI, Lamb C. 1997. Programmed Cell Death in Plants. *The Plant Cell* **9**, 1157-1168.

Piszczek E, Gutman W. 2007. Caspase-like proteases and their role in programmed cell death in plants. *Acta Physiologiae Plantarum* **29**, 391-398.

Pontier D, Balague C, Roby D. 1998. The hypersensitive response. A programmed cell death associated with plant resistance. *Comptes rendus de l'Academie des sciences. Serie III, Sciences de la vie* **321**, 721-734.

Pontier D, Godiard L, Marco Y, Roby D. 1994. Hsr203j, a Tobacco Gene Whose Activation Is Rapid, Highly Localized and Specific for Incompatible Plant/Pathogen Interactions. *Plant Journal* **5**, 507-521.

Presti LL, Lanver D, Schweizer G, Tanaka S, Liang L, Tollot M, Zuccaro A, Reissmann S, Kahmann R. 2015. Fungal Effectors and Plant Susceptibility. *Annual Review of Plant Biology* **66**, 513-545.

Qi YP, Tsuda K, Glazebrook J, Katagiri F. 2011. Physical association of pattern-triggered immunity (PTI) and effector-triggered immunity (ETI) immune receptors in Arabidopsis. *Molecular Plant Pathology* **12**, 702-708.

Rahman, Mahmudur. 2010. Biochemical Analysis of Type II Metacaspase (mcII-*Pa*) *Dept. of Molecular Biology*.

Reina-Pinto JJ, Yephremov A. 2009. Surface lipids and plant defenses. *Plant Physiology and Biochemistry* **47**, 540-549.

Repka V, Fischerova I, Silharova K. 2004. Methyl jasmonate is a potent elicitor of multiple defense responses in grapevine leaves and cell-suspension cultures. *Biol Plant* **48**, 273 - 283.

Reynolds P. 1999. Inducible control of gene expression: an overview. In Inducible Gene Expression in Plants, 1-9. .

Schroder S, Telle S, Nick P, Thines M. 2011. Cryptic diversity of Plasmopara viticola (Oomycota, Peronosporaceae) in North America. *Organisms Diversity & Evolution* **11**, 3-7.

Seibicke T. 2002. Untersuchungen zur induzierten Resistenz a Vitis spec. **PhD thesis University of Freiburg**

Slee EA, Harte MT, Kluck RM, Wolf BB, Casiano CA, Newmeyer DD, Wang HG, Reed JC, Nicholson DW, Alnemri ES, Green DR, Martin SJ. 1999. Ordering the cytochrome c-initiated caspase cascade: Hierarchical activation of caspases-2, -3, -6, -7, -8, and -10 in a caspase-9-dependent manner. *Journal of Cell Biology* **144**, 281-292.

Smale ST, Kadonaga JT. 2003. The RNA polymerase II core promoter. *Annual review of biochemistry* **72**, 449-479.

Spoel SH, Dong XN. 2012. How do plants achieve immunity? Defense without specialized immune cells. *Nature Reviews Immunology* **12**, 89-100.

Suarez MF, H.Filonova L, Smertenko A, Savenkov EI, H.Clapham D, Arnold Sv, Zhivotovsky B, V.Bozhkov P. 2004. Metacaspase-dependent is essential for PCD in plant embryogenesis. *Current Biology* **14**, 339-340.

Sundström JF, Vaculova A, Smertenko AP, Savenkov EI, Golovko A, Minina E, Tiwari BS, Rodriguez-Nieto S, Jr AAZ, Välineva T, Saarikettu J, Frilander MJ, Suarez MF, Zavialov A, Ståhl U, Hussey PJ, Silvennoinen O, Sundberg E, Zhivotovsky B, Bozhkov PV. 2009. Tudor staphylococcal nuclease is an evolutionarily conserved component of the programmed cell death degradome. *nature cell biology* **11**, 1347-1356.

Svyatyna K, Jikumaru Y, Brendel R, Reichelt M, Mithofer A, Takano M, Kamiya Y, Nick P, Riemann M. 2014. Light induces jasmonate-isoleucine conjugation via OsJAR1-dependent and -independent pathways in rice. *Plant, cell & environment* **37**, 827-839.

Tamaoki M. 2008. The role of phytohormone signaling in ozone-induced cell death in plants. *Plant signaling & behavior* **3**, 166-174.

Tang YJ, Wang RP, Gong PJ, Li SX, Wang YJ, Zhang CH. 2016. Gene Cloning, Expression and Enzyme Activity of Vitis vinifera Vacuolar Processing Enzymes (VvVPEs). *Plos One* **11**.

This P, Lacombe T, Thomas MR. 2006. Historical origins and genetic diversity of wine grapes. *Trends in Genetics* **22**, 511-519.

Tian R-H, Zhang G-Y, Yan C-H, Dai Y-R. 2000. Involvement of poly(ADP-ribose) polymerase and activation of caspase-3-like protease in heat shock-induced apoptosis in tobacco suspension cells. *FEBS Letters* **474**, 11-15.

Tsiatsiani L, Breusegem FV, Gallois P, Zavialov A, Lam E, Bozhkov P. 2011. Metacaspases. *Cell Death and Differentiation* **18**, 1279–1288.

Tsiatsiani L, Timmerman E, De Bock PJ, Vercammen D, Stael S, van de Cotte B, Staes A, Goethals M, Beunens T, Van Damme P, Gevaert K, Van Breusegem F. 2013. The Arabidopsis METACASPASE9 Degradome. *Plant Cell* **25**, 2831-2847.

Tsuda K, Katagiri F. 2010. Comparing signaling mechanisms engaged in pattern-triggered and effector-triggered immunity. *Current Opinion in Plant Biology* **13**, 459-465.

Uren AG, O'Rourke K, Aravind L, Pisabarro MT, Seshagiri S, Koonin EV, Dixit VM. 2000. Identification of Paracaspases and Metacaspases: Two Ancient Families of Caspase-like Proteins, One of which Plays a Key Role in MALT Lymphoma. *Molecular Cell* **6**, 961-967.

van Doorn WG, Woltering EJ. 2005. Many ways to exit? Cell death categories in plants. *Trends in Plant Science* **10**, 117-122.

Vercammen D, Declercq W, Vandenabeele P, Van Breusegem F. 2007. Are metacaspases caspases? *The Journal of Cell Biology* **179**, 375-380.

Vercammen D, van de Cotte B, De Jaeger G, Eeckhout D, Casteels P, Vandepoele K, Vandenberghe I, Van Beeumen J, Inze D, Van Breusegem F. 2004. Type II metacaspases Atmc4 and Atmc9 of Arabidopsis thaliana cleave substrates after arginine and lysine. *Journal of Biological Chemistry* **279**, 45329-45336.

Wang X, Feng H, Tang C, Bai P, Wei G, Huang L, Kang Z. 2012. TaMCA4, a novel wheat metacaspase gene functions in programmed cell death induced by the fungal pathogen Puccinia striiformis f. sp. tritici. *Molecular plant-microbe interactions : MPMI* **25**, 755-764.

Watanabe N, Lam E. 2004. Recent advance in the study of caspase-like proteases and Bax inhibitor-1 in plants: their possible roles as regulator of programmed cell death. *Molecular Plant Pathology* **5**, 65-70.

Watanabe N, Lam E. 2005. Two *Arabidopsis* Metacaspases AtMCP1b and AtMCP2b Are Arginine/Lysine-specific Cysteine Proteases and Activate Apoptosis-like Cell Death in Yeast. *The Journal of biological chemistry* **280**, 14691–14699.

Watanabe N, Lam E. 2011a. Arabidopsis metacaspase 2d is a positive mediator of cell death induced during biotic and abiotic stresses. *The Plant Journal*, 969–982.

Watanabe N, Lam E. 2011b. Calcium-dependent Activation and Autolysis of Arabidopsis *metacaspase* 2d. *The Journal of biological chemistry* **286**, 10027–10040.

Welter LJ, Gokturk-Baydar N, Akkurt M, Maul E, Eibach R, Topfer R, Zyprian EM. 2007. Genetic mapping and localization of quantitative trait loci affecting fungal disease resistance and leaf morphology in grapevine (Vitis vinifera L). *Molecular Breeding* **20**, 359-374.

Wolter M, Hollricher K, Salamini F, Schulze-Lefert P. 1993. The mlo resistance alleles to powdery mildew infection in barley trigger a developmentally controlled defense mimic phenotype. *Molecular and General Genetics MGG* **239**, 122-128.

Woltering EJ, van der Bent A, Hoeberichts FA. 2002. Do plant Caspases exist? *Plant Physiology* **130**, 1764-1769.

Xu WR, Yu YH, Ding JH, Hua ZY, Wang YJ. 2010. Characterization of a novel stilbene synthase promoter involved in pathogen- and stress-inducible expression from Chinese wild Vitis pseudoreticulata. *Planta* **231**, 475-487.

Xu WR, Yu YH, Zhou Q, Ding JH, Dai LM, Xie XQ, Xu Y, Zhang CH, Wang YJ. 2011. Expression pattern, genomic structure, and promoter analysis of the gene encoding stilbene synthase from Chinese wild Vitis pseudoreticulata. *Journal of Experimental Botany* **62**, 2745-2761.

Yamada K, Shimada T, Nishimura M, Hara-Nishimura I. 2005. A VPE family supporting various vacuolar functions in plants. *Physiologia Plantarum* **123**, 369-375.

Zhang CH, Gong PJ, Wei R, Li SX, Zhang XT, Yu YH, Wang YJ. 2013. The metacaspase gene family of Vitis vinifera L.: Characterization and differential expression during ovule abortion in stenospermocarpic seedless grapes. *Gene* **528**, 267-276.

Zhang LR, Xing D. 2008. Methyl jasmonate induces production of reactive oxygen species and alterations in mitochondrial dynamics that precede photosynthetic dysfunction and subsequent cell death. *Plant and Cell Physiology* **49**, 1092-1111.

Zhang X, Wu Q, Cui S, Ren J, Qian WQ, Yang Y, He SP, Chu JF, Sun XH, Yan CY, Yu XC, An CC. 2015. Hijacking of the jasmonate pathway by the mycotoxin fumonisin B1 (FB1) to initiate programmed cell death in Arabidopsis is modulated by RGLG3 and RGLG4. *Journal of Experimental Botany* **66**, 2709-2721.

Zhang Y, Lam E. 2011. Sheathing the swords of death: post-translational modulation of plant metacaspases. *Plant signaling & behavior* **6**, 2051-2056.

Zipfel C. 2008. Pattern-recognition receptors in plant innate immunity. *Current Opinion in Immunology* **20**, 10-16.

Zipfel C. 2009. Early molecular events in PAMP-triggered immunity. *Current Opinion in Plant Biology* **12**, 414-420.

Zipfel C, Kunze G, Chinchilla D, Caniard A, Jones JDG, Boller T, Felix G. 2006. Perception of the bacterial PAMP EF-Tu by the receptor EFR restricts Agrobacterium-mediated transformation. *Cell* **125**, 749-760.

Publication

Gong PJ, Riemann M and Nick P 2017. Expression and function analysis of *metacaspase* gene family during pathogen-triggered PCD in grapevine (in preparation)

Zhang CH*, **Gong PJ* (Co-first author)**, Wei R, Li SX, Zhang XT, Yu YH, Wang YJ. 2013. The metacaspase gene family of Vitis vinifera L.: Characterization and differential expression during ovule abortion in stenospermocarpic seedless grapes. *Gene* 528, 267-276.